ISSN 1450 – 7404

Journal of Research in Physics

SPECIAL ISSUE
Contributed Papers of III YCSLS

Volume 28
Number 3
1999

INSTITUTE OF PHYSICS

Faculty of Sciences
University of Novi Sad – Novi Sad – Yugoslavia

Journal of Research in Physics

Published by: Institute of Physics, Faculty of Sciences, University of Novi Sad,
Trg Dositeja Obradovića 4, 21000 Novi Sad, Yugoslavia
Phone: +381-21-55318 Fax: +381-21-55662 E-mail: fizika@uns.ns.ac.yu
http://www.ns.ac.yu/prez/fiz/index.html

Printed by: Zavod za grafičku tehniku
TMF - Beograd, Yugoslavia

PREFACE

This book contain 3 invited lectures, 2 abstracts of invited lectures and 25 contributed papers presented at the third Yugoslav Conference on Spectral Line Shapes (YCSLS). The Conference was held in Brankovac from October 4 to October 6, 1999. The meeting was attended by 35 participants from Yugoslavia and guest from Belarus.

The conference deals with various aspects of physical processes associated with the formation of spectral line profiles in plasma.

The invited speakers and contributors have been asked to send their manuscripts in final form for publication, so no spelling and typing errors have been corrected in the course of the preparation of this book.

We would like to express our gratitude to DDOR Banka Novi Sad and Ikarbus Zemun which partially sponsored organization of the Conference.

The editors

3rd Yugoslav Conference on Spectral Line Shapes

Brankovac, October 4th to 6th, 1999

Scientific Organizing Committee

S. Djurović, Chairman
(Institute of Physics, Novi Sad)

N. Konjević	(Faculty of Physics, Belgrade)
J. Purić	(Faculty of Physics, Belgrade)
S. Djeniže	(Faculty of Physics, Belgrade)
M. Dimitrijević	(Astronomical Observatory, Belgrade)
I. Vince	(Astronomical Observatory, Belgrade)
M. Ćuk	(Faculty of Physics, Belgrade)
R. Kobilarov	(Institute of Physics, Novi Sad)
A. Mihajlov	(Institute of Physics, Belgrade)

Local Organizing Committee

Z. Mijatović, Chairman
(Institute of Physics, Novi Sad)

S. Djurović	(Institute of Physics, Novi Sad)
R. Kobilarov	(Institute of Physics, Novi Sad)
B. Vujičić	(Institute of Physics, Novi Sad)
D. Nikolić	(Institute of Physics, Novi Sad)
I. Savić	(Institute of Physics, Novi Sad)

Editors of the Conference Proceedings

Z. Mijatović
S. Djurović

Journal of Research in Physics Vol.28, No. 3, 185-198 (1999)

Invited lecture

QUASI - STATIC STARK PROFILE AS A MODEL OF THE SPECTRAL LINE SHAPE OF HEAVY NEUTRAL NON - HYDROGEN EMITTERS

D. NIKOLIĆ, S. DJUROVIĆ, Z. MIJATOVIĆ, R. KOBILAROV and N. KONJEVIĆ*
Institute of Physics, trg Dositeja Obradovića 4, 21000 Novi Sad, Yugoslavia
**Institute of Physics, P.O. Box 68, 11080 Belgrade, Yugoslavia*

1. INTRODUCTION

In accordance with plasma line broadening theory, the shapes of isolated spectral lines of the heavy neutral emitters, in plasmas of medium and high densities are predominately the result of collisions with the plasma electrons. These electron impacts cause a symmetric profile of Lorentzian shape. Griem et al. (1962) developed a semi-classical theory for the shapes of non-hydrogen lines emitted from plasmas and broadened by the local electric fields of both electrons as well as ions. First applied to neutral helium, Griem (1962) subsequently extended theory to heavier elements. The effects on spectral line shape due to collisions of electrons with the radiating atoms were treated by an impact approximation, while influences of local electric fields generated by the plasma ions were assigned to asymmetries near the center of isolated spectral lines. Such asymmetries can be caused by the microfield-induced quadratic Stark shifts of the energy levels of the radiating atoms. Under usually encountered experimental conditions, where ion motion can be neglected for heavy element lines, local electric field due to plasma ions is treated by a quasi-static approximation. Griem (1974) developed criterium, considering plasma conditions, when time-dependent ion-fields should be used and when ion motion becomes significant. Performing numerical calculations, Griem (1974) showed that electron impact broadening is the dominant contributor to the broadening for neutral atoms, while ion broadening contributes mostly about 10% of the total line width. This is the case of medium density plasma conditions, which are realized in stabilized arcs. The ion contributions for the line shifts are somewhat greater, and the shifts both due to electron impact and ion broadening are 'red' shifts for the majority of lines. Upper levels of radiating atoms (and to a much smaller extent, the lower levels) are exposed to relatively small shifting (proportional to the square of the electric microfield strength) under the influence of the local fields from environmental ions. Such shifts, when smeared out by the electric microfield distribution (Baranger and Mozer, 1959; Mozer and Baranger, 1960; Hooper Jr., 1966; Hooper Jr., 1968*a*), cause the electron-broadened symmetric Lorentzian line shape to become slightly asymmetric and broader as well as shifted beyond position due to electron broadening. Appearance of asymmetry in spectral line profile provides the possibility for experimental separation of the quasi-static ion broadening contribution from the electron-impact broadening. The numerous experiments were devoted to assembling of width and shift data (Fuhr et al., 1972; Fuhr and Lesage, 1993; Konjević and Roberts, 1976; Konjević et al., 1984). However, very small and thus hardly noticeable asymmetries in the line profiles have been mostly ignored until investigations of Roder and Stampa (1964) on several helium lines. They utilized the difference in the intensity decays of the blue and the red wings of the lines, which was theoretically predicted by Griem et al. (1962). Namely, the asymptotic intensity distributions in the line wings of the quasi-static $j_{A,R}(x)$ profile are (Griem et al., 1962; Griem, 1974; Woltz, 1986):

$$j_{A,R}(x) = \frac{1}{\pi} \cdot \int_0^{\infty} \frac{W_R(\beta)\, d\beta}{1+\left(x - A^{4/3} \cdot \beta^2\right)^2} \approx \begin{cases} \frac{1}{\pi} \cdot x^{-2} \cdot \left[1+\left(\frac{3\pi}{4}\right) \cdot A \cdot x^{1/4}\right] & x >> 1 \\ \frac{1}{\pi} \cdot x^{-2} & x << -1 \end{cases} . \quad (1)$$

Here $j_{A,R}(x)$ denotes the profile of an isolated spectral line emitted by a non-hydrogen radiator in the quasi-static ion approximation; A (α in ref. Griem, 1974) denotes ion broadening parameter as a measure of the relative significance of ion to electron broadening. Parameter R is the ratio of the mean ion separation to the Debye length:

$$R = (36\pi)^{1/6} \cdot \sqrt{\frac{e^2}{kT_e}} N_e^{1/6} , \quad (2)$$

where k is the Boltzmann constant and T_e is the plasma electron temperature. The scaled frequency (wavelength) x is given by

$$x = \frac{\omega - \omega_{ul} - d_e}{w_e} = \frac{\lambda - \lambda_{ul} - d_e}{w_e} , \quad (3)$$

with angular frequency ω and wavelength λ; ω_{ul} is the unperturbed frequency (wavelength λ_{ul}) of the line, while d_e and w_e are electron impact shift and half-halfwidth respectively. The argument β in relation (1) denotes the field strength F in units of the normal field strength F_0, while $W_R(\beta)$ is the ion microfield distribution function (Baranger and Mozer, 1959; Mozer and Baranger, 1960; Hooper Jr., 1966; Hooper Jr., 1968*a*). Roder and Stampa (1974), measured for some neutral helium lines, the ratios $Q = j_{A,R}(x) / j_{A,R}(-x)$ for several wavelength distances $\pm x$ from the line center (d_e and w_e may be obtained from the tables of Griem, 1974) , and calculated a mean value for parameter A according to

$$A = (Q-1) \cdot \frac{4}{3\pi} \cdot x^{-1/4} . \quad (4)$$

Kelleher (1981) has used much improved instrumentation to investigate most of these and several others He I lines. With the same approach good agreement with earlier experimental results and theory was obtained. Brandt et al. (1981) also performed a similar investigation of differences in the two line wings for a neutral krypton lines, and Nubbemeyer (1980) for vacuum ultraviolet lines of neutral nitrogen. Utilizing the general theoretical line profiles calculated and tabulated by Griem (1974), Goly and Grabowski (1976) perfomed best fit procedures on the shape of several neutral carbon lines. For known plasma conditions, parameter R (Eq. 2) is also known, so using tabulated electron shifts d_e and half-halfwidths w_e (Griem, 1974) it was possible to adjust value of ion broadening parameter A by iterative interpolation of tabulated quasi-static $j_{A,R}(x)$ profiles (Griem, 1974). Goly and Grabowski (1976) thus derived, for the first time by least-square procedure, values only for ion broadening parameter A.

In Refs. (Jones and Wiese, 1984; Jones et al., 1986; Jones and Wiese, 1987; Badie and Bacri, 1991), Lorentzian profiles were fitted to the experimental and theoretical $j_{A,R}(x)$

profiles. A functional relationship between the maximum of the Lorentzian - $j_{A,R}(x)$ deviation curve and parameter A was established. This function then was used for determination of values for A from the maximum deviations between the experimental points and the fitted Lotentzian. Such deviation method uses experimental points near the maximum deviation between the experimental profile and the fitted Lorentzian, and further more requires interpolation to determine the peak of the deviation curve; this interpolation procedure can be an additional source of error. Using an alternate approach, Hahn and Woltz (1990) developed a computer code, which fits the experimental profile with an asymmetric theoretical $j_{A,R}(x)$ profile by varying the width, shift, ion broadening parameter, and the cubic background of the theoretical curve. Namely, theoretical profiles $j_{A,R}(x)$ of known A were fitted to the experimental profiles of some neutral argon and carbon lines. Theoretical profiles $j_{A,R}(x)$ were generated for three initial guesses for A (A_1, A_2 and A_3) and for a known R, determined from the plasma density and temperature. Then the parameters d_e and w_e (Eq.3) are varied to minimize the sum of squared deviations χ_i^2 (χ_1^2, χ_2^2 and χ_3^2) between the experimental and theoretical profiles for each A_i. The fitting was done within one half width at half maximum (HWHM) of the line center where the experimental data are most reliable due to large signal-to-noise ratio, and where other sources of wing asymmetries are minimal. A cubic polynomial background is fitted to the experimental points beyond one HWHM from line center. It was found that the value of A is relatively insensitive to this background as well as to the value of parameter R. The next guess for A was taken as the minimum point of a parabola fitted through the three points (A_i, χ_i^2). The worst A_i (whose χ_i^2 is the largest) is discarded and procedure was repeated until the function $\chi^2(A)$ was minimized within a given tolerance. Hahn and Woltz (1990) concluded that the quasi-static ion approximation and quadratic level shifts due to the ion microfield give a good theoretical description of the asymmetries of the spectral line profiles studied in their work, and that a proposed least-square fitting technique can be of use in determining the experimental ion broadening parameter A. Neglecting a distinctions among above mentioned techniques of various authors, one common characteristic could be emphasized: experimental methods and instrumentation were used to provide such the plasma conditions necessary for validity of quasi-static approximation for ions and domination of the Stark effect in broadening of spectral lines. The other broadening mechanisms (natural, resonance, Van der Waals, Doppler and apparatus) were either neglected or later on taken into account by the simple corrections. When the Gaussian portion (corresponding to Doppler and apparatus broadening) of the experimental profile is of the same order or greater than the Lorentzian part (arising from Stark broadening with negligible asymmetry due to ions), Voigt profiles of general type (Goly and Weniger, 1986; Bakshi and Kearney, 1989; Davies and Vaughan, 1963) can be used as model functions. When the influence of the ion broadening on the line shape can not be neglected, the important Gaussian portion have to be taken into account by folding the profile $j_{A,R}(x)$ after Griem (1974) with Gaussian profile (Goly and Weniger, 1986; Mijatović et al.,1993; Knauer and Kock, 1996; Nikolić, 1998; Schinkoth et al., 1998):

$$K(x) = \int_{-\infty}^{+\infty} G(x-s) \cdot j_{A,R}(s)\, \mathrm{d}s\,. \qquad (5)$$

It is assumed that all others broadening mechanisms are negligible; on the contrary, their resulting profiles should be also taken account by folding them with the convolution $K(x)$ (Knauer and Kock, 1996).

This paper deals with the convenience of using the model (5) with the purpose to evaluate the Stark parameters directly from the experimental profiles of isolated or overlapped spectral lines of neutral atoms. In that manner, a method used by Nikolić (1998) will be presented through the short discussion of the nonlinear fitting of synthetic and of some experimental profiles.

2. NON-LINEAR REGRESSION AS A MODELING TOOL

Common modeling application in scientific research is that of predicting an outcome on the basis of experience. This statistical method, known as regression analysis, requires that functional relationship between the dependent Y and independent X variables be specified. In the past, regression analysis has been largely limited to linear models. Such models can be solved by hand with a single matrix inversion, although they are more easily solved using a computer. Certain other models can be made linear by parameter transformation in order to utilize linear regression techniques. Such transformations can introduce unwanted and sometimes unsuspected limitations or assumptions into the model and must be used with care. The majority of models encountered in spectral line shapes research, however, are nonlinear (related to parameters of the model) and cannot be transformed into linear form. Certain requirement exists for a general-purpose non-linear regression technique, which is both sufficiently general and robust to be applicable to a wide variety of research interests.

Most of today's software for non-linear regression is based on an algorithm by Marquardt (1963), which uses a Taylor's series expansion to give successive improvements to an initial set of parameter estimates. The method is actually a compromise between the inverse Hessian matrix method (Press et al., 1995) and the method of steepest descent (gradient method). It combines the best features of both methods while avoiding theirs most serious limitations (Draper and Smith, 1966). It shares with the gradient methods their ability to converge from an initial guess which may be outside the region of convergence of other methods (Press et al., 1995) and with the inverse Hessian matrix methods their ability to rapidly converge once in the vicinity of the minimum. An attenuation parameter (ξ) is used to switch smoothly between the two methods when is needed. Making ξ large favors the gradient method, and expands the region of convergence. Making ξ small selects the inverse Hessian matrix method and favors rapid convergence. Although no single method can be considered as the best one for all non-linear problems, Marquardt's method is a sensible first choice, providing the reasonable initial parameter estimates.

The goal of nonlinear regression is to fit a model to experimental data. More precisely, the goal is to minimize the sum of the squares of the vertical distances of the points (e.g. χ^2 - function) from the model curve (MC). A model is a formal presentation of a scientific idea. To be useful for nonlinear regression, the model must be expressed as an equation that defines Y, the outcome which one measures, as a function of X and one or more parameters $\vec{p}$ that one wants to fit. Choosing a model is a scientific decision and has to be based on understanding of scientific problem and should not be based solely on the shape of the graph. The key assumption is that the data really do follow a specified MC, and

that all scatters are attributable to random variation. For least-square regression to be valid, it has to be assumed that this variation (approximately) follows a Gaussian distribution, and that the standard deviation of the scattering is the same for all parts of the MC. In other words, the degree of scattering is completely unrelated to X. Except for a few special cases, it is not possible to directly solve the χ^2 - function minimum set of equations to find the values $\vec{p}_*$ of the model parameters which minimize the χ^2 - function. Instead, nonlinear regression requires an iterative approach. Here are the steps that every nonlinear regression procedure follows:

1. Starting with an initially estimated value for each parameter $\vec{p} \equiv (p_1, p_2, \ldots p_M)$ in the model curve: $Y = Y(X; p_1, p_2, \ldots p_M)$.
2. Generating the MC determined by the initial values; after that, calculation of the value of χ^2 - function defined as, $\chi^2(\vec{p}) = \sum_{i=1}^{N} \frac{(Y_i - Y(X_i; \vec{p}))^2}{\sigma_i^2}$, where (X_i, Y_i) is the set of N experimental points and σ_i is set of their measurement errors (standard deviations).
3. Adjusting the parameters $\vec{p}$ to make the MC come closer to the data points. There are several algorithms for adjusting parameters. Levenberg and Marquardt (Press et al., 1995) derived the most commonly used method discussed in the next section.
4. Adjusting the parameters again so that MC comes even closer to the points.
5. Proceeding with step 4 until the adjustment makes virtually no difference in the value of χ^2 - function.
6. Reporting the best - fit results. The obtained precise values will depend partially on the initial values chosen in step 1, and the stopping criteria of step 5. This means that repeated analyses of the same data will not always give exactly the same results.

If obtained data are 'clean' that clearly define a curve, then it is usually doesn't matter if the initial values are fairly far from the 'correct' values. One will get the same answer no matter what initial values uses, unless the initial values are far from 'correct'. Initial values matter more when experimental data have a lot of scatter, don't span a large enough range of X values to define a full curve, or don't really fit the model. In these cases, one may get different answers depending on which initial values were used. This problem (called *finding a local minimum*) is intrinsic to nonlinear regression, no matter what procedure is used. Fitting procedure will rarely encounter a local minimum if data have little scatter or were collected over an appropriate range of X values, and an appropriate model equation is chosen . To test for the presence of a false minimum it is necessary to:

- Note the values of the parameters $\vec{p}$ and the χ^2 - function from the first fit
- Make a large change to the initial values of one or more parameters $\vec{p}$ and run the fit again
- Repeat preliminar step several times
- Ideally, procedure will report nearly the same values of χ^2 - function and same parameters $\vec{p}$ regardless of the initial values. If the values are different, the one with the lowest value of χ^2 - function should be accepted.

3. LEVENBERG - MARQUARDT METHOD

Sufficiently near to the minimum, it is reasonable to expect that the χ^2 - function can be approximated by a quadratic form due to Taylor's series expansion (Press et al., 1995):

$$\chi^2(\vec{p}) \approx \chi^2(\vec{p}_*) + \left.\frac{\partial \chi^2(\vec{p})}{\partial \vec{p}}\right|_{\vec{p}_*} \cdot (\vec{p} - \vec{p}_*) + (\vec{p} - \vec{p}_*) \cdot \left.\frac{\partial^2 \chi^2(\vec{p})}{\partial \vec{p}^2}\right|_{\vec{p}_*} \cdot (\vec{p} - \vec{p}_*), \tag{6}$$

where $\mathbf{g} \equiv \dfrac{\partial \chi^2(\vec{p})}{\partial \vec{p}}$ is an M-vector and $\mathbf{H} \equiv \dfrac{\partial^2 \chi^2(\vec{p})}{\partial \vec{p}^2}$ is an $M \times M$ (Hessian) matrix. If the approximation (6) is a good one, only one step divides the current trial parameters $\vec{p}$ from minimizing ones $\vec{p}_*$:

$$\vec{p}_* = \vec{p} + \mathbf{H}^{-1} \cdot \mathbf{g} \ . \tag{7}$$

Approximation (6) may be unfavorable for the shapes of the χ^2 - function at $\vec{p}$, so step down the gradient is necessary like in the steepest descent method:

$$\vec{p}_{next} = \vec{p} + const. \cdot \mathbf{g} \ , \tag{8}$$

where the *const.* has to small enough not to loose the direction down the χ^2 - function surface. Making the use of Eqs. (7, 8) one has to compute $\mathbf{g}$ (the gradient of the χ^2 - function at any set of model parameters $\vec{p}$), and also the matrix $\mathbf{H}$ which is the second derivative matrix of the χ^2 - function at any $\vec{p}$. To do so, one has to specify the model curve $Y = Y(X; \vec{p})$ and the $\chi^2(\vec{p})$ merit function. The gradient of $\chi^2(\vec{p})$ with respect to the parameters $\vec{p}$ has the components:

$$[\mathbf{g}]_q \equiv \frac{\partial \chi^2}{\partial p_q} = -2 \sum_{i=1}^{N} \frac{(Y_i - Y(X_i; \vec{p}))}{\sigma_i^2} \cdot \frac{\partial Y(X_i; \vec{p})}{\partial p_q} \qquad q = 1, 2, \ldots M, \tag{9}$$

while after taking additional derivatives, Hessian matrix has the components:

$$[\mathbf{H}]_{sq} \equiv \frac{\partial^2 \chi^2}{\partial p_s \partial p_q} = 2 \sum_{i=1}^{N} \frac{1}{\sigma_i^2} \cdot \left[\frac{\partial Y(X_i; \vec{p})}{\partial p_s} \cdot \frac{\partial Y(X_i; \vec{p})}{\partial p_q} - (Y_i - Y(X_i; \vec{p})) \cdot \frac{\partial^2 Y(X_i; \vec{p})}{\partial p_s \partial p_q} \right] \tag{10}$$

$$s, q = 1, 2, \ldots M$$

It is common in practice to introduce new components of gradient and Hessian:

$$\beta_q \equiv -\frac{1}{2} \cdot [\mathbf{g}]_q \quad \text{and} \quad \alpha_{sq} \equiv \frac{1}{2} \cdot [\mathbf{H}]_{sq}, \tag{11}$$

so that Eq.(7) can be rewritten in terms of the increments $\delta\vec{p} = \vec{p}_* - \vec{p}$ as the set of linear equations:

$$\sum_{q=1}^{M} \alpha_{sq} \cdot \delta p_q = \beta_s \qquad s = 1, 2, \ldots M . \tag{12}$$

After solving the set (12) for the increments $\delta\vec{p}$, adding them to the current approximation for parameters $\vec{p}$ it is possible to get the next approximation ($\vec{p}_{next} = \vec{p} + \delta\vec{p}$). Equation (8), the steepest descent formula, translates to:

$$\delta p_q = const. \cdot \beta_q \qquad q = 1, 2, \ldots M . \tag{13}$$

Curvature matrix $[\alpha]$ has the components dependant both on the first and on the second derivatives of the model curve with respect to the model parameters (Eq. (10)). The second derivative term can be dismissed when it is zero (model curve depends linearly on parameters $\vec{p}$) or small enough comparing to the first derivative term. An additional possibility arises in practice, when the term $\left(Y_i - Y_i(X_i;\vec{p})\right)$, multiplying the second derivative in Eq. (10), is sufficiently small for a successful model because this term should be the random measurement error of each point. This error can have both signs, and in general should be uncorrelated with the model, so that the second derivative terms tend to cancel out each other when summed over *i*. Following the definition of curvature matrix components, next relation will be used instead Eq. (11):

$$[\alpha]_{sq} = \sum_{i=1}^{N} \frac{1}{\sigma_i^2} \cdot \left[\frac{\partial Y(X_i;\vec{p})}{\partial p_s} \cdot \frac{\partial Y(X_i;\vec{p})}{\partial p_q} \right] \qquad s = 1, 2, \ldots M . \tag{14}$$

From the fact that the χ^2 - function is nondimensional, the constants of proportionality between δp_q's and β_q's in Eq. (13) therefore must have dimensions of p_q^2 since β_q have dimension of p_q^{-1}. According to definition (14) for the components of $[\alpha]$, only the reciprocals of the diagonal elements $1/\alpha_{qq}$ have the dimensions of p_q^2. Levenberg-Marquardt method is based on the two facts. First is that the *const.* in Eq. (13) should be replaced with $\frac{1}{\xi \cdot \alpha_{qq}}$, where the attenuation nondimensional parameter ξ serves to cut down the step (setting $\xi >> 1$), and the second one is that eqs. (12,13) can be built into only one set of linear equation for increments $\delta\vec{p}$:

$$\sum_{q=1}^{M} \alpha'_{sq} \cdot \delta p_q = \beta_s \qquad s = 1, 2, \ldots M , \tag{15}$$

where the new curvature matrix $[\alpha']$ is defined by the following prescription:

$$\alpha'_{sq} \equiv (1 + \xi \cdot \delta_{sq}) \cdot \alpha_{sq} \qquad s, q = 1, 2, \ldots M , \tag{16}$$

where δ_{sq} is the Kronecker's symbol. When ξ is very large, the matrix $[\alpha']$ is forced to be diagonally dominant and (16) tends to (13); on the other hand, as ξ approaches zero, Eq. (16) goes over to (12).

With the given initial guess for the set of model parameters $\vec{p}$, Marquardt (1963) recommended an effective algorithm:

- Compute $\chi^2(\vec{p})$.
- Set a modest value for ξ, commonly $\xi = 0.001$.
- (❖) Solve the set of the linear equations (15) for the increments $\delta\vec{p}$ and evaluate $\chi^2(\vec{p}+\delta\vec{p})$
- If $\chi^2(\vec{p}+\delta\vec{p}) \geq \chi^2(\vec{p})$, increase ξ by a factor of 10 and go to (❖)
- If $\chi^2(\vec{p}+\delta\vec{p}) \leq \chi^2(\vec{p})$, decrease ξ by a factor of 10, set the new trial solution $\vec{p} \leftarrow \vec{p}+\delta\vec{p}$, and go to (❖)
- Condition of stopping is determined with first or second occasion that χ^2 decreases by a negligible amount (say fractional amount like 10^{-3})
- When acceptable minimum has been found, set $\xi = 0$ in order to compute estimated covariance matrix $[C] \equiv [\alpha]^{-1}$ of standard errors in the fitted parameters $\vec{p}$ (Press et al., 1995).

4. EVALUATION OF STARK PARAMETERS

According to Section 1 of this work and under conditions mentioned therein, it is reasonably to assume that isolated spectral lines of neutral emitters could be modeled by Eq. (5). This model has to be accommodated to real experimental situations. Experimental profiles are mostly represented as some relationship between signals from detector and wavelength of observed radiation. So, transition from the scaled wavelengths x to real wavelengths λ is needed. Amplitudes of signals from detector are usually normalized to maximal detected value, but almost never to the area under the experimental profile. That's why a normalized constant C_n has to be introduced. The Gaussian part of the convolution (5) decays fast on the wings, and practically tends to zero at distances of the several halfwidths from the center of the Gaussian profile. This fact justify the reduction of integration limits in (5) from $\lambda \in (0,\infty)$ to $\lambda \in (\lambda_0^* - \Delta\lambda, \lambda_0^* + \Delta\lambda)$, where λ_0^* denotes the center of the line and $\Delta\lambda$ has to be chosen in such manner to optimize accuracy of numerical integration against the computing time. The electric microfield distribution function $W_R(\beta)$ is tabulated for neutral point and charged point cases in Refs. (Hooper Jr., 1966; Hooper Jr., 1968*a*) and for the values $\beta \in (0,10)$. For $\beta > 10$ distribution function $W_R(\beta)$ is practically zero, so integration limits $\beta \in (0,\infty)$ in Eq. (1) can be replaced with limits $\beta \in [0,10]$ unless the more accurate computations have to be performed (Hoper Jr., 1968*b*). With the two-dimensional interpolation of mentioned tables for $W_R(\beta)$, it is possible to compute values of $j_{A,R}(\lambda)$ profile for given values of the parameters A and R. Since the spectral line always has underlying continuum, it is necessary to add in Eq. (5) unknown function $cont(\lambda)$, which represents continuum dependence on the wavelength. According to many laboratory experimental results, the isolated spectral lines of the neutral emitters are relatively narrow (the total halfwidths for the medium plasma conditions are

below 0.5 nm) and in the case of the Ar I lines (Nikolić, 1998) the observations were made inside of approximately eight halfwidths around the line center. In such spectral intervals it is justified to consider the continuum as independent or weakly linearly dependent function of the wavelength. Extensive simulations (Nikolić, 1998; Nikolić et al., 1998) have shown that, the preliminary subtraction of the fitted underlying continuum from the experimental profiles, do influence the adjusted values for the fitted stark parameters $\vec{p} \equiv (w_e, d_e, A)$ but always under 2%. On the other hand, such preliminary subtraction of the continuum reduces the number of the model parameters, and therefore the time needed for the overall fitting. Taking into account all the facts mentioned above, the convolution model (5) adapted for the real situations has the form:

$$\overline{K}(\lambda) \approx \frac{2\sqrt{ln2}}{\pi^{3/2} w_G} \cdot \frac{C_n}{w_e} \cdot \Psi_{1,0,0}(\lambda), \tag{17}$$

where overbar denotes continuum reduction. Here w_G means the halfwidth of the Gaussian portion of the convolution (17):

$$w_G = \sqrt{w_D^2 + w_I^2}, \tag{18}$$

with Doppler w_D and apparatus w_I broadening effects included. Concise notation has been introduced for the convolution integral (17):

$$\Psi_{a,b,c}(\lambda) \equiv \int_{\lambda_0 - \Delta\lambda}^{\lambda_0 + \Delta\lambda} d\lambda' (\lambda')^b \cdot e^{-\frac{4ln2}{w_G^2}(\lambda' - \lambda)^2} \int_0^{10} d\beta (\beta)^c \cdot \frac{W_R(\beta)}{\left[1 + \left(\frac{\lambda' - \lambda_0 - d_e}{w_e} - A^{4/3} \cdot \beta^2\right)^2\right]^a}, \tag{19}$$

where λ_0 is the wavelength corresponding to the center of the observed line emitted from the referent low pressure source (as Geissler tube, for example) . The gradient components of the model function (17) are:

$$\frac{\partial \overline{K}}{\partial w_e} = \frac{4\sqrt{ln2}}{\pi^{3/2} w_G} \cdot \frac{C_n}{w_e^4} \cdot \left[\Psi_{2,2,0} - 2 \cdot (\lambda_0 + d_e) \cdot \Psi_{2,1,0} - \gamma \cdot w_e \cdot \Psi_{2,1,2} + (\lambda_0 + d_e)^2 \cdot \Psi_{2,0,0} + \right.$$
$$\left. + \gamma \cdot w_e \cdot (\lambda_0 + d_e) \cdot \Psi_{2,0,2} - \frac{1}{2} \cdot w_e^2 \cdot \Psi_{1,0,0}\right], \tag{20}$$

$$\frac{\partial \overline{K}}{\partial d_e} = \frac{4\sqrt{ln2}}{\pi^{3/2} w_G} \cdot \frac{C_n}{w_e^3} \cdot \left[\Psi_{2,1,0} - (\lambda_0 + d_e) \cdot \Psi_{2,0,0} - \gamma \cdot w_e \cdot \Psi_{2,0,2}\right], \tag{21}$$

$$\frac{\partial \overline{K}}{\partial \gamma} = \frac{4\sqrt{ln2}}{\pi^{3/2} w_G} \cdot \frac{C_n}{w_e^2} \cdot \left[\Psi_{2,1,2} - (\lambda_0 + d_e) \cdot \Psi_{2,0,2} - \gamma \cdot w_e \cdot \Psi_{2,0,4}\right], \tag{22}$$

$$\frac{\partial \bar{K}}{\partial C_n} = \frac{2\sqrt{ln2}}{\pi^{3/2} w_G} \cdot \frac{1}{w_e} \cdot \Psi_{1,0,0} \quad , \text{ and} \tag{23}$$

$$\frac{\partial \bar{K}}{\partial w_G} = \frac{16(ln2)^{3/2}}{\pi^{3/2} w_G^4} \cdot \frac{C_n}{w_e} \cdot \left[\Psi_{1,2,0} - 2 \cdot \lambda \cdot \Psi_{1,1,0} - \lambda^2 \cdot \Psi_{1,0,0} - \frac{w_G^2}{8 ln2} \cdot \Psi_{1,0,0} \right], \tag{24}$$

where $\gamma = A^{4/3}$. The last gradient component (24) could be eliminated from fitting procedure due to the fact that the Gaussian halfwidth can be experimentally determined (Nikolić, 1998). To summarize, implementing Levenberg-Marquardt algorithm for χ^2-function minimization, it is possible to adjust fitting parameters $(w_e, d_e, \gamma, C_n, w_G)$ in such manner that convolution (17) properly describes experimental profiles of the neutral non-hydrogen emitters. Furthermore, in the case of two overlapping spectral lines similar procedure gives satisfactory results, but the fitting time is much longer, since one has the eight parameters to adjust $(w_{e1}, d_{e1}, \gamma_1, C_{n1}, w_{e2}, d_{e2}, \gamma_2, C_{n2})$. The model function in that case has the form:

$$\bar{K}(\lambda) \approx \frac{2\sqrt{ln2}}{\pi^{3/2} w_{G1}} \cdot \frac{C_{n1}}{w_{e1}} \cdot \Psi^{(1)}_{1,0,0}(\lambda) + \frac{2\sqrt{ln2}}{\pi^{3/2} w_{G2}} \cdot \frac{C_{n2}}{w_{e1}} \cdot \Psi^{(2)}_{1,0,0}(\lambda) \tag{25}$$

and the gradient components have the same form as eqs. (20-24) with the parameters corresponding to the overlapped lines. In the next section will be briefly presented several steps of the isolated synthetic spectral line profile fitting by the program code written in *Mathematica 3.0* (Wolfram, 1996) and given in Appendix 1 of ref. Nikolić (1998).

5. SIMULATIONS

For the testing purposes of given fitting procedure, discussed in the previous section, first step is to generate synthetic convolution profile defined by Eq. (17). The exact values of parameters, which are fixed during the fitting, were: $\Delta\lambda = 0.5$ nm, $w_G = 0.021$ nm and $R = 0.45$, while artificial values for adjustable parameters were $w_e = 0.025$ nm, $d_e = 0.020$ nm, $\gamma = 0.15$ and $C_n = 0.5$ arb.u.$\cdot$nm. With these values an synthetic convolution (17) was generated in $N = 100$ equally spaced points with the step of 0.005 nm. Such synthetic profile was then disturbed by a normally (Gaussian) distributed random noise centered at each point with the standard deviation of 0.01 arb.u.. This noise is almost three times larger than the experimental one (Nikolić, 1998). After that, fitting procedure was performed, accordingly to the described method, with an initial set of adjustable parameters: $w_e = 0.015$ nm, $d_e = 0.015$ nm, $\gamma = 0$ and $C_n = 0.3$ arb.u.$\cdot$nm. Fig. 1 shows the result of such initial guess. After eight iterations, with the stopping criteria that the relative change in the χ^2 value should not exceed 0.5%, optimal values were obtain; namely: $w_e = 0.0265$ nm, $d_e = 0.0217$ nm, $\gamma = 0.117$ and $C_n = 0.5025$ arb.u.$\cdot$nm. Fig. 2 shows the final result of fitting. Relative discrepancies between the artificial and fitted values are: 6% for w_e, 8.5% for d_e, 16.5% for A and 0.5% for C_n.

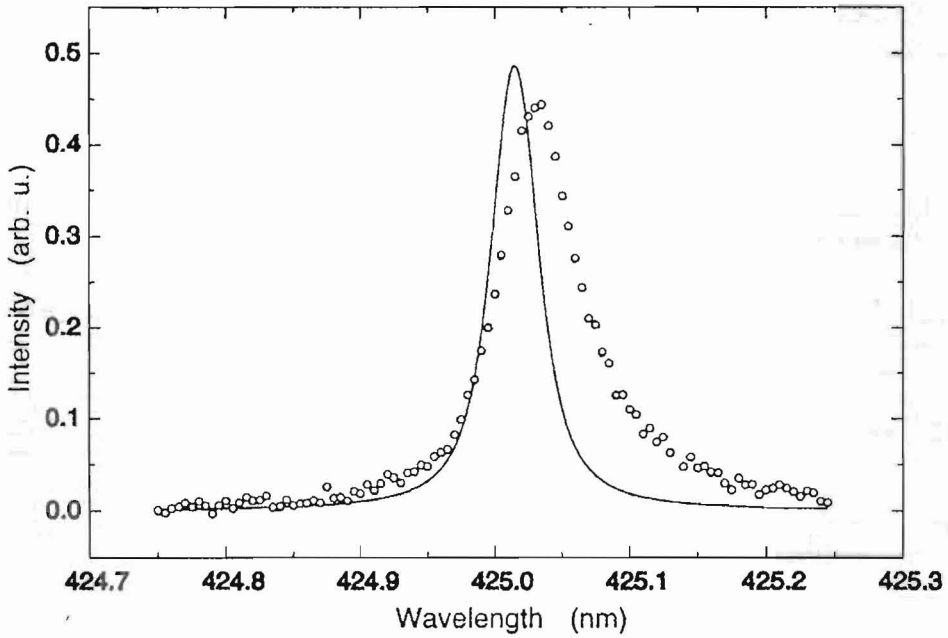

Fig. 1. Comparison of the randomly disturbed synthetic convolution (∘ ∘ ∘) with the model convolution (——) generated with an initial set of adjustable parameters: $w_e = 0.015$ nm, $d_e = 0.015$ nm, $\gamma = 0$ and $C_n = 0.3$ arb.u. · nm, before fitting.

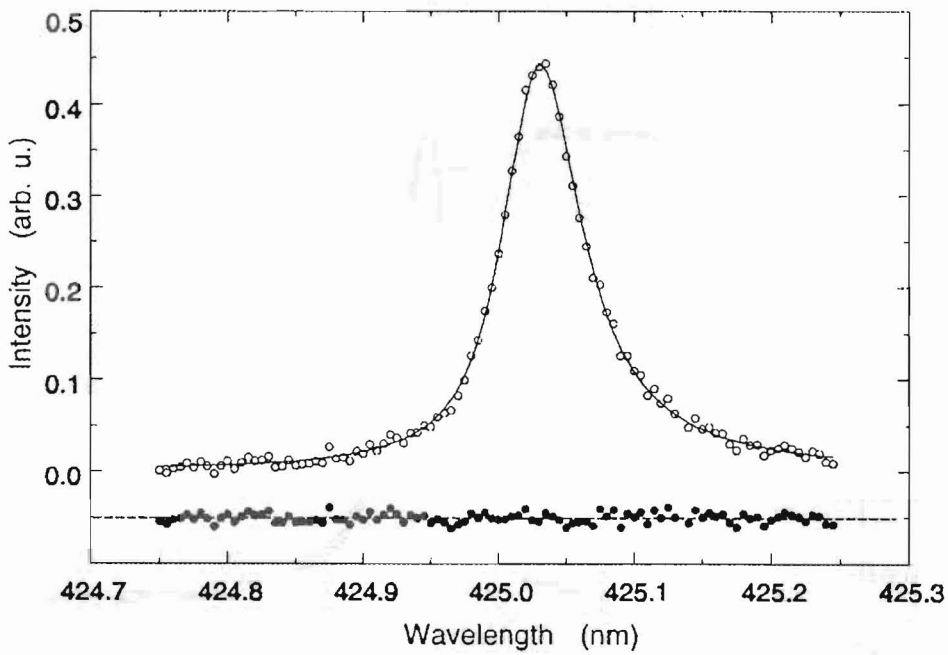

Fig. 2. Comparison of the randomly disturbed synthetic convolution (∘ ∘ ∘) with the model convolution (——) generated with an optimized set of adjustable parameters: $w_e = 0.0265$ nm, $d_e = 0.0217$ nm, $\gamma = 0.117$ and $C_n = 0.5025$ arb.u. · nm, at the end of the fitting. Diferences between those two convolutions (• • •) exibit random scatering.

The estimated covariance matrix of the performed fitting procedure has the form given in Table 1. According to Press et al. (1995), the 68.3% confidence intervals for the values of the fitted parameters are: $\delta w_e = 0.0012$ nm, $\delta d_e = 0.0013$ nm, $\delta\gamma = 0.021$ and $\delta C_n = 0.011$ arb.u.·nm

Table 1. Elements of the covariance matrix necessary for the estimation of the model parameters standard deviations

[C]	w_e (10^{-1} nm)	d_e (10^{-1} nm)	γ	C_n (arb.u.·nm)
w_e (10^{-1} nm)	$3.08\cdot10^{-5}$	$1.38\cdot10^{-5}$	$-3.57\cdot10^{-5}$	$1.4\cdot10^{-5}$
d_e (10^{-1} nm)	$1.38\cdot10^{-5}$	$3.54\cdot10^{-5}$	$-4.55\cdot10^{-5}$	$5\cdot10^{-6}$
γ	$-3.57\cdot10^{-5}$	$-4.55\cdot10^{-5}$	$8.96\cdot10^{-5}$	$2.2\cdot10^{-6}$
C_n (arb.u.·nm)	$1.4\cdot10^{-5}$	$5\cdot10^{-6}$	$2.2\cdot10^{-6}$	$2.48\cdot10^{-5}$

7. RESULTS AND DISCUSSION

For the demonstrating purpose, some results (Nikolić, 1998) of exposed modeling method for the neutral argon spectral will be presented. In the case of the isolated ArI lines, the 425.9 nm spectral line is selected and given in Fig. 3.

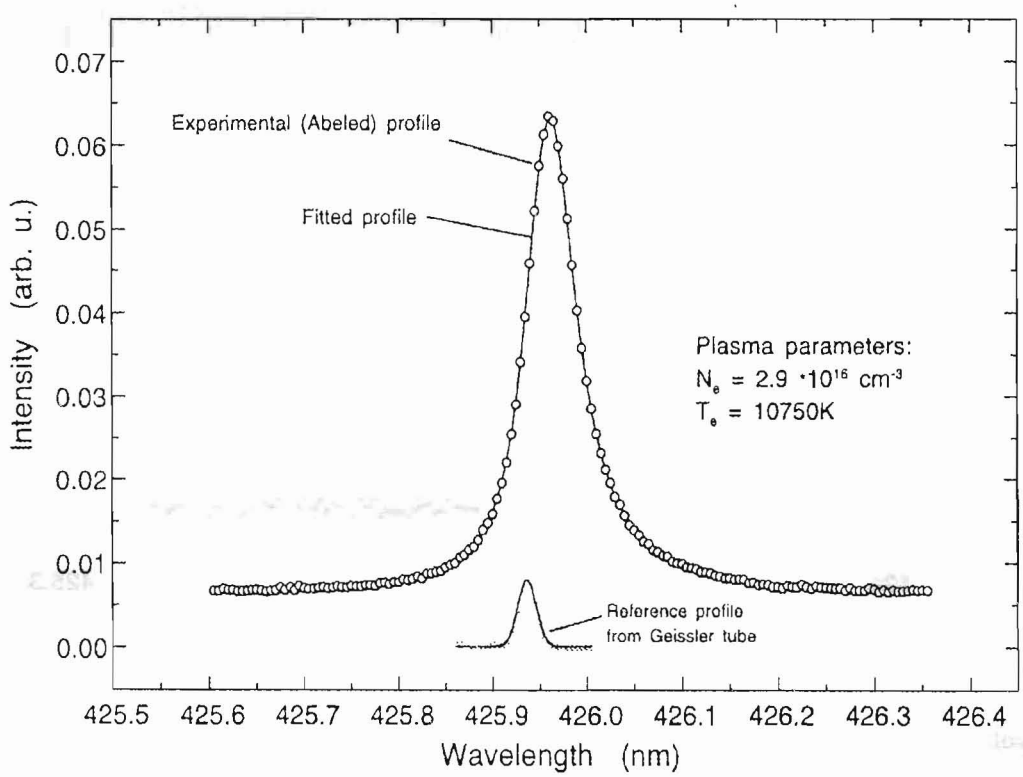

Fig. 3. Demonstration of fitting procedure in the case of Ar I 425.9 nm spectral line (Nikolić, 1998)

As representatives of two significantly overlapped neutral argon lines, Ar I 419.07 nm and Ar I 419.10 nm were taken (Nikolić et al., 1999). The final result of fitting procedure for these lines is illustrated in Fig.4.

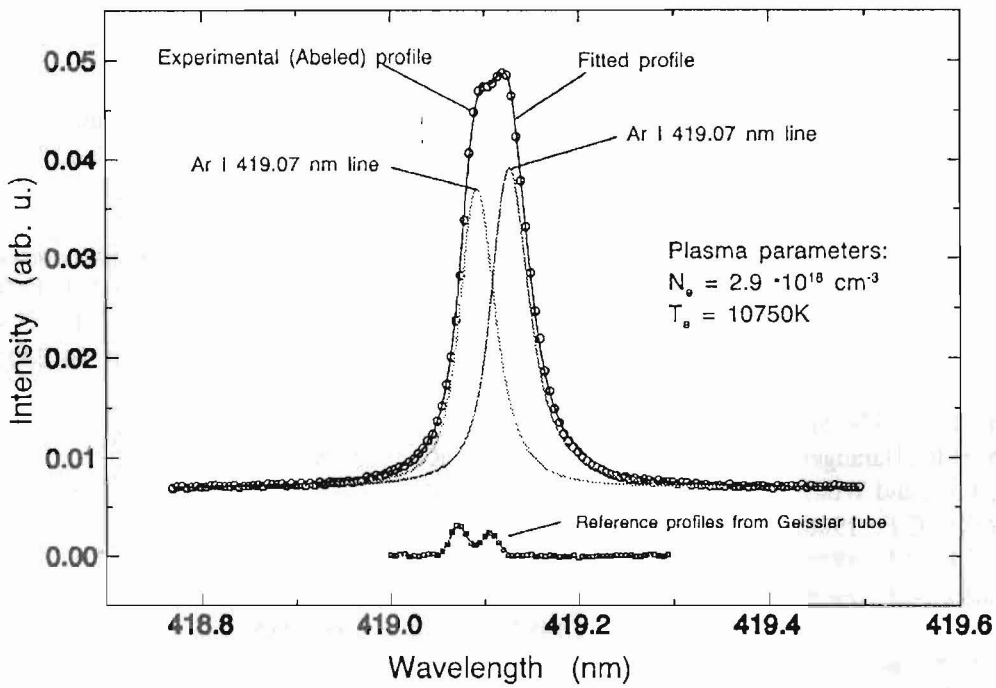

Fig. 4. Demonstration of fitting procedure in the case of two overlapped Ar I 419.07 nm and Ar I 419.10 nm spectral line (Nikolić, 1998)

As it can be seen from presented examples, described method results in fitted profiles which are in very good agreement with the experimental one. The only drawback of this method is long computing time - few hours for two overlapping lines - on pentium based PC with 32 MB RAM.

8. CONCLUSION

The herein presented method for modeling the spectral line shape of neutral atoms emitted from plasmas can be successfully applied under specified conditions. Existing theoretical predictions for Stark parameters of investigated spectral lines can be verified directly from high-precision measurements, providing proper separation of all significant broadening effects.

References

Badie, J.M., and Bacri, J.: 1991, *J. Phys. D* **24**, 809

Bakshi, V., and Kearney, R.J.: 1989, *J. Quant. Spectrosc. Radiat. Transfer* **42**, 405

Baranger, M., and Mozer, B.: 1959, *Phys. Rev.* **115**, 521

Brandt, T., Helbig, V., and Nick, K.P.: 1981, in: *Spectral Line Shapes* (B. Wende, Editor), 265, Walter de Gruyter, Berlin

Davies, J.T., and Vaughan, J.M.: 1963, *Astrophys. J.* **137**, 1302

Draper, N.R., and Smith, H.: 1966, *Applied Regression Analysis*, John Wiley&Sons, Inc., N.Y.

Fuhr, J.R., and Lesage, A.: 1993, *Bibliography on Atomic Line Shapes and Shifts (July 1978 through March 1992)*, National Standards Reference Data Series, National Bureau of Standards, U.S. Government Printing Office, Washington, DC

Fuhr, J.R., Wiese, W.L., and Roszman, L.J.: 1972, *Bibliography on Atomic Line Shapes and Shifts*, Natl. Bur. Stds. Spec. Publ. 366; ibid. Suppl. 1 (1974); Suppl. 2 (1975); Suppl. 3 (1978)

Goly, A., and Grabowski, B.: 1976, *Zesz. Nauk. Wyzsz. Szk. Pedagog. Opolu, Fiz. No.* **17**, 93

Goly, A., and Weniger, S.: 1986, *J. Quant. Spectrosc. Radiat. Transfer* **36**, 147; ibid. **38**, 225 (1987)

Griem, H.R.: 1962, *Phys. Rev.* **128**, 515

Griem, H.R.: 1974, *Spectral Line Broadening by Plasmas*, Academic Press

Griem, H.R., Baranger, M., Kolb, A.C., and Oertel, G.K.: 1962, *Phys. Rev.* **125**, 177

Hahn, T.D., and Woltz, L.A.: 1990, *Phys. Rev. A* **42**, 1450

Hooper Jr., C.F.: 1966, *Phys. Rev.* **149**, 77

Hooper Jr., C.F.: 1968 *a*, *Phys. Rev.***165**, 215

Hooper Jr., C.F.: 1968 *b*, *Phys. Rev.* **169**, 193

Jones, D.W., Pichler, G., and Wiese, W.L.: 1987, *Phys. Rev. A* **35**, 2585

Jones, D.W., and Wiese, W.L.: 1984, *Phys. Rev. A* **30**, 2602

Jones, D.W., Wiese, W.L., and Woltz, L.A.: 1986, *Phys. Rev. A* **34**, 450

Kelleher, D.E.: 1981, *J. Quant. Spectrosc. Radiat. Transfer* **25**, 191

Knauer, J.P. and Kock, M.: 1996, *J. Quant. Spectrosc. Radiat. Transfer* **56**, 563

Konjević, N., and Roberts, J.R.: 1976, *J. Phys. Chem. Ref. Data* **5**, 209

Konjević, N., Dimitrijević, M.S., and Wiese, W.L.: 1984, *J. Phys. Chem. Ref. Data* **13**, 619; ibid. **19**, 1307 (1990)

Marquardt, D.W.: 1963, *J. Soc. Indust. Appl. Math.*, **2**, 431

Mijatović, Z., Kobilarov, R., Vujičić, B.T., Nikolić, D., and Konjević, N.: 1993, *J. Quant. Spectrosc. Radiat. Transfer* **50**, 329

Mozer, B., and Baranger, M.: 1960, *Phys. Rev.* **118**, 626

Nikolić, D.: 1998, '*Influence of plasma temperature on shape and shift of argon spectral lines*', MSc Thesis, University of Belgrade, Belgrade (in Serbian)

Nikolić, D., Djurović, S., Mijatović, Z., Kobilarov, R., and Konjević, N.: 1999, *14th International Conference on Spectral Line Shapes* (Ed. R. Herman), AIP, New York, **10**, 191

Nikolić, D., Mijatović, Z., Djurović, S., Kobilarov, R., and Konjević, N.: 1998, *Deconvolution of Plasma Broadened Non-Hydrogenic Neutral Atom Lines*, accepted for publication in *J. Quant. Spectrosc. Radiat. Transfer*

Nubbemeyer, H.: 1980, *Phys. Rev. A* **22**, 1034

Press, W.H., Teukolsky, S.A., Vetterling, W.T., and Flannery, B.P.: 1995, *Numerical Recipes in C, Fortran and Pascal, 2nd ed.*, Cambridge University Press

Roder, O., and Stampa, A.: 1964, *Z. Physik* **178**, 348

Schinkoth, D., Kock, M., and Schulz-Gulde, E.: 1998, 'Experimental Stark Broadening Parameters for Near-Infrared Ar I and Kr I Lines', submitted to *J. Quant. Spectrosc. Radiat. Transfer*

Wolfram, S.: 1996, *The Mathematica Book, 3rd ed.*, Wolfram Media / Cambridge University Press)

Woltz, L.A.: 1986, *J. Quant. Spectrosc. Radiat. Transfer* **36**, 547

Journal of Research in Physics Vol.28, No. 3, 199-207 (1999)

Invited lecture

THE PROBLEMS OF PLASMA ACCELERATOR SPECTROSCOPY DIAGNOSTICS

V.M.Astashynski

Institute of Molecular and Atomic Physics
National Academy of Sciences of Belarus
F.Scaryny pr., 70, 220072 Minsk, Belarus
E-mail: lrpd@imaph.bas-net.by

1. Introduction

The reliable data on distribution of basic gas- and thermodynamic parameters of plasma, as well as distributions of electric and magnetic fields in such systems are necessary for adequate description of physical processes in plasma accelerators. In examinations of plasma accelerators, various methods of diagnostics are applied, such as methods of high-speed photo-recording, interferometry and shadowgraphy, probe and calorimeter methods, corpuscular and microwave methods, photoelectric methods of recording of radiation, and also spectroscopic methods of diagnostics of plasma formations.

We shall consider the use of some of the listed above plasma diagnostic methods on an example of concrete experimental examinations of quasi-stationary plasma accelerators with their own magnetic field, which are carried out in Group of Plasma Accelerators at the Institute of Molecular and Atomic Physics of National Academy of Sciences of Belarus. It should be noted here, that a feature of plasma accelerators under investigation is that the acceleration of plasma along the axis of the discharge device is accompanied by pinching at the output of accelerating system. As a result, the compression plasma flow is formed behind the edge of interior electrode. The parameters of plasma in this flow are much higher, than that in interelectrode gap of the accelerator [1]. Three types of plasma accelerators were studied: magneto-plasmadynamic compressor (MPC) [2-5], the double-stage quasi-stationary high-current plasma accelerator (QHPA) P-50M [6,7], working in vacuum with pulse (valve) delivery of working gas, and erosive plasmadynamic systems [8,9], which are capable to generate (in air at atmospheric pressure) compression erosion plasma flows of designated composition, which is determined by material of an interior electrode.

2. Determination of basic gas-dynamic and electrical parameters of the discharge in plasma accelerators

Dynamics of plasma generation and the formation of compression plasma flows was studied by methods of high-speed photorecording. Photographic recordings of

plasma luminescence were carried by high-speed photorecording installations SFR and VFU-1, which were working in streak mode or in frame mode. For time referencing of velocity photoscans and current and voltage oscillograms of the discharge, a simple method of synchronization by photodiode FD-10G (time resolution of the photodiode ~ $1{,}2\ 10^{-7}$ sec), which was introduced in one of the windows of lens insert (during frame mode operation) or in photorecording device film channel (during continuous scan operation), was used [2]. A signal from the photodiode was connected to the same beam of an oscilloscope, as one from Rogovsky coil.

Such examinations allow to study micro- and macrostructure of plasma flow and to determine characteristic velocities of plasma formations [2,4,6,8]. Summarizing results of the specified examinations, it is possible to present the following pattern of discharge development in the magneto-plasmadynamic compressor. After delivery of start pulse on a driving electrode of ignitron discharger, an electrical breakdown of an interelectrode gap is taking place at the point, where this gap has minimal value. The formed plasma is accelerated in the discharge device under action of electromagnetic (Ampere) force and is taken out behind the tip (edge) of the accelerator, where the compression plasma flow is formed on an axis of system. Under operating conditions, the plasma comes behind the tip of interior electrode (cathode) to ~ 15 μsec from the beginning of discharge current. As shown by continuous photoscans received with orientation of SFR slit normally to the axis of the discharge device, a compression flow in first 15 ÷ 20 μsec after coming of plasma to the tip of an interior electrode displays appreciable radial macro-oscillations, which get stronger as initial pressure of working gas is reduced. Approximately after 30 μsec from the beginning of discharge current, the flow becomes macro-stable, the diameter therewith comprises 0.3 ÷ 1 cm, and the length — 5 ÷10 cm (depending on the initial conditions of experiment). The time of stable existence of compression plasma flow makes ~ 40÷50 μsec (at total duration of the discharge of ~ 80 μsec).

The compression plasma flow during all the time of its existence evidently displays discrete (intermittent) microstructure, which is well visible on continuous photoscans under condition of orientation of the slit along the axis of the flow as alternation of light and dark stripes. The light stripes are projections of trajectories of motion of separate plasma formations onto the slit of moving-image camera. The frequency of following of plasma formations grows from 5 up to 15 MHz as initial pressure of working gas in the MPC camera increase from 133 up to 665 Pa. The presence of plasma sub-flow behind the tip of interior electrode, moving from compression region into divertor hole is evident. The demarcation of compression region and specified sub-flow of plasma is, in essence, "a zero point ", i.e. place, where the longitudinal velocity of plasma on an axis of system goes to zero.

In [7], the velocity of plasma formations generated by QHPA was estimated from continuous photoscans. At initial voltage of the store of the second stage of the

accelerator U_0 = 3 kV, the velocity of plasma comprises ~ 7 $\cdot 10^6$ cm/sec. Experimentally, velocity of plasma flow reaches it's peak value at U_0 = 4 kV and makes ~ 1,7 $\cdot 10^7$ cm/sec, while at U_0 = 5 kV it makes ~ 10^7 cm/sec.

The basic electrotechnic characteri stics of the discharges in plasma accelerators, a discharge current I_d and voltage on electrodes U_d were measured by gauged Rogovsky coils with integration of the signal by RC-chain and by frequency compensated RC-voltage dividers. On the basis of received oscillograms of current and voltage of the discharge, an instantaneous power $P_i(t) = I_d(t) \cdot U_d(t)$, energy, which is put in the discharge, $W_c = \int P_i(t)dt$ and energy efficiency of the accelerator $\eta = W_c/W_0$ (here W_0 is energy reserved in the store) were determined. In MPC- and QHPA-type systems, η usually makes ~ 0.6-0.8 [2,6,8]. The volt-ampere characteristics, showing dependence between voltage on electrodes and current during one discharge of MPC during time since 20 till 60 μsec (when transients were finished and plasma flow is in stable state), are nonlinear and have power character with an exponent ~ 2.

3. Measuring electrical and magnetic fields

The studies of electric and magnetic field distributions in QHPA were carried out by probe methods [7,10]. Floating potential of plasma was measured by single Langmuir probe, and distribution of magnetic fields was studied by magnetic probe. The probes were inserted into the discharge device of QHPA perpendicularly to plasma flow between anode rods. The probe-induced perturbations were checked by investigation of integral performances (current and voltage) of the discharge, and by symmetry and stability of plasma flow in QHPA. For perturbation of plasma reduction, only one magnetic or electrical probe at a time was inserted into the channel. The insertion of probe does not render appreciable influence on the shape and values of discharge current practically in the whole volume of the channel, except for narrow layer (1-2 cm) near the surface of cathode transformer, where the influence of probe insertion on I_d could be appreciable. For example, the introduction of probes in near-cathode layer before critical section of the channel (10 cm from its inlet) is causing increase of discharge current amplitude on ~ 25% and diminution of duration of the first half-period by ~ 15%. If the probe is introduced into the channel behind critical section (40 cm from the inlet), the amplitude of current is rising by ~ 15%, the duration of a half-period thus decreases by ~ 10%. The study of frames of plasma luminescence received by VFU -1 have shown that the presence of probe in the channel does not influence symmetry and stability of plasma flow in QHPA.

The spatial-time pattern of distribution of isolines of current ($I=5HR=const$), which was constructed on the basis of measured azimuth component of magnetic field H_θ, has allowed to reveal, in addition to usually gained distribution of current with "slippage", two types of current distribution in the channel of QHPA: quasi-radial

distribution and distribution with "antislippage" [7,10]. It was shown, that for receiving of any pattern of distribution of current in the channel of QHPA it is necessary to match in appropriate way quantities of a discharge current and rate of flux of ions in near-anode and near-cathode regions or, what is the same, to match an exchange parameters ξ_c and ξ_a. The quasi-radial distribution of a current is set, when $\xi_c = \eta\xi_a$. Here, η is a loss coefficient for current-carrying ions, depending on a construction of transformers and on interaction of specified ions with plasma in the channel of the accelerator; after matching of operation of first and second stages of QHPA this coefficient comes close to one. If $\xi_c > \eta\xi_a$, distribution of current with "antislippage" along cathode transformer (T_c) is observed. When $\xi_c < \eta\xi_a$, the distribution of a current with "antislippage" is implemented in the accelerating channel. It is obvious, that, having placed inside of cathode transformer an ion source (it could be plasma, which is filling interior volume of T_c), it is possible to move from a mode with "antislippage" of current to the mode with quasi-radial distribution or with "antislippage" one.

For classifying of patterns of potential distribution Φ in QHPA channel, the dimensionless coefficients χ_c and χ_a, were defined. This coefficients are showing accordingly the ratio of potential difference in narrow near-cathode and near-anode layer to potential difference between electrodes (transformers) as a whole [7,10]. It was shown, that when distribution of current in the channel of a QHPA with "antislippage" is taking place than $\chi_c < \chi_a$, while at "antislippage" of current and its quasi-radial distribution one have $\chi_c > \chi_a$. It should be noted, that χ_c at "antislippage" of current for appropriate moments of time always exceeds χ_c for quasi-radial distribution of current, but χ_a values for "slippage" of current, on the contrary, are always less than χ_a for its quasi-radial distribution. Hence, it is possible to make judgements about the character of distribution of discharge current in the channel of QHPA on the basis of relation of values χ_c and χ_a. The received relations allow to reduce essentially and to simplify procedure of diagnosing of modes of operations of the accelerator, that is especially important in operation with powerful and complex accelerating plasmadynamic systems.

4. Methods of definition of thermodynamic parameters of plasma in plasma accelerators

The use of traditional spectroscopic methods of diagnostics fo r studies of quasi-stationary plasma accelerators under conditions, when working gas is hydrogen, causes some difficulties. Under such conditions, temperature of plasma can be determined from results of experiments on supersonic compression flow incidence on thin wedge with sharp forward edge, which is a source of weak perturbations. In studies of plasma flows of QHPA a wedge was set under zero angle of attack to an axis of system, 35 cm apart from the tip of cathode transformer [10]. Visualization of Mach lines on forward edge of the wedge was carried out by shadow method with double passage of probing bundle of

laser radiation through explored region. Recording of shadow pattern was carried out by high speed photographic camera working in a frame mode. The frame frequency of shadow pattern was equal to 245000 frame/sec. The time of exposure of each separate frame is defined by duration of spikes of laser radiation, it is less than 1 μsec.

As is known, the slope angle of Mach lines (Mach angle) depends on velocity of incident compression flow and on velocity of sound in plasma as follows : $sin\alpha = C_s/V$, where α is Mach angle; V is velocity of an incident plasma flow, C_s is velocity of sound. Then, from expression for velocity of sound in plasma $C_s^2 = (\gamma k(T_i + zT_e)/M_i$, where T_i and T_e are temperatures of ions and electrons; M_i is ion mass; z is ion charge; k is Boltzmann constant; γ — the exponent of Poisson adiabat, is possible to find temperature of plasma: $T_{pl} = (V \cdot sin\ \alpha)^2 \cdot M_i/\gamma k(1+z)$, where $T_{pl} \equiv T_i = T_e$. Under QHPA conditions, the temperature of plasma of compression flow, determined by specified method, comprises 10-15 eV [10].

Most informative, and at the same time most complex method of diagnostics of plasma accelerators, is interferometry method. Advantage of this method is the opportunity of reception of extensive and reliable information without entering perturbations into explored plasma. The application of an interferometer in combination with high-speed recording camera allows not only to visualize processes, which are not accessible for photographic recording, but also to determine spatial-time distribution of parameters in explored plasma with high accuracy.

The spatially and time-resolved electron concentration of plasma of compression flow in MPC and QHPA was determined by two-mirrors autocollimation interferometer [11] with visualization field, varied, depending on conditions of experiment, from 50 up to 200 mm. Interference figure recording was carried out by high-speed moving-image cameras SFR or VFU working in a frame mode, that allows to gain a series of interferograms for single experiment showing time change of phase refraction coefficient of studied plasma formation in the whole field of view.

For most symmetric interferograms, a definition of radial distribution of fringes shifts was carried out. In a symmetric case the radial distribution and registered quantities of fringe shifts at observation along a chord are interlinked through Abel equation. For the solution of this equation, a series of methods was designed, for example [12]. However, it is not always possible to receive required radial distribution by using simple computational methods, as the integral Abel equation belongs to a class of so-called ill-posed problems of mathematical physics. Tikhonov method of regularization was applied for determination of radial distribution of shifts of fringes [13], implementing computer build-up of stable approximate solution. The test checkouts have shown good precision of restoration of model radial distributions by used program and its considerable advantages in comparison to traditional methods such as Bokasten's.

The interferometric studies of MPC and QHPA P-50M were carried out with single wave length probing laser. Therefore as a preliminary, an opportunity of definition of electron concentration of plasma formations was analyzed, accounting for various factors influencing refraction of plasma in the range of parameters $T_e \sim 1 \div 15$ eV, $N_e \sim 10^{15} \div 10^{17}$ cm^{-3}, which is characteristic for MPC and QHPA. First of all, the contribution of heavy particles, i.e. atoms and ions of hydrogen, to a refraction of plasma was estimated. The calculations with use of value of a specific polarizability of hydrogen atoms have shown, that the contribution of heavy particles becomes comparable to the contribution of electrons at a degree of ionization ~ 0.03. At a degree of ionization more than ~ 0.3, contribution of atoms of hydrogen can be neglected, as it becomes comparable with an error of measurements. Let's note here, that the degree of ionization of plasma formations in MPC and QHPA is close to 1.

The shifts of interference fringe s caused by replacement of neutral gas from area, filled by compression plasma flow, was estimated too. Experimentally, it has appeared equal 0.02 fringes and was not taken into account in calculations. Then possible influence of "resonant" effect was analyzed. Wave length of H_α ($\lambda = 656$ nm), having a half-width of about 5 nm, is nearest to probing laser wave length ($\lambda = 694$ nm) in spectrum of radiation of compression region. According to calculations, "resonant" influence of H_α - line on an refraction coefficient is small (~ 0.03 fringes) and it was not taken into account at determination of N_e.

Further, at definition of density of charged particles by means of optical interferometry, some indeterminacy exists, which is caused by the lack of sharp transition between mobile electrons and electrons of the upper excited levels. However, the quantity of this indeterminacy for plasma formations with parameters, close to implemented in QHPA, does not exceed 1%.

At last, the passage of probing laser beam through e xplored plasma is accompanied by its diversion from a tentative direction owing to refraction of light on phase inhomogeneities, that can give in additional interferometry fringes shifts. However, this effect can be neglected in our case, because values of electron concentration ($10^{17} \div 10^{18}$ cm^{-3}) implemented even in compression region are at least three - four orders below critical density (~ 10^{21} cm^{-3}). Thus, as the analysis carried out shows, the refraction of plasma in MPC and QHPA contexts is defined mainly by mobile electrons.

Interferometric studies of MPC and QHPA executed in [14-17] have allowed to measure concentration of charged particles in the accelerating channel and to receive a spatial-time pattern of distribution of density of electrons in an output of the accelerator. The analysis of time change N_e in the accelerating channel shows, that there is some characteristic (boundary) range of values of electron density in QHPA (experimentally, it is equal to $\sim (1.5 - 2) \cdot 10^{15}$ cm^{-3}), in which quasi-radial distribution of current isolines is set at quasi-stationary stage of the discharge (after ~ 150 μsec). If electron concentration

is higher than this range, the distribution of current with slippage is set. In the case, when density of electrons of plasma in the channel becomes below this boundary, the distribution of isolines of current with antislippage is observed.

The measuring of an electron concentration in the accelerating channel and in the output of accelerating system has enabled to determine the contraction ratio of compression flow, which, experimentally, varies from 20 up to 50.

5. Features of spectroscopic diagnostics of plasma in QHPA

The presence of areas of plasma with essentially different temperatures and densities of particles in discharge volume is characteristic for QHPA-type systems. Temperature of electrons can comprise ~ 1 eV in the drift channel and hundreds of eVs in compression flow, the electron concentration thus also varies for several orders ($10^{14} \div 10^{15}$ cm^{-3} in the channel and ~ 10^{17} cm^{-3} in compression region). It causes particular difficulties for spectroscopic diagnostics of QHPA, when working gas is hydrogen. Let's note also, that in the areas of QHPA, where the electron concentration reaches values ~ 10^{17} cm^{-3}, at temperatures exceeding 2 eV, hydrogen is practically completely ionized.

Under such conditions, procedures of definition of plasma parameters with the use of spectral lines of atoms and ions of inert gases, which are specially added as impurities into working gas of the accelerator [18] can be more convenient experimentally. The parameters of broadening for these lines are lower, and temperature interval, in which they are effectively excited, is wider in comparison to hydrogen lines. The addition in working gas of small portions of inert gas impurities with different potentials of ionization can allow not only to determine temperature and density of plasma, but also to visualize regions with various parameters in QHPA.

At the present time there are numerous data on parameters of Stark broadening, transition probabilities or oscillator forces and energy levels for many spectral transitions in Ar, Xe, Ne and especially He atoms and ions [19-21]. For spectroscopic diagnostics based on introduction of impurities of inert gases in hydrogen plasma, calculations of limits of applicability of concrete procedures using various spectral lines of atoms and ions of these gases for definition of parameters of plasma and calculations of limits of applicability of concrete procedures using various spectral lines are needed.

The tentative experiments on determination of parameters of plasma in QHPA P-50M by spectroscopic methods were carried out by addition of helium impurity in hydrogen, i.e. an intermixture of hydrogen and helium in the ratio 3:1 as working gas was used. The spectrums of emission filed were obtained with the help of time resolved spectrography (ISP-30 + SP-452). The time interval, in which radiation was registered, comprise ~ 40 μsec.

Electron concentration in plasma was determined by line broadening $H\beta$ 486.1 nm and *HeI* 587.5 nm caused by linear and square-law Stark effect accordingly. The precision

of definition of density of electrons in plasma with the use of *HeI*-line 587.5 nm is not worse than at measuring N_e by broadening of $H\beta$ -line. Averaged through beam of sight values of electron concentration measured at line broadening $H\beta$ and *HeI* have made accordingly $\sim 3.5 \cdot 10^{15}$ and $\sim 3.6 \cdot 10^{16}$ cm^{-3} for section, which was ~ 35 cm apart from an edge of interior electrode [22]. The discrepancy of N_e, received with the use of specified lines, falls outside the measuring error limits and is due to spatial inhomogeneity of plasma flow in QHPA. It is clearly visible on spectrums of plasma luminescence slit, registered with orientation of spectrograph slit normally to compression flow axe, that the hydrogen Balmer series lines are displayed through all length of the chosen sections of plasma flow, while *HeI* lines with higher (in comparison to hydrogen atom lines) energies of the upper levels are emitting only from central, hotter region. The values of density of electrons received with use of helium atom lines correspond to this region.

6. Conclusion

As is known, distributions of electrical and magnetic fields in plasma accelerators are defined in the final by both the process of acceleration and by parameters of formed plasma flows. However use of probes can import essential contortions to real-life pattern of electrical and magnetic fields distribution in plasma accelerators. Therefore the studies, which are directed on development of non-contact methods of diagnostics, are very important. The spectroscopic methods using spectral lines of atoms and ions of inert gases purposely introduced as admixtures in the working gas can be useful for decision of those problems.

References

1. A.I.Morozov Nucl. Fusion, Special Suppl., (1969) 111.
2. V.M.Astashynski, G.I.Bakanovich, L.Ya.Min'ko. J. Appl. Spectroscopy 33 (1980) 629.
3. V.M.Astashynski, G.I.Bakanovich, L.Ya.Min'ko. Sov. J. Plasma Phys. (Engl.transl). 10 (1984) 1058.
4. V.M.Astashynski, G.I.Bakanovich, E.A.Kostyukevich et al. J. Appl. Spectroscopy 50 (1989) 887.
5. V.M.Astashynski, G.I.Bakanovich, A.M.Kuz'mitski et al. Injenerno-fizicheskii J. 62 (1992) 386.
6. S.I.Ananin, V.M.Astashynski, G.I.Bakanovich et al., Sov. J. Plasma Phys. (Engl. transl.) 16 (1990) 102.
7. V.M.Astashynski, A.A.Man'kovskii, L.Ya. Min'ko, and A.I.Morozov, Sov. J. Plasma Phys. (Engl. transl.), 18 (1992) 47.

8. V.M.Astashynski, A.A.Man'kovskii, L.Ya.Min'ko. J. Appl. Spectroscopy 55 (1991) 903.
9. V.M.Astashynski, A.A.Man'kovskii, L.Ya. Min'ko. Publications of the Astronomical Observatory of Belgrade N 53 (1996) 59.
10. V.M.Astashynski, L.Y.Min'ko. The Physics of Ionized Gases / Edited by N.Konjevic, M.Cuk and S.Djurovic. — Publisher: University of Belgrade, Yugoslavia, 1999. — P. 285.
11. E.A.Kostyukevich, L.Ya.Min'ko. Proceedings of XIV Int. Conf. High-speed Photography. Moscow (1980) 581.
12. K.Bockasten. J. Opt. Soc. Am. 51 (1961) 943.
13. A.N.Tikhonov, A.V.Goncharskii, V.V.Stepanov et al. Numerical Methods for Solution of Ill-Posed Problems. Moscow: Nauka, 1990.
14. V.M.Astashynski, E.A.Kostyukevich. Sov. J. Plasma Phys. (Engl. transl.) 7 (1981) 282.
15. V.M.Astashynski, E.A.Kostyukevich, A.M.Kuzmitsky et al. SPIE Proceedings 1121 (1990) 650.
16. V.M.Astashynski, V.V.Efremov, E.A.Kostyukevich et al. Sov. J. Plasma Phys. (Engl. transl.) 17 (1991) 645.
17. S.I.Ananin, V.M.Astashynski, E.A.Kostyukevich et al. Plasma Physics Reports 24, N 11 (1998) 936.
18. G.I.Bakanovich. VII Sov. Conf. on Plasma Accelerators. Contr. Papers. Kharkov (1989) 179.
19. N.Konjevic. Proc. XIX Intern. Conference in Ionized Gases. Invited Papers. Belgrade. (1989) 382.
20. M.S.Dimitrievic, S.Sahal-Brechot. Bull. Obs. Astron. Belgrade. N 141 (1989) 57.
21. J.Puric. J. Appl. Spectoscopy 63 (1996) 816.
22. V.M.Astashynski, G.I.Bakanovich, N.A.Bukova et al. J. Appl. Spectroscopy 55 (1991) 331.

Acknowledgements

This work was supported in part by the Belarus Foundation of Basic Investigation, grant F98-336.

Journal of Research in Physics Vol.28, No. 3, 209-217 (1999)

Invited lecture

ON THE ELECTRON TEMPERATURE MEASUREMENTS IN A MEDIUM ELECTRON DENSITY PLASMAS

B.Blagojević, M.V.Popović and N.Konjević
Institute of Physics, P.O.Box 68, Belgrade, Yugoslavia

Abstract – This paper reports the results of the spectroscopic electron temperature (T_e) measurements in plasmas with electron densities ranging (0.3 - 1.4)·10^{17} cm^{-3}. The results of T_e measurements obtained from various spectroscopic methods are mutually compared and discussed in relation to the condition for partial local thermodynamic equilibrium (PLTE). For the cases when the application of the spectroscopic techniques for T_e measurements can not be justified on the bases of PLTE criterion, new method for determination of plasma electron temperature is proposed and tested.

Measurements of plasma parameters, electron temperature and electron density were performed in a low pressure pulsed arc in helium and argon with small admixture of nitrogen or oxygen whose ions were used as thermometric species. The electron densities were determined from the width of the He II P_α 468.6 nm line.

1. INTRODUCTION

The plasma electron temperature T_e is one of the most important parameters used for plasma modeling, in opacity calculations, plasma line broadening studies etc. The most popular nonperturbative spectroscopic techniques for T_e determination involve absolute and/or relative line intensity measurements. The plasma electron temperature determined in this way is sometimes referred as an excitation temperature. If one excludes corona equilibrium from further considerations, the common for all line-intensity spectroscopic techniques is requirement of thermal equilibrium i.e. the Boltzmann distribution of the population of energy levels involved in the procedure of T_e measurements. Since most of laboratory plasmas are not in complete thermodynamic equilibrium the Boltzmann distribution of energy levels population is achieved only above certain energy level whose principal quantum number depends upon electron density, spectroscopic charge number Z and the electron temperature, see e.g. Griem, 1964; 1997; Stokes, 1971. Here, we exclude from further considerations the influence of strong gradients and fast time changing plasmas, see Griem, 1964; 1997.

In many cases when T_e measurements have to be performed it is difficult to select spectral lines in the accessible spectral region, which originate from the energy levels populated in accordance with the Boltzmann distribution. In addition, for these lines reliable atomic data should be available. All these requirements frequently limit the applications of spectroscopic methods fur T_e measurements.

In this paper the method for plasma electron temperature measurement using spectral lines originating from the energy levels not fulfilling PLTE criterion is described. This method is applied and tested for temperature measurements in a plasma of a low pressure pulsed arc in helium.

2. DESCRIPTION OF THE METHOD

The validity criteria for PLTE and consequently determination of the conditions for application spectroscopic methods for T_e measurements are extensively discussed by Griem, 1964; 1997 and Drawin, 1975. Simple formula (Griem, 1964) derived for the steady state plasma (applicable also to slow time varying plasmas) may be used to estimate the importance of emitter characteristics for estimation of PLTE criterion

$$N_e \geq 7\times10^{18}\frac{Z^6}{n^{17/2}}\sqrt{\frac{kT_e}{E_H}} \qquad (1)$$

where N_e is plasma electron density in cm^{-3} units, Z - spectroscopic ion charge, n - principal quantum number, T_e plasma electron temperature and E_H – hydrogen ionization energy. Although the fulfillment of above PLTE criterion is essential for the application of spectroscopic techniques and this was discussed in many plasma spectroscopy textbooks, see e.g. Griem, 1964; 1997; Drawin, 1975; Lochte-Holtgreven, 1968, some authors measure T_e assuming but not proving fulfillment of PLTE criterion.

Whenever spectral lines of consecutive stages of ionization of a single element in plasma spectrum appear several spectroscopic methods may be used to determine T_e. Apart from the Boltzmann plot of relative line intensities for each ionization stage, the lines of two consecutive stages of ionization may be used for T_e measurements also. To apply this method one has to measure plasma electron density and the ionization equilibrium is required. For more details see Griem, 1964; 1997.

In the cases when, according to PLTE criterion, Eq. (1), none of the discussed spectroscopic techniques may be applied, we propose method which may be used for T_e determination from the results of standard spectroscopic methods applied to non-PLTE conditions. The proposed method requires at least two T_e measurements from the spectral lines belonging to two consecutive ionization stages of the same element. Since PLTE criterion, Eq. (1) is not fulfilled measured electron temperatures are erroneous. The difference from the correct T_e is related to the deviation from the criterion expressed by Eq. (1). So in this case incorrect T_e values can be used in an extrapolation procedure to derive correct (or true) plasma T_e^c using linear fit through ($\ln(N_e^c/N_e)$, $\ln T_e$) points or exponential fit through ($\ln(N_e^c/N_e)$, T_e) points where N_e^c is calculated from Eq.(1). Thus the extrapolated value T_e^c is obtained for $\ln(N_e^c/N_e)=0$. Each N_e^c comes out from the condition of the fulfillment of PLTE criterion. Eq. (1), for appropriate T_e, N_e, Z and n. Therefore the proposed procedure for T_e^c determination requires independent N_e measurements. An illustration of the described method for T_e^c determination is presented in Fig. 1.

Furthermore the whole procedure may be iterated by using $T_e^{c,1}$ obtained in the first step into the system of equations (1), to calculate new N_e^c values which are further used to evaluate new set of ($\ln(N_e^c/N_e)$, $\ln T_e$) data points. The extrapolation of this new set of points gives $T_e^{c,2}$ value and so on. The iterations can be repeated until required precision of the iterative method is achieved. In our case the temperatures T_e^c obtained from the first and the last iterations differ no more than 3%.

Here, we draw attention to an important assumption made by applying spectroscopic methods for non-LTE conditions. Namely only Boltzmann distribution of energy levels population gives straight line of the Boltzmann plot. Numerous experimental measurements performed within this experiment showed for non-LTE conditions that Boltzmann plots may be, within experimental uncertainty, approximated with the straight line. So we assumed that,

if energy levels are overpopulated or underpopulated in comparison with LTE distribution, they still have an analytical form of the Boltzmann distribution. This assumption will be further discussed in relation to the experimental results.

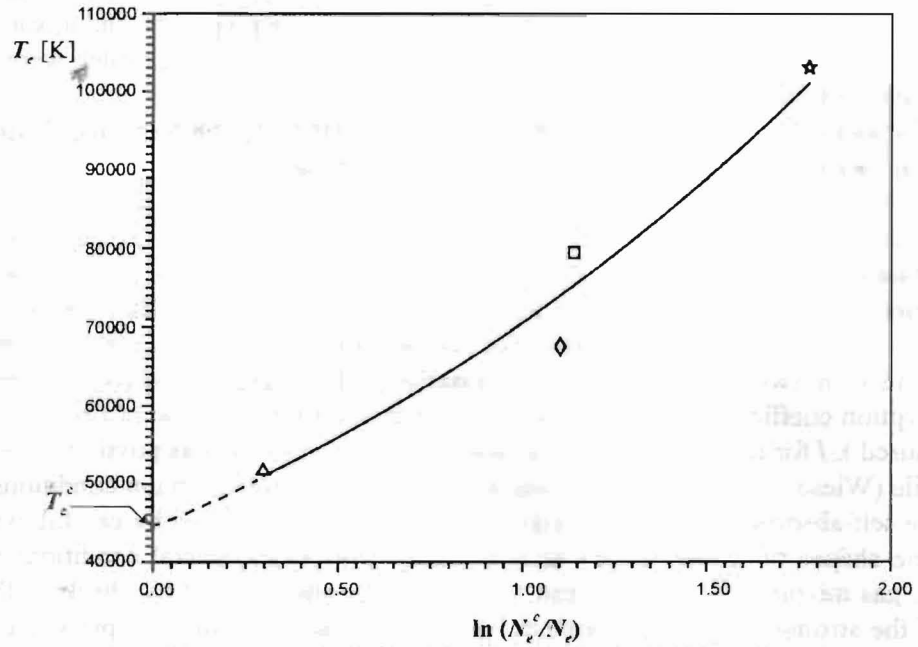

Figure 1. Sample of the extrapolation fit through ($\ln(N_e^c/N_e)$, T_e) points gives T_e^c=44360 K for $\ln(N_e^c/N_e)$=0. Four ($\ln(N_e^c/N_e)$, T_e) points on this plot are calculated from relative intensities of O III lines (Δ), O III and O IV lines (◊), O IV lines (□), O IV and O V lines (☆), radiated from helium-oxygen plasma for t=6 μs, see Figure 4.

3. EXPERIMENT

The light source was a low pressure pulsed arc with quartz discharge tube 10 mm internal diameter. The distance between aluminum electrodes was 161 mm and 3 mm diameter holes were located at the center of both electrodes to allow end-on plasma observations. The central part around the pulsed arc axis was imaged 1 : 1 onto the entrance slit of the 1 m monochromator by means of the concave 1 m focal length, focusing mirror. A 30 mm diaphragm placed in front of the focusing mirror ensures that light comes from the narrow cone about the arc axis, see Fig.2. The monochromator with inverse linear dispersion 0.833 nm/mm in the first order of the diffraction grating was equipped with the photomultiplier tube (PMT) and a stepping motor. Signals from the PMT were led to a digital storage oscilloscope, which was triggered by the voltage pulse from the Rogowski coil induced by the current pulse through the discharge tube. The experiments are performed in He-N_2, He-O_2, Ar-N_2 and Ar-O_2 gas mixtures. The discharge in the experiments was driven by a 15.2 μF low inductance capacitor charged to 3 kV (14.5 kA peak current) and fired by an ignitron. Greatest care was taken to find the optimum conditions with the negligible line self-absorption. The ratios N_2 : He = N_2 : Ar = 2 : 98 and O_2 : He = O_2 : Ar = 1 99 were determined after a number of experiments in which N_2 and O_2 were diluted gradually until strong spectral line intensities of N and O ions were found proportional to the concentration of N_2 and O_2 in the gas mixture. During the spectral line recording continuous flow of gas mixture was maintained at a pressure of about 3 Torr. The stepping motor and

oscilloscope were controlled by a personal computer, which was also used for data acquisition. Recordings of spectral line shapes were performed shot by shot. At each wavelength position of the monochromator the digital oscilloscope recorded time evolution and decay of the plasma radiation. Eight such signals were averaged at each wavelength. To construct the line profiles these averaged signals at different wavelengths and at various times of the plasma existence were used. In all experiments spectral line profiles were recorded with the instrumental half widths of 0.0168 nm.

For electron density measurements width of the He II P_α 468.6 nm line (Büscher et al, 1996) was used. Our main concern in the electron-density measurements was a possible presence of self-absorption of the He II P_α line, which may distort the line profile. This would result in erroneous reading of the line width, which would introduce an error in the electron-density measurements. In order to determine the optical thickness of the investigated lines we have introduced in the discharge an additional movable electrode (Kobilarov et al, 1981). By placing the movable electrode (10 mm thick) at two different positions and by recording the line profiles from two plasma lengths, it is possible to determine $k_\lambda l$, where k_λ is the spectral line absorption coefficient and l is the plasma length along the direction of observation. Since the measured $k_\lambda l$ for the He II P_α line was always smaller than 1 it was possible to recover the line profile (Wiese, 1965). Great care was also taken to find the optimum conditions with the negligible self-absorption of the investigated lines. This was achieved by careful examination of the line shapes of N and O ions as a function of the experimental conditions (total gas pressure, gas mixture composition, and capacitor bank energy), and by checking the optical depth of the strongest lines by measuring the intensity ratios within multiplets, see Konjević and Wiese, 1976, and comparing them with theoretical predictions (Wiese et al, 1996).

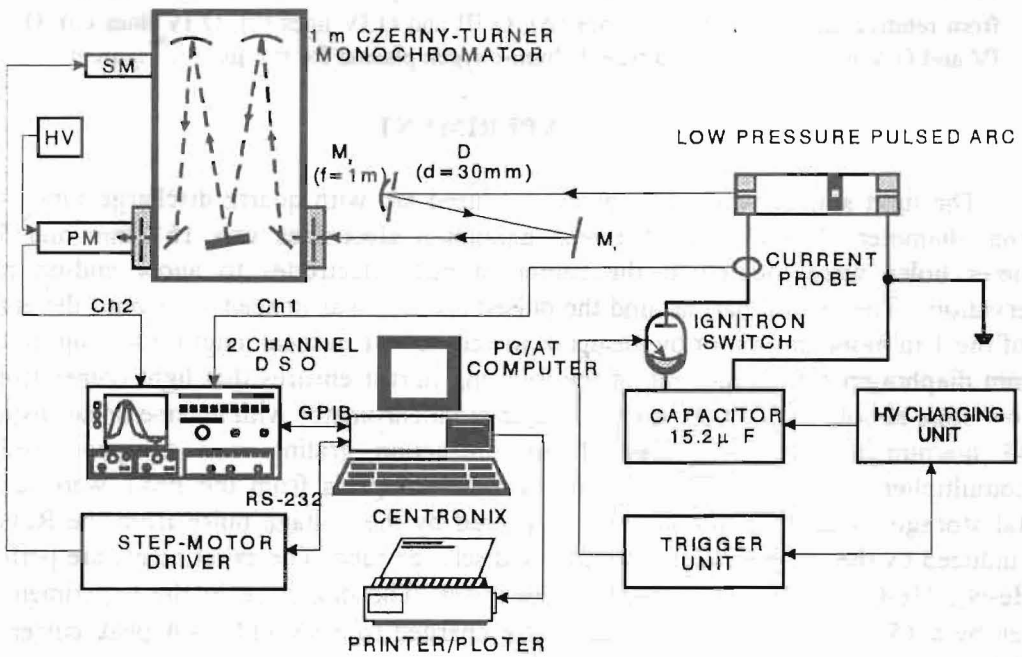

Figure 2. The experimental setup.

The axial electron temperatures were determined in He-N_2 mixture from the Boltzmann plots of the relative intensities of: N II 399.500, 463.054, 444.703, 480.329 nm; N III 409.736, 410.339, 463.413, 464.064 nm; N IV 347.872, 348.300, 374.754, 405.776 nm; also from the relative intensities of two lines: N II 463.054

and N III 409.736 nm; N III 409.736 and N IV 405.776 nm; N IV 405.776 and N V 460.374 nm.

The axial electron temperatures were determined in He-O_2 mixture from the Boltzmann plots of the relative intensities of: O III 375.470, 375.988, 370.727, 371.509 nm; O IV 306.343, 307.160, 340.123, 341.169 nm; also from the relative intensities of two lines: O III 375.988 and O IV 341.169 nm; O IV 341.169 and O V 278.699 nm.

Transition probabilities and other atomic data, needed for determination of plasma electron temperatures were taken from Wiese et al, 1996.

The spectral response of the photomultiplier-monochromator system was calibrated against a standard coiled-coil quartz iodine lamp.

4. RESULTS AND DISCUSSION

Helium-nitrogen plasma

As a consequence of relatively low plasma electron density in our experiment, only electron temperatures evaluated from N II lines were derived under condition described by expression (1). All other T_e measured from the lines of higher ionization stages of nitrogen were determined without PLTE criterion, Eq.(1) fulfilled so they are incorrect. The electron temperatures evaluated from the Boltzmann plot of N III lines, see Fig.3, are the closest to the correct value, T_e^c, because N_e is only about 50% smaller than the one estimated from Eq.(1). Other electron temperatures derived from the lines of higher nitrogen ions show larger deviation from T_e^c. This is in qualitative agreement with Z dependence of the Eq.(1). The results in Fig.3 show that the overestimation of the correct plasma electron temperatures is proportional to the deviation from the PLTE criterion. The dashed curve in Fig.3 represents T_e^c values calculated by the extrapolation method interpolated by qubic spline. There is good agreement between T_e^c values (dashed curve in Fig.3) and plasma electron temperatures derived from the Boltzmann plot of N II lines.

Helium-oxygen plasma

The helium-oxygen experiment was performed under same discharge conditions as the preceding one (see 3. Experiment). The results are presented in Fig.4. Unfortunately, PLTE criterion, Eq.(1), is not fulfilled for any observed transition of O III, O IV and O V used for temperature measurements. By applying the extrapolation method plasma electron temperature, T_e^c, was determined (see also example in Fig.1) and presented as a dashed curve in Fig.4. As one would expect for the same discharge conditions used in both experiments the part of T_e^c curve, which describes plasma electron temperature decay, see Fig.4, looks like an extension of T_e^c curve in helium-nitrogen mixture, see Fig.3.

From the comparison of T_e obtained using different ions of a single element as thermometric species, see Figs.1, 3, 4, it is interesting to notice that measured T_e from one ionization stage to another differs less than one would expect from the

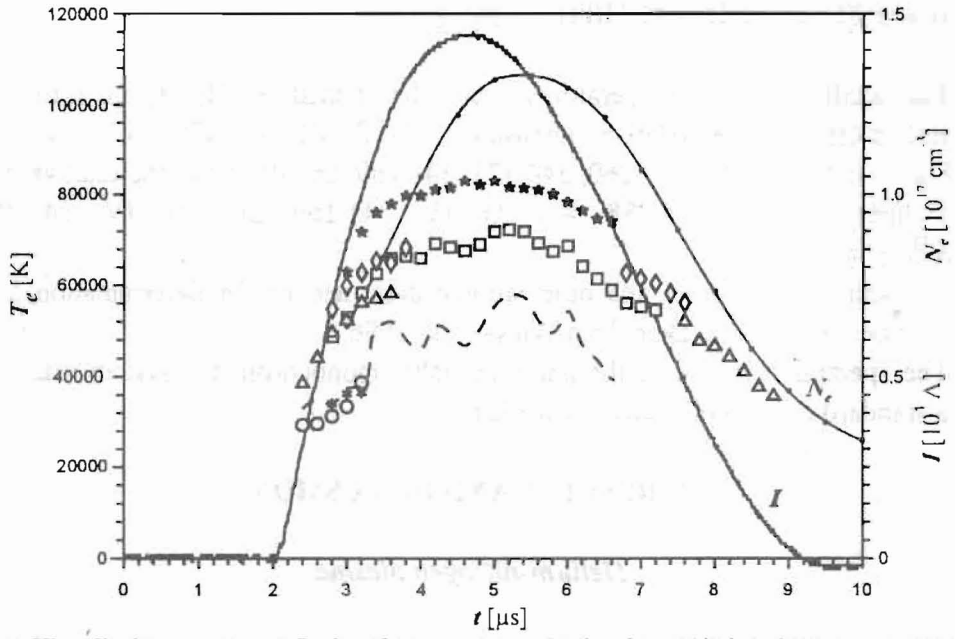

Figure 3. The discharge current I, the electron concentration N_e and the electron temperatures T_e measured from the relative intensities of nitrogen ion spectral lines in helium-nitrogen plasma experiment: N II lines (O), N II and N III (✻), N III lines (Δ), N III and N IV lines (◊), N IV lines (□), N IV and N V lines (☆). Dashed curve presents T_e^c values calculated by the extrapolation method and interpolated by qubic spline.

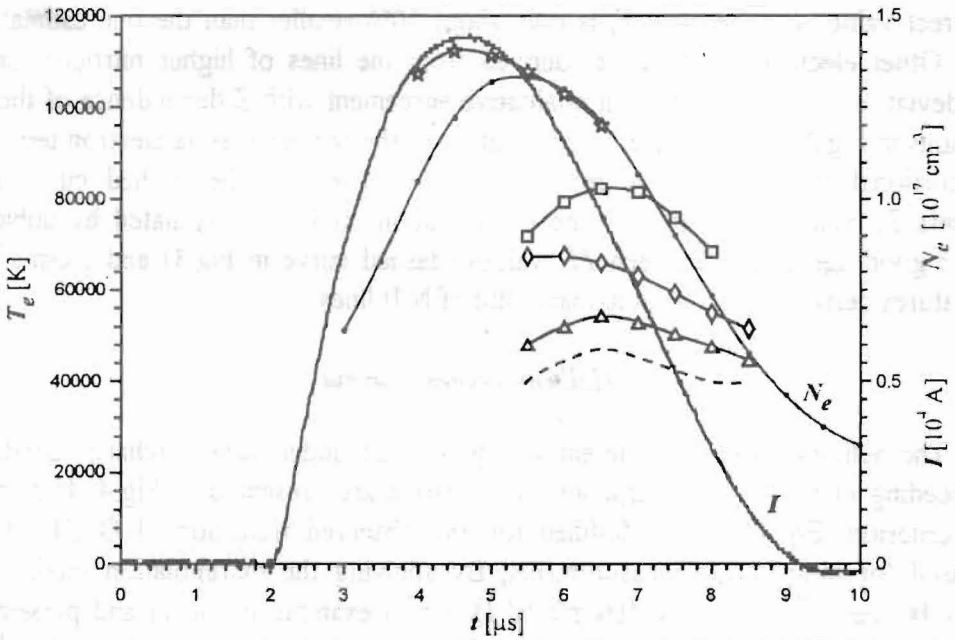

Figure 4. The discharge current I, the electron concentration N_e and the electron temperatures T_e measured from the relative intensities of oxygen ion spectral lines in helium-oxygen plasma experiment: O III lines (Δ), O III and O IV lines (◊), O IV lines (□), O IV and O V lines (☆). Dashed curve presents T_e^c values calculated by the extrapolation method and interpolated by qubic spline.

corresponding change of PLTE N_e evaluated from Eq.(1). Here one should mention that all lines taken for T_e measurements are from n = 3 (3s-3p and 3p-3d transitions). Another

interesting result is a good agreement (approximately within 10%) between temperatures obtained from the lines of two consecutive stages of ionization and from the Boltzmann plot of the lines from upper ionization stage. For both methods N_e^c values in Figs.1, 3, 4 are calculated from Eq.(1) using same Z and n. This result suggests that the criterion for application of two ionization stages method for T_e measurements should be relaxed.

Finally one can notice in both experiments, see Figs.1, 3, 4 that whenever PLTE criterion is not fulfilled measured plasma T_e is always higher than correct value. T_e^c. This may be explained by overpopulation of the energy levels involved in T_e measurements.

Argon-nitrogen and argon-oxygen plasmas

The argon-nitrogen and argon-oxygen experiments were performed under the same discharge conditions as the helium-nitrogen and helium-oxygen experiments respectively. Only difference is that helium is replaced by argon in gas mixtures. The results are presented in Figs.5 and 6. Relative intensities of singly and doubly ionized nitrogen and oxygen are detected only. Self-absorption of recorded nitrogen line shapes are detected in region 3-9 [μs] in the argon-nitrogen experiment (see Fig.5). In the argon-oxygen experiment, self-absorption of oxygen line shapes was present in region 7-8 [μs] (see Fig.6). Plasma electron temperatures, determined by using the methods of relative line intensities, obtained from self-absorbed line intensities are incorrect in above mentioned time regions. Transition from region of self-absorption to region without self-absorption is characterized by changing the T_e trend, see 9[μs] on Fig.5 and 8 [μs] on Fig.6. New method for determination of plasma electron temperature was not applied in these two experiments, because the T_e obtained by using methods of relative intensities which not fulfilled PLTE criterion are close to true T_e obtained from Boltzmann plots of N II (9-10 [μs]) and O II (8-10 [μs]) lines which satisfied PLTE criterion.

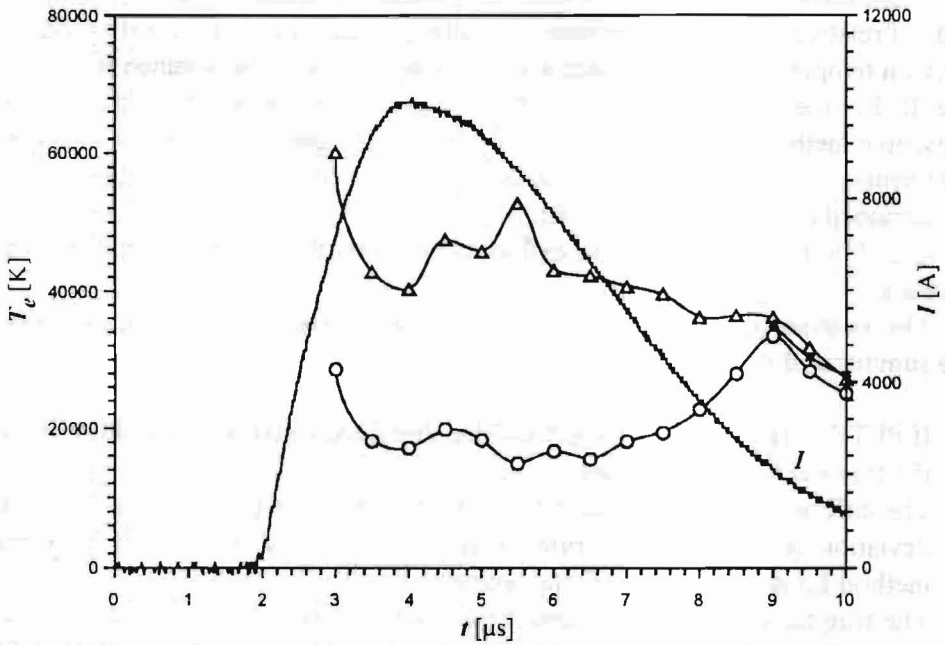

Figure 5. The discharge current I, the electron temperatures T_e measured from the relative intensities of nitrogen ion spectral lines in argon-nitrogen plasma experiment: N II lines (O), N II and N III (∗), N III lines (Δ).

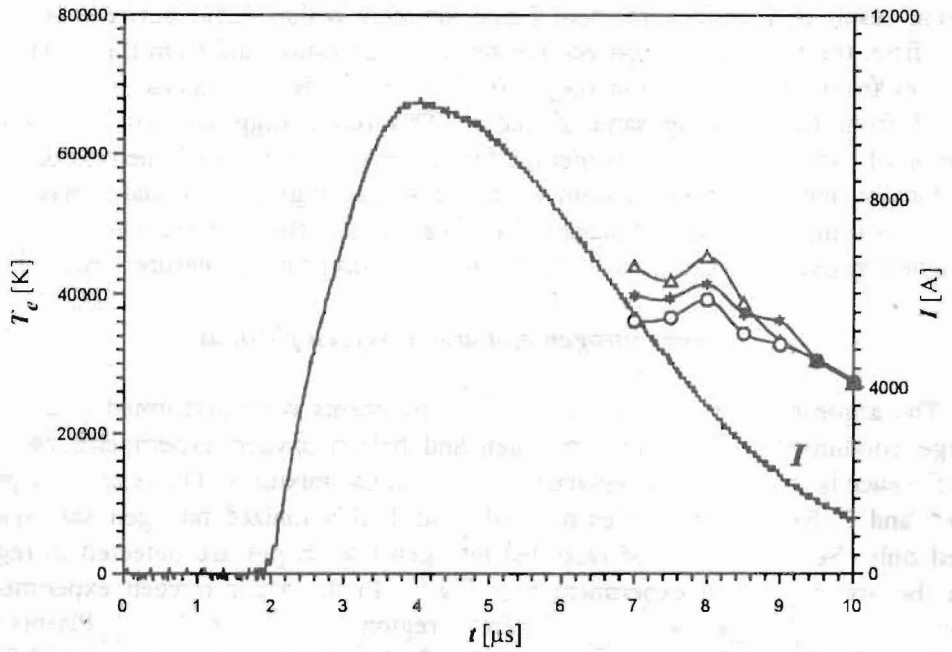

Figure 6. The discharge current I, the electron temperatures T_e measured from the relative intensities of nitrogen ion spectral lines in argon-oxygen plasma experiment: O II lines (O), O II and O III (*), O III lines (Δ).

5. SUMMARY

The medium electron density plasma generated in a low pressure pulsed arc in helium with admixtures of nitrogen and oxygen was used to demonstrate the possibility of proposed extrapolation method for plasma electron temperature T_e^c measurements. The spectroscopic methods of relative spectral line intensities of nitrogen and oxygen ions were used to measure the electron temperature T_e. The plasma electron density, N_e, is determined from the width of the He II P_α line. According to the PLTE criterion expressed by Eq.(1) none of the spectroscopic methods can be used with the lines of nitrogen or oxygen ions for temperature measurements). The only exception was the Boltzmann plot technique applied to N II lines. It was demonstrated however, that temperatures obtained without fulfillment of the PLTE criterion, Eq.(1) may be used with an extrapolation method to determine true plasma electron temperature.

The analysis of the results of systematic plasma electron temperature measurements may be summarized as follows:

I. If PLTE criterion, Eq.(1), is not fulfilled measured electron temperature is higher than the true electron temperature.

II. The difference between measured and true electron temperature is proportional to the deviation from PLTE criterion. This proportionality is used in an extrapolation method for determination of true temperature.

III. The true temperature determined from the PLTE Boltzmann plot of spectral lines of ion with the charge Z is lower than the temperature of Z+1 ion derived from non-PLTE Boltzmann plot for about 20%. If the method of two subsequent stages of ionization is used difference between true and measured temperatures applied to the

same pair of ions is smaller for about 10%. These two factors may be applied to any other consecutive ionization stages to predict approximate overestimation of the true temperature. It is necessary only to estimate the ionization stage with fulfilled PLTE criterion for unchanged principal quantum number n.

At the end one should mention that the preceding conclusions are derived from the data obtained in a limited range of electron densities and temperatures and therefore any extrapolation outside of this range of plasma parameters should be done with great precautions. Similar experiments at different plasma conditions would be very desirable.

ACKNOWLEDGMENTS

This research is supported by the Ministry of Science and Technology of the Republic of Serbia.

REFERENCES

Griem H.R.: 1964, *Plasma Spectroscopy*, McGraw-Hill, New York.
Griem H.R.: 1997, *Principles of Plasma Spectroscopy*, Cambridge University Press.
Stokes U.S.: 1971, in *Reactions under Plasma Conditions*,
Vol.II, Ed.M.Venugopalan, Wiley-Interscience, New York.
Drawin H.W.: 1975, in *Progress in Plasmas and Gas Electronics*,
Eds. Rompe R., Steenbeck M., Vol.I, Akademie Verlag, Berlin.
Lochte-Holtgreven W.: 1968, Editor, *Plasma Diagnostics*,
North-Holland Publishing Co., Amsterdam.
Büscher S., Glenzer S., Wrubel Th. and Kunze H.-J.: 1996, J.Phys.B **29**, 4107.
Kobilarov R., Konjević N. and Popović M.V.: 1981, Phys.Rev.A **40**, 3871.
Wiese W.L.:1965, in *Plasma Diagnostic Techniques*,
edited by Huddleston R.M. and Leonard S.L., Academic, New York.
Konjević N., Wiese W.L.: 1976, J.Phys.Chem.Ref.Data **5**, 259.
Wiese W.L., Fuhr J.R. and Deters T.M.: 1996, *Atomic Transition Probabilities of Carbon, Nitrogen and Oxygen*, J.Phys.Chem.Ref.Data, Monograph No.7.

Journal of Research in Physics Vol.28, No. 3, 219-219 (1999)

Abstract of Invited lecture

SPECTROSCOPIC INVESTIGATIONS DURING SOLAR ECLIPSES

ISTVAN VINCE

Astronomical Observatory, 11000 Belgrade, Volgina 7, Yugoslavia

Total solar eclipse occurs when the Moon passes in between the Sun and the observer on the Earth and the angular diameter of the Moon is slightly larger than that of the Sun, so the solar disc (the photosphere) can be covered by it. This enables us to separate out the bright photosphere, so the total solar eclipses provide unique opportunities for study of the much less bright outer atmospheric layers of the Sun, the chromosphere and corona.

The chromosphere appears just after the beginning (the second contact) and before the end (the third contact) of totality for a few seconds. During these several seconds the bright spectral lines flash out through the whole spectrum. According to Young this sudden appearance of emission spectrum is called the flash spectrum. It consists of a large number of emission lines and a continuum. By taking successive spectra of the chromosphere, as the Moon moves across it, we can observe the changes of spectral line profiles with high spatial resolution. From these observations extensive studies of the vertical structure of chromosphere can be made. There are two methods of observation of flash spectrum at the total solar eclipse. One is the slitless and the other one is the slit spectrograph method. The type of spectrography depends on the problem that has to be solved. For instance if we intend to measure the whole energy of the chromospheric line we have to use the slitless method. This method allows us to make observations with very high height resolution (about 100 km). On the other hand, this method is not suitable for the spectral line profile measurements, because the line profile will be affected by the extension of the chromosphere and by the atmospheric turbulence. Because of that the slit method has to be introduced for line profile observations. The disadvantage of slit method is the difficulty of determining the position of the slit in the chromosphere. Unfortunately, both methods have a disadvantage that observations integrate the radiation over a long path which includes various parts with different properties that are very difficult to disentangle. Although the chromospheric spectrum has been observed at many eclipses from 1870. large gaps still exist in our knowledge of the spectrum. For instance, the transition of the photospheric into chromospheric spectra and the behaviour of line profiles are still of importance in attempts to find the energy sources that produce the temperature rise not only in the chromosphere but in the corona, too. Spectra of active regions observed at the limb at an eclipse are also of great interest.

The solar corona is a very hot, low dense and optically thin gas. The radiation of the solar corona consists of three components: the K, F and E corona. The K corona is the photospheric light scattered by electrons, but due to high velocity and the Doppler broadening the spectral lines of the photosphere are washing out. The F corona, which is created by scattering of photospheric light on dust particles between the Earth and Sun, shows the photospheric absorption spectral lines. As these particles are slow moving, the photospheric lines are not washed out. The E corona is combined light of different emission lines. Some of these lines have the intensity which exceeds their background continuum many times (often by a factor 100). Their widths are usually about 0.1 nm. These emission lines in the visible spectrum derive from forbidden transitions of highly ionized atoms like FeX, FeXIII or FeXIV and they are very useful for study of the temperature and velocity structure of the corona that is of crucial importance for understanding the coronal heating mechanism.

Journal of Research in Physics Vol.28, No. 3, 221-221 (1999)

Abstract of Invited lecture

QUASIMOLECULAR BANDS IN OPTICAL SPECTRA OF WEAKLY IONIZED PLASMAS

Lj. M. IGNjATOVIĆ[1], A. A. MIHAJLOV[1,2] AND M. S. DIMITRIJEVIĆ[1]
1) Institute of Physics, Pregrevica 118, 11080 Beograd, Yugoslavia
2) Astronomical Observatory, Volgina 7, 11050 Beograd, Yugoslavia

Even though the ion-atom radiative charge exchange and photoassociative processes has known for a long time, their investigation, as a sources of continuous electromagnetic spectra of low temperature plasmas, has been begun recently The aim of this work is that underlines necessity of taking into account above mentioned radiative processes during the analysis of molecular bands or atomic spectral lines.

The significant progress in this area has been reached by very detailed investigations of the influence of the slow symmetrical radiative collisions

$$A^+ + A \leftrightarrow \hbar\omega + A + A^+, \tag{1.a}$$
$$A^+ + A \leftrightarrow \hbar\omega + A_2^+, \tag{1.b}$$

at the radiative characteristics of weakly ionized plasmas. Their importance were shown convincingly in the cases *A=H, He, Li* and *Na* for different types of both astrophysical and laboratorical plasmas, which could be treated as a chemically homogenous plasmas (Mihajlov et al 1993, Mihajlov et al 1994, Ermolaev et al 1995). However, in the chemically inhomogenous, weakly ionized plasmas, we have to take into account the non-symmetrical ion-atom processes. The following processes will be considered:

$$A^+ + B \leftrightarrow \hbar\omega + A + B^+, \tag{2.a}$$
$$A^+ + B \leftrightarrow \hbar\omega + AB^+, \tag{2.b}$$
$$(AB^+)^* \leftrightarrow \hbar\omega + A + B^+. \tag{2.c}$$

In dependence on varying of ionization potentials I_A and I_B, the character of the considered ion-atom systems changes in the wide borders: from the almost symmetrical systems, which are composed of the atom and ion of different isotopes of the same element, to the quite non-symmetrical systems. Accordingly to that, the features of ion-atom systems are change very strong, as well as the spectra of photons emmited/absorbed in the course of reactions (2). Because of that, in the frame of this work we shall consider two characteristical cases:

- the collisional system is weakly non-symmetrical; representative for this case will be the system with *A=Li* and *B=Na*,
- the collisional system is extremely non-symmetrical; representative for this case will be the system with *A=H* and *B=Li*.

References

Ermolaev A.M., Mihajlov A.A., Ignjatović Lj.M. and Dimitrijević M.S.: 1995, *J. Phys. D: Appl. Phys.*, **28**, 1047

Mihajlov A.A., Dimitrijević M.S. and Ignjatović Lj.M.:1993, *Astronomy and Astrophys.*, **276**, 187

Mihajlov A.A., Dimitrijević M.S. and Ignjatović Lj.M.:1994, *Astronomy and Astrophys.*, **287**, 1026

Journal of Research in Physics Vol.28, No. 3, 223-226 (1999)

EXPERIMENTAL STUDY OF LS COUPLING ALONG LITHIUM ISOELECTRONIC SEQUENCE

B.Blagojević, M.V.Popović and N.Konjević

Institute of Physics, 11080 Belgrade, P.O.Box 68, Yugoslavia

1. INTRODUCTION

LS or Russell-Saunders coupling is dominant for many transitions in the spectra of light elements. This is the case spin-orbit interaction in atomic Hamiltonian is more important than the electrostatic separation between levels of the same principal quantum number n. Since electrostatic separation increases as Z while the spin-orbit interaction grows as $z^4\alpha^2$ where z is charge number of atomic nucleus and α is fine structure constant, the LS-coupling scheme becomes inappropriate at a certain point. Systematic failure of the LS-coupling approximation is expected from lower to higher elements of an isoelectronic sequence for nl-nl' transitions. The aim of this paper is to test predictions of LS-coupling theory for the transitions within $3s^2S$-$3p^2P^0$ multiplets along lithium isoelectronic sequence. In addition we tested whether plasma electron density influences spontaneous emission coefficients as suggested by Chung et al, 1988.

2. THEORY

For LS coupling theory see e.g. (Cowan, 1981). Theoretical values calculated from wave function obtained using Coulomb approximation are compared with our measured intensity ratios. For the case of pure LS coupling the relative line strength for a transition between levels J_1 and J_2 is proportional to the factor (Cowan, 1981, Appendix I)

$$D^2_{line} = (2J_1+1)(2J_2+1)\begin{Bmatrix} L_1 & S_1 & J_1 \\ J_1 & 1 & L_2 \end{Bmatrix}^2 \qquad (1)$$

Values of the 6j symbol are given in Appendix D of (Cowan, 1981). The intensity ratio of two multiplet components is represented by (Cowan, 1981)

$$\frac{I}{I'} = \left(\frac{\lambda'}{\lambda}\right)^4 \left(\frac{D_{line}}{D'_{line}}\right)^2 \exp\left(\frac{E'-E}{kT_e}\right) \qquad (2)$$

where I, λ and I', λ' are the total intensities and wavelengths of the two components, and E and E' are the energies of the upper levels of the two components, respectively.

3. EXPERIMENT

The light source was a low pressure pulsed arc with quartz discharge tube 10 mm internal diameter. The distance between aluminum electrodes was 16.2 cm and 3 mm diameter holes were located at the center of both electrodes to allow end-on plasma observations to be made. The central part around the pulsed arc axis was imaged 1 : 1 onto the entrance slit of the 1 m monochromator by means of the concave 1 m focal length, focusing mirror. A 30 mm diaphragm placed in front of the focusing mirror ensures that light comes from the narrow cone about the arc axis. The monochromator with inverse linear dispersion 0.833 nm/mm in the first order of the diffraction grating was equipped with the photomultiplier tube (PMT) and a stepping motor. Signals from the PMT were led to a digital storage oscilloscope, which was triggered by the voltage pulse from the Rogowski coil induced by the current pulse through the discharge tube. The discharge was driven by a 15.2 μF low inductance capacitor charged to 3.0 kV and fired by an ignitron. Greatest care was taken to find the optimum conditions with the least line self-absorption. It was found that the percentage of each studied element in the appropriate gas mixture was of crucial importance for the elimination of self-absorption. During the spectral line recording continuous flow of gas mixtures was maintained at a pressure of about 400 Pa.

4. PLASMA DIAGNOSTICS

For the electron-density measurements we use the width of He II P_α 468.6 nm line. The full width at half-maximum $\Delta\lambda_{FWHM}$ of this line is related to the electron density N_e using the following relationship (Büscher et al, 1996)

$$N_e(cm^{-3}) = 2.238 * 10^{16} \Delta\lambda^{1.204}{}_{FWHM} \qquad (3)$$

where $\Delta\lambda_{FWHM}$ is in 0.1 nm units. This equation is based on the fitting of the experimental data, and in fact closely agrees with calculations by Griem and Shen, 1961. Our main concern in electron-density measurements is a possible presence of self-absorption of the 468.6 nm line, which may distort the line profile. This would result in erroneous reading of the line half width, which, after the use of Eq.(3), introduces an error in electron-density

measurements. There are several experimental methods which can be used for self-absorption check (Konjević and Wiese, 1976) but unfortunately, none of them is convenient for the He II 468.6 nm line or for our long, pulsed plasma source. Recently, in order to determine the optical thickness of the investigated line Kobilarov et al, 1981, have introduced in the discharge an additional movable electrode. By positioning the movable electrode at two different positions and by recording the line profiles from two plasma lengths it is possible to determine $k_\lambda l$ where k_λ is the spectral line absorption coefficient and l is the plasma length along the direction of observation. If $k_\lambda l$ is not large ($k_\lambda l < 1$ (Wiese, 1965)) it is possible to recover the line profile (Fig.2 of Kobilarov et al, 1981) for the optically thin case. The same method is used here for the He II 468.6 nm line self absorption testing. For this purpose an additional aluminum electrode (10 mm thick) is located inside the discharge tube and the profiles of 468.6 nm line are recorded with two plasma lengths. Since the measured $k_\lambda l$ was smaller than 0.74 it was possible to recover the line profile for the optically thin case.

5. EXPERIMENTAL RESULTS AND DISCUSSION

The theoretical intensity ratios R_{th} of two most intensive ion spectral lines within $3s^2S\text{-}3p^2P^0$ multiplets of B III, C IV, N V and O VI ions of lithium isoelectronic sequence are given in Table 1. R_{th} are calculated from wave functions obtained in Coulomb approximation. The experimental intensity ratios R_m of two most intensive ion spectral lines within $3s^2S\text{-}3p^2P^0$ multiplets of B III, C IV, N V and O VI ions are compared with appropriate theoretical intensity ratios in Table 2. The R_m values are averaged over set of measurements which corresponding different electron concentrations N_e in plasma.

Table 1.

Transition	R_{th}
B III $3s^2S\text{-}3p^2P^0$	2.00
C IV $3s^2S\text{-}3p^2P^0$	2.01
N V $3s^2S\text{-}3p^2P^0$	2.03
O VI $3s^2S\text{-}3p^2P^0$	2.05

The agreement between averaged $<R_m>$ and theoretical R_{th} ratios along lithium isoelectronic sequence in Table 2 is within ±6% which is under estimated relative experimental error of ±10%. Table 2 is good indication that theory [8] predicts well spectral line intensity ratios

within multiplets in case of C IV, N V and O VI emitters. Within the investigated plasma electron density range spontaneous emission coefficients remain constant what is in agreement with results and discussion in Refs.[9-10].

Table 2.

Ion	N_e [10^{17}cm^{-3}]	$\left(\frac{R_m}{R_{th}}\right)_{3s-3p}$
B III	0.28	0.99
	0.58	0.99
		<0.99>
C IV	0.58	0.93
	0.76	0.96
	0.86	0.94
		<0.94>
N V	0.86	0.93
	0.99	1.02
	1.13	1.06
	1.21	1.02
	1.33	0.92
		<0.99>
O VI	1.09	1.01
	1.38	1.00
	1.41	0.96
	1.57	0.94
	1.68	0.97
		<0.98>

REFERENCES

Chung Y., Lemaire P. and Sucewer S.:1988, Phys.Rev.Lett. **60**, 1122.

Cowan R.D.:1981, *The Theory of Atomic Structure and Spectra*, University of California Press, Berkeley.

Büscher S., Glenzer S., Wrubel Th. and Kunze H.-J.:1996, J.Phys.B, **29**, 4107.

Griem H.R. and Shen K.Y.: 1961, Phys.Rev. **122**, 1490.

Konjević N. and Wiese W.L.:1976, J.Phys. Chem. Ref. Data **5**, 259.

Kobilarov R., Konjević N. and Popović M.V.:1981, Phys.Rev.A **40**, 3871.

Wiese W.L.:1965, in *Plasma Diagnostic Techniques*, eds. by Huddleston R.M. and Leonard S.L., Academic, New York.

Wiese W.L., Fuhr J.R. and Deters T.M.:1996, *Atomic Transition Probabilities of Carbon, Nitrogen and Oxygen*, J.Phys.Chem.Ref.Data Monograph No.7.

Griem H.R., Huang Y.W., Wang J.-S. and Moreno J.C.:1991, Phys.Fluids B **3** 2430.

Griem H.R.:1991, Phys.Rev.Lett. **66**, 521.

Journal of Research in Physics Vol.28, No. 3, 227-230 (1999)

ON THE STARK WIDTH REGULARITIES IN THE DOUBLY IONIZED OXYGEN SPECTRUM

S.Djeniže
Faculty of Physics, University of Belgrade, P.O.B.368, Serbia, Yugoslavia

1. INTRODUCTION

Extensive studies of the star atmospheres (and other cosmic emitters) on the basis of the shape and position of spectral lines ,emitted by atomic or ionic emitters, have enhanced the effort to develop a fast and reliable method to find the Stark widths of spectral lines. If the Stark broadening is the principal pressure broadening mechanism in plasmas (with 10^{22} -10^{27} m^{-3} electron density), on the basis of Stark HWHM (half-width at half intensity maximum,w) values it is possible to obtain the other basic plasma parameters e.g. electron temperature (T) and density (N),essential in the modeling of the stellar atmospheres or other laboratorical plasmas (Dimitrijević 1989; Lesage 1994).The simplest way to quick and reliable estimation of the values of w is to use an established regularities for a given type of quantum transition in a particular ionic spectrum.The main objective of this study is to establish regularities of Stark HWHM values using existing experimental results and,on that basis,to predict the w values for spectral lines of the doubly ionized oxygen atoms (O III),that have been not measured or calculated before.Trends of the Stark HWHM values within four types of transitions (3s-3p, $2p^2$ 3s-$2p^2$ 3p, 3p-3d , $2p^2$ 3p-$2p^2$ 3d) have been established in doubly ionized oxygen spectrum. On that basis Stark width values for 25 intensitive spectral lines, not measured or calculated before, have been predicted. These can be applied in the plasma spectroscopy.

2. REGULARITIES

The simplest way to estimate the value of a Stark HWHM (w) is to use established regularities of w along the same type of quantum transition in the ionic spectra (Djeniže et al.1989, and references therein). Namely,on the basis of the existing experimental results of a Stark HWHM of the spectral lines that belong to the 4p-4d transition in the Ar II spectrum it was found that simple analytical relationship exist between w and corresponding upper-level ionization potential (I) of a particular spectral line for the same type of transitions. This relationship, normalized to a N= 10^{23} m^{-3} electron density, is of a form:

$$w(\mathrm{rad/s}) = a\, T^{-1/2}\, I^{-b}. \qquad (1)$$

The upper-level ionization potential I (in eV) specifies the emitting ion,while the electron temperature T (in K) characterizes the assembly.The coefficients a and b are independent of I and T.Successful application of Eq.(1) (including the all existing experimental w data) in the cases of nine singly ionized spectra is presented by Djeniže et al.(1999).Inclusion the all existing experimental Stark HWHM data for O III spectral lines in the Eq.(1), in the cases of the investigated transitions, leads to the coefficients a and b which are presented in Fig.1. The found Stark HWHM trends along various type of the transition are graphically presented in the Fig.1.The error bars of 15%,in the Fig.1, shows the magnitude of the scatter of the experimental data of the reduced Stark HWHM ($wT^{1/2}$) values.Stark width

values,predicted on the basis of the Eq.(1),at T= 40 000 K electron temperature (as example) and $N=10^{23}$ m^{-3} electron density,are presented in Tab.1. The necessary atomic data are taken from Wiese et al.(1966).

Transition	Multip.	lλ(nm)	2w(nm)	Acc(%)
$2p^2\ 3s - 2p^2\ 3p$	$^5P - {}^5D^0$ (21)	370.34	0.0182	12
	$^5P - {}^5S^0$ (22UV)	268.61	0.0126	12
		267.46	0.0125	12
		266.57	0.0124	12
	$^3P - {}^3P^0$ (23)	407.39	0.0279	12
	$^3P - {}^3P^0$ (24)	355.69	0.0237	12
3p - 3d	$^3S - {}^3P^0$ (12)	313.29	0.0119	22
		312.17	0.0118	22
	$^3P - {}^3D^0$ (14)	370.72	0.0154	22
	$^3P - {}^3P^0$ (15)	344.41	0.0144	22
	$^1D - {}^1D^0$ (16)	550.01	0.0311	22
	$^1D - {}^1P^0$ (18)	381.68	0.0199	22
$2p^2\ 3p - 2p^2\ 3d$	$^3S - {}^3P$ (23 UV)	268.75	0.0124	18
	$^5D^0 - {}^5F$ (25)	345.51	0.0165	18
		345.09	0.0164	18
		344.81	0.0163	18
	$^5D^0 - {}^5D$ (26)	308.36	0.0149	18
	$^5P^0 - {}^5D$ (27)	338.49	0.0180	18
		338.27	0.0179	18
	$^3D^0 - {}^3F$ (30)	372.88	0.0250	18
		372.85	0.0248	18
		372.97	0.0248	18
	$^5S^0 - {}^5P$ (33)	446.16	0.0315	18
	$^3P^0 - {}^3D$ (35)	363.87	0.0286	18
		364.68	0.0287	18

Tab.1 Predicted Stark FWHM (2w) values at T=40 000 K electron temperature and $N=10^{23}$ m^{-3} electron density with theire estimated accuracies.

3. RESULTS

3s - 3p transition

Ten spectral lines from six multiplets (parenthesis on the Fig.1) in the 3s-3p transition have been investigated in four experiments (Platiša et al.1975; Purić et al.1988; Djeniže et al.1996; Blagojević et al.1998).Measured Stark HWHM values satisfy our Eq.(1).

$2p^2\ 3s - 2p^2\ 3p$ transition

Three spectral lines from three multiplets in the $2p^2 3s - 2p^2 3p$ transition have been investigated in only one experiment (Purić et al.1988).Measured Stark HWHM values satisfy our Eq.(1).Predicted Stark width data for six spectral lines,not measured or calculated before (Lesage & Fuhr 1998), are presented in Tab.1.

3p - 3d transition

Ten spectral lines from six multiplets in the 3p - 3d transition have been investigated in two experiments (Platiša et al.1975; Purić et al.1988). Measured Stark HWHM values satisfy our Eq.(1).Predicted Stark width data for six spectral lines,not measured or calculated before,are presented in Tab.1.

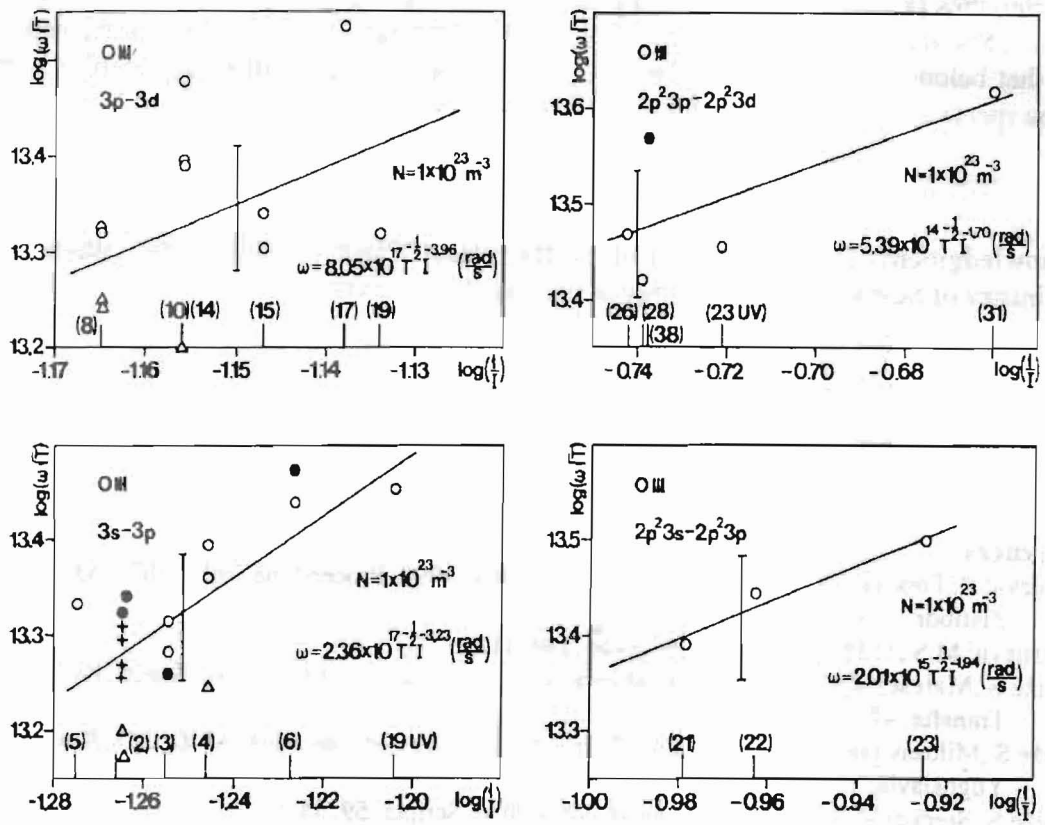

Fig.1

Reduced Stark HWHM ($wT^{1/2}$) versus inverse value of the upper-level ionization potential for various transitions. Δ,Platiša et al.(1975);o,Purić et al.(1988); •,Djeniže et al.(1996) and +,Blagojević et al.(1998).

$2p^2\ 3p - 2p^2\ 3d$ transition

Five spectral lines from five multiplets in the $2p^2\ 3p - 2p^2\ 3d$ transition have been investigated in two experiments (Purić et al.1988; Djeniže et al.1996). Measured Stark HWHM values satisfy our Eq.(1). Predicted Stark width data for thirteen spectral lines,not measured or calculated before,are presented in Tab.1.

4. CONCLUSION

On the basis of existing experimental data, trends of Stark HWHM values for spectral lines from doubly ionized O III spectrum have been established in four types of transitions. They confirm the correct form of the dependence of w on the upper-level ionization potential. It should be pointed out that the investigated spectral lines origin from the upper levels (i) whose energies lies in the wide energy interval (ΔE_i) :2.83 eV; 1.126 eV, 1.006 eV and 0.95 eV for the 3s - 3p, $2p^2$ 3s-$2p^2$ 3p, 3p - 3d and $2p^2$ 3p-2p2 3d transitions, respectively. The ΔE_i values is in order the magnitude of the plasma characteristics (kT) of the investigated plasma sources (kT; 2 eV - 4 eV).The minor scatter (within 15% accuracy) among reduced Stark HWHM values in the cases of the spectral lines that belong to the 3s-3p and $2p^2$ 3s-$2p^2$ 3p transitions makes them applicatible in the plasma spectroscopy (Djeniže 1999).

Acknowledgment: This research is a part of the project "Plasma Spectroscopy" supported by Ministry of Science and Technology of the Republic of Serbia.

References

Blagojević B.,Popović M.,Konjević N.,Dimitrijević M.S.,1998, Proceed.the 19th SPIG, 353, Zlatibor, Yugoslavia.

Dimitrijević M.S.,1989, Bull.Astron.Belgrade.,**140**, 111.

Djeniže S.,Malešević M,,Srećković A.,Milosavljević M.,Purić J.,1989, J.Quant. Spectr. Radiat. Transfer, **42**, 429.

Djeniže S.,Milosavljević V.,Srećković A.,Platiša M.,1996,Proceed.the 18 th SPIG, 267, Kotor, Yugoslavia.

Djeniže S.,Srećković A.,Labat J.,Platiša M.,1999, Phys.Scripta, **59**, 98.

Djeniže S.,1999, Physica Scripta (to be published).

Lesage A.,1994,in the Proceed. of the XXIInd General Assembly of the International Astronomical Union, le Haie.

Lesage A.,Fuhr J.,1998, *"Bibliography on Atomic Line Shapes and Shifts"*, Supp.5 (April 1992 through December 1997) Publication de l' Observatoire de Paris.

Platiša M.,Popović,M.,Konjević N.,1975, Astron.Astrophys. **45**, 325.

Purić J.,Djeniže S.,Srećković A.,Platiša M.,Labat J.,1988, Phys.Rev.A **37**, 498.

Wiese W.L.,Smith M.W.,Glennon B.M.,1966, *"Atomic Transition Probabilities"*, Vol.I NSRDS-NBS 4(DC,U.S.Government Printing Office,Washington).

Journal of Research in Physics Vol.28, No. 3, 231-234 (1999)

MEASURED,CALCULATED AND ESTIMATED STARK WIDTH OF THE 381.135 nm O VI SPECTRAL LINE

S.Djeniže
Faculty of Physics, University of Belgrade , P.O.B.368, Serbia, Yugoslavia

1. INTRODUCTION

Spectral lines of multiply ionized emitters, like O VI, were discovered in the spectra of stellar atmospheres of hot stars (Bruhweiler 1985; Kostyakova 1981).Thus, the necessity of knowledge of Stark widths of these lines was imposed. On the basis of Stark HWHM (half-width at half intensity maximum, w) values it is possible to obtain the other basic plasma parameters e.g. electron temperature (T) and electron density (N),important in the modeling of the stellar atmospheres (Lesage 1994) or other laboratorical plasmas (Griem 1974).After Hubble space telescope was launched to orbit, the UV radiation detection has became reality. It is of interest to find intensive spectral lines with well-known Stark width values, convenient in a plasma diagnostics. In this view, the 381.135 nm O VI spectral line would be recommended for a plasma diagnostics. Namely, the existing measured, calculated and estimated Stark width values of this line shows mutually agreement in a wide range of the electron temperatures.

2. MEASUREMENTS

Three experiments deal with the Stark width investigation of the 381.135 nm O VI spectral line. This was measured by Böttcher et al.(1988) at 145 000 K electron temperature, and by Glenzer et al. (1992) for an electron temperatures compused between 90 000 K and 200 000 K. Measurements of Blagojević et al.(1999) were realized in the temperature range between 61 900 K and 79 700 K. The observed electron densities in the mentioned experiments lies between 0.86 10^{23} m^{-3} and 24 10^{23} m^{-3}.

3. CALCULATIONS

The previous calculation the Stark width values of the 381.135 nm.O VI spectral line was performed by Dimitrijević & Konjević on the basis of the simplified semiclassical approximation after Griem (1974) (GM) and of the modified semiempirical formulae (SEM) (Dimitrijević & Konjević 1980). Seaton's calculations, using the close-coupling theory (CC),have been presented in 1988. Böttcher et al.(1988) have calculated the Stark width value of this line at 145 000 K electron temperature using the impact and classical path approximations (Hey & Breger 1980,1982) and Baranger's (1962) theory for nonhydrogenic ions.Blagojević et al.(1999) have calculated the newly values of the Stark widths in a wide range of the electron temperatures (20 000 K - 300 000 K) in the semiclassical perturbation formalism (SCPF) (Sahal-Bréchot 1969a, 1969b). This is a extension the calculations performed by Dimitrijević & Sahal-Bréchot (1992).

4. ESTIMATIONS

The simplest way to estimate the value of a Stark HWHM (w) is to use established regularities of w along the isonuclear (INS) isoelectronic (IES) sequences for given type of

quantum transition. It was found (Djeniže et al.1988 ; Purić et al.1988) that a simple analytical relationship may exist, for same transition, between w and the corresponding upper-level ionization potential (I) of a particular spectral line.The found relationship, normalized to a $N = 10^{23}$ m^{-3} electron density, is of a form:

$$w\ (rad/s) = az^2\ T^{-1/2}\ I^{-b}. \qquad (1)$$

The upper-level ionization potential I (in eV) and net core charge z (z=1,2,3,4,... for neutral, singly, doubly, triply,... ionized atoms, respectively) specifies the emitting ion, while the electron temperature T (in K) characterizes the assembly. The coefficients a and b are independent of I and T. In the case of the lithium-like isoelectronic sequence (IES) (Li I, Be II, B III, CIV, N V, O VI, F VII, Ne VIII) for the 3s - 3p transition, this dependence is expressed (Purić et al.1988) as :

$$w(rad/s) = 5.31x10^{14}\ z^2\ T^{-1/2}\ I^{-1.74} \qquad (2)$$

In the case of the oxygen isonuclear sequence (INS), (O I, O II, O III, O IV, O V, O VI, O VII, O VIII), for the 3s - 3p transition, the following form was found (Djeniže & Labat 1996,and references therein):

$$w(rad/s) = 6.6\ x10^{13}\ z^2\ T^{-1/2}\ I^{-1.15} \qquad (3)$$

Using the Eqs.(2-3) it is possible to predict the Stark width values for: z = 1,2,3,4,5,6,7 at various electron temperatures. The estimated Stark FWHM (2w) values of the 381.135 nm O VI (z=6) spectral line are presented in Tab.1. The necessary atomic data were taken from Wiese et al.(1966).

$T(10^3 K)$	INS	IES	$T(10^3 K)$	INS	IES
40	0.0180	0.0135	110	0.0109	0.0082
50	0.0161	0.0122	120	0.0104	0.0078
60	0.0147	0.0111	130	0.0100	0.0075
70	0.0136	0.0103	140	0.0096	0.0073
80	0.0128	0.0096	150	0.0093	0.0070
90	0.0120	0.0091	200	0.0081	0.0061
100	0.0114	0.0086	300	0.0066	0.0050

Table 1

Estimated Stark FWHM values (2w in nm) on the basis of the regularities along a isonuclear (INS) and isoelectronic (IES) sequences at various electron temperatures and 10^{23} m^{-3} electron density.

5. DISCUSSION

In order to make easy comparison among measured, calculated and estimated Stark width values, in the Fig.1, the dependence of 2w (FWHM) values on the electron temperatures is given. Theoretical values present only electronic contribution to the Stark width, because the ion contribution is negligible (Blagojević et al. 1999).

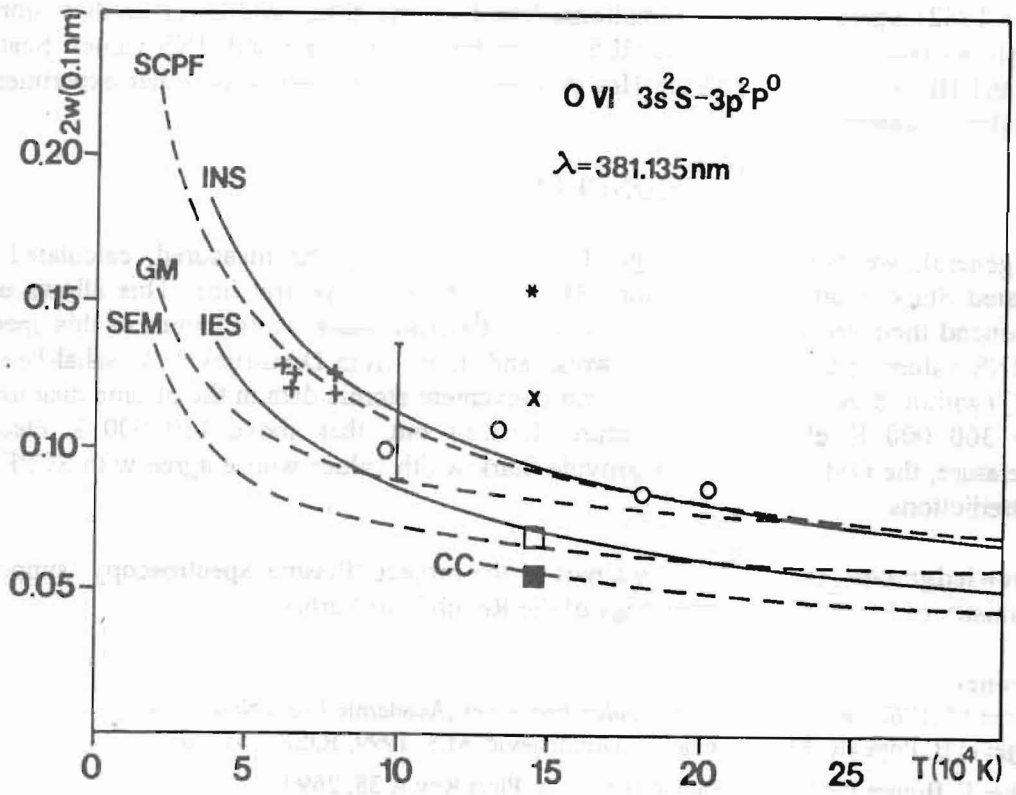

Fig.1

Stark FWHM dependence on the electron temperature at 10^{23} m^{-3} electron density Measured values: o,Glenzer et al.(1992),+ ,Blagojevic et al.(1999);*,Böttcher et al.(1988).Calculated values; ■,Hey & Breger (1980); □,Hey & Breger (1982); x,Baranger (1962). For other symbols see the text. Error bar corresponding to 20% uncertainties is given for indication.

It is evident that excellent agreement among calculated Stark width values (based on the semiclassical perturbation formalism, SCPF) and our estimated values (based on the isonuclear sequence, INS), exist in the wide range of the electron temperatures (40 000 K - 300 000 K). On the other hand, the existing experimental data agree, within a few percent of accuracies,with these calculated and estimated values. Only exception makes data from Böttcher et al.(1988).This lies above the all other Stark width values up to 60 % . Here would be pointed out, that the results of the: GM, SEM and Hey's calculations (□ in Hey &

Breger 1982) agree with the estimations, based on the Stark width regularities along a lithium-like isoelectronic sequence (IES).These lies under SCPF and INS values. Seaton's (CC) and Hey's determinations (in Hey & Breger 1980) are below the other experimental, calculated and estimated data.

6. CONCLUSION

In general, we noticed a very good agreement among the measured, calculated and estimated Stark width values of the 381.135 nm O VI spectral line. This allows us to recommend their use for plasma spectroscopy.Existing Stark width values of this spectral line: INS values in the Tab.1 in this work and those from Dimitrijević & Sahal-Brechot (1992) (within 8 % uncertainties) present convenient atomic data in the plasma diagnostics up to 300 000 K electron temperature. It turns out, that above 150 000 K electron temperature, the GM aproximation provide Stark width values whose agree with SCPF and INS predictions.

Acknowledgment: This research is a part of the project "Plasma Spectroscopy "supported by Ministry of Science and Technology of the Republic of Serbia.

References

Baranger M.,1962, *in Atomic and Molecular Processes* ,Academic Press,New York.
Blagojević B.,Popović M.,Konjević N.,Dimitrijević M.S.,1999, JQSRT **61**, 361.
Böttcher F.,Breger P.,Hey J.D.,Kunze H.J.,1988, Phys.Rev.A **38**, 2690.
Bruhweiler F.C.,1985, BAAS, **17**, 559.
Dimitrijević M.S.,Konjević N.,1980, JQSRT **24**, 451.
Dimitrijević M.S.,Sahal-Brechot S.,1992, A & A,Supp.S. **93**, 359.
Djeniže S.,Srećković A.,Milosavljević M.,Labat O. Platiša M.,Purić J.,1988, Z.Phys.D **9**, 129.
Djeniže S.,Labat J.,1996, Bull.Astron.Belgrade. **153**, 35.
Glenzer S.,Uzelac N.I.,Kunze H.J.,1992, Phys.Rev. A **45**, 8795.
Griem H.R.,1974, *Spectral Line Broadening by Plasmas*, Academic Press,New York.
Hey J.D.,Breger P.,1980, JQSRT, **24**, 349 and 427.
Hey J.D.,Breger P.,1982, S.Afr.J.Phys.**5**, 111.
Kostyakova E.B.,1981, *in Zvezdy i zvezdnye sistemy,* Nauka, Moskva.
Lesage A.,1994,in the Proceed.of the XXIInd General Assembly of the International Astronomical Union, le Haie.
Purić J.,Djeniže S.,Labat J.,Platiša M.,Srećković A., Ćuk M.,1988, Z.Phys.D **10**, 431.
Sahal-Brechot S.,1969a, A & A **1**, 91.
Sahal-Brechot S.,1969b, A & A **2**, 322 .
Seaton M.J.,1988, J Phys.B **21**, 3033.
Wiese W.L.,Smith M.W.,Glennon B.M.,1966, *Atomic Transition Probabilities*,NSRDS NBS 4 Vol.1 (DC:US Govt Printing Office,Washington).

Journal of Research in Physics Vol.28, No. 3, 235-238 (1999)

MEASURED STARK WIDTHS OF SEVERAL Ar II AND Ar III SPECTRAL LINES

S.Djeniže, S.Bukvić and D.Mišković
Faculty of Physics, University of Belgrade, P.O.B. 368, Serbia, Yugoslavia

1. INTRODUCTION

A number of experimental and theoretical papers have dealt with Stark broadening of singly (Ar II) and doubly (Ar III) ionized argon spectral lines (Lesage & Fuhr 1998, and references therein). The aim of this paper is to provide some new data on the Stark width of ionized argon spectral lines at 22 500 K electron temperature (T) and 1.90 10^{23} m^{-3} electron density (N). We have measured Stark FWHM (full-width at half intensity maximum, w) of four Ar II and seven Ar III spectral lines. The Stark widths of the 371.474 nm Ar II, as well of the 248.886 nm and 250.442 nm Ar III spectral lines have not been measured before, to the knowledge of the authors.

2. EXPERIMENT

The modified version of the linear low pressure pulsed arc (Djeniže et al 1989, Djeniže et al 1998) has been used as a plasma source. A pulsed discharge driven in a quartz discharge tube of 5 mm inner diameter and has an effective plasma length of 5.8 cm. The tube has end-on quartz windows. On the opposite side of the electrodes the glass tube was expanded in order to reduce sputtering of the electrode material onto the quartz windows. The working gas was argon and helium mixture (72% Ar + 28 % He) at 130 Pa filling pressure in flowing regime. Spectroscopic observation of isolated spectral lines were made end-on along the axis of the discharge tube. A capacitor of 14 μF was charged up to 2.5 kV. The line profiles were recorded by a shot-by-shot technique using a photomultiplier (EMI 9789 QB) and a grating spectrograph (Zeiss PGS-2, reciprocal linear dispersion 0.73 nm/mm in the first order) system. The exit slit (10 μm) of the spectrograph with the calibrated photomultiplier was micrometrically traversed along the spectral plane in small wavelength steps (0.0073 nm). The photomultiplier signal was digitized using oscilloscope, interfaced to as computer. A sample output, as example, is shown in Fig.1. The measured profiles were of the Voigt type due to the convolution of the Lorentzian Stark and Gaussian profiles caused by Doppler and instrumental broadening. For electron density and temperature obtained in our experiment the Lorentzian fraction in the Voigt profile was dominant. Van der Waals and resonance broadening were estimated to be smaller by more than an order of magnitude in comparison to Stark, Doppler and instrumental broadening. A standard deconvolution procedure (Davies & Vaughan 1963) was used. The deconvolution procedure was computerized using the least square algorithm. (see Fig.2 for a example). The Stark widths were measured with ±8% error.

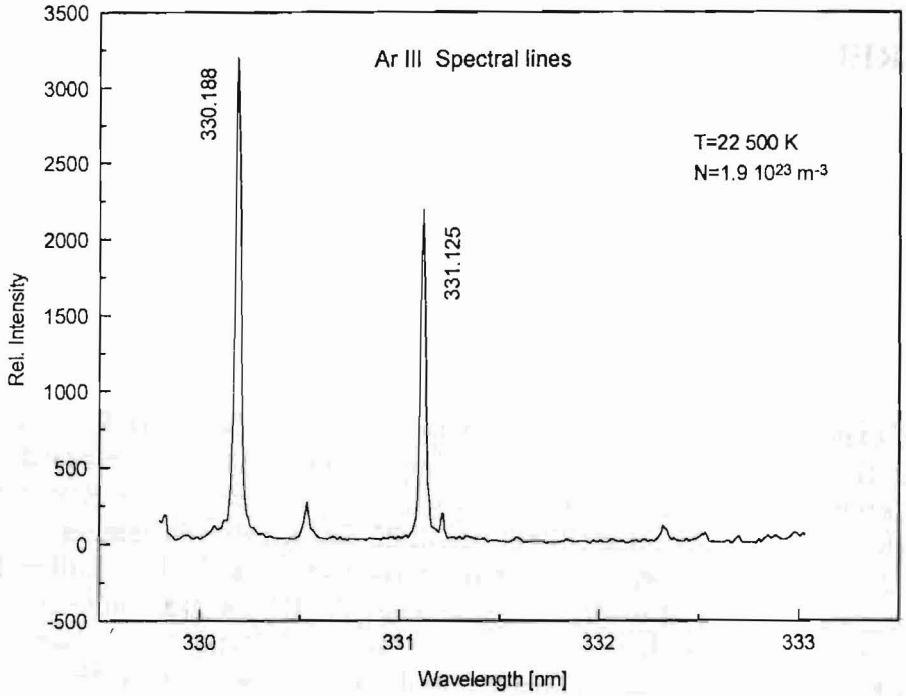

Fig.1.

Recorded spectrum at 15th μs after the beginning of the discharge (when the line profiles were analyzed) with the investigated Ar III spectral lines from the multiplet No.1.

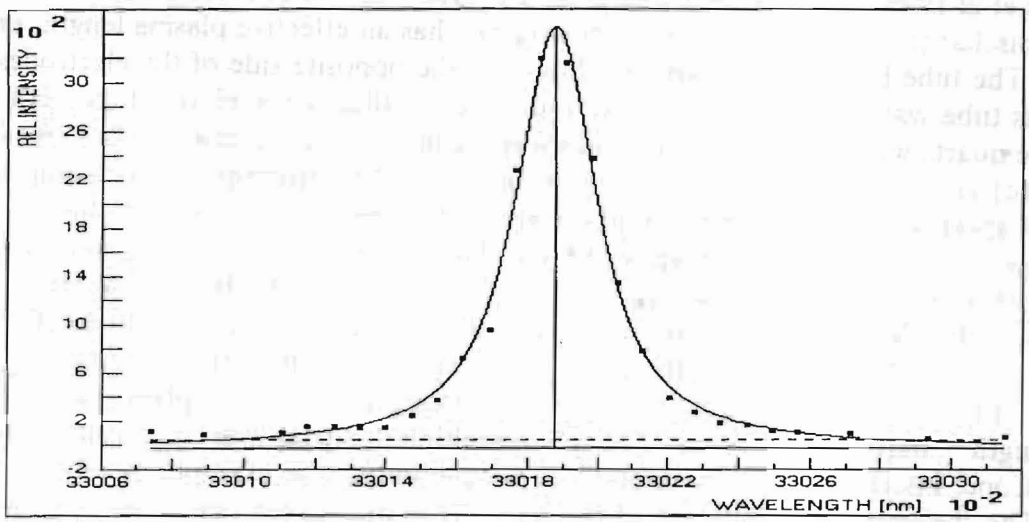

Fig.2.

Profile of the 3301.88 nm Ar III spectral line. *, experimental points; —, Voigt fitting

Great care was taken to minimize the influence of self-absorption on Stark width determinations. The opacity was checked by measuring line-intensity ratios within multiplets No. 1 and No.3 in the case of the Ar III spectrum. The values obtained were compared with calculated ratios of the products of the spontaneous emission

probabilities and the corresponding statistical weights of the upper levels of the lines. It turns out that these ratios differed by less than ± 4 % in the 15th μs of the discharge.

The plasma parameters were determined using standard diagnostics methods. The electron temperature was determined from the Boltzmann-slope of seven investigated Ar III lines with a corresponding upper-level energy interval of 8.32 eV. The necessary atomic parameters were taken from Wiese et al (1969) and Striganov & Sventickii (1966). At 15th μs after the beginning of the discharge (when the spectral line profiles were analyzed) the found electron temperature was 22 500 K ± 10 % (see Fig.3).

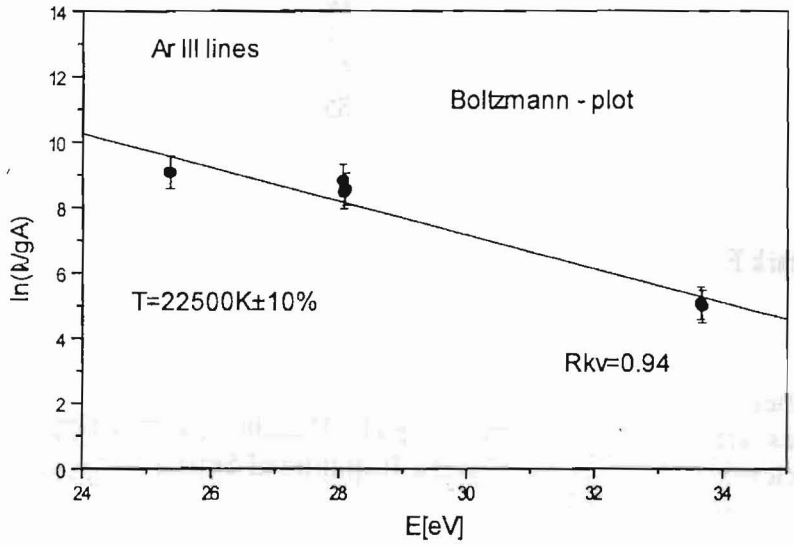

Fig.3.
Boltzmann-plot of seven Ar III spectral lines with 0.94 correlation factor.

For electron density measurement we used the convenient Stark width of the He II Paschen-α 468.57 nm spectral line. The obtained value was N= 1.90 10^{23} m^{-3} ±9 %.

3. RESULTS

Our experimental results of the measured Stark FWHM values (in 0.1 nm) at 22 500 K electron temperature and N = 1.90 10^{23} m^{-3} electron density are given in the Table 1.

It turns out that our measured Stark width values agree with those from other experimental works (Djeniže et al 1996, and references therein) in the case of Ar III spectral lines and with values presented by Pellerin et al (1997) in the case of Ar II spectral lines. The results of comparison between our new experimental Stark widths values and existing theoretical data will be presented in Djeniže et al (2000).

Emitter	Transition	λ (nm)	FWHM (0.1nm)
Ar II			
	$3d\ ^4D - 4p\ ^2D^0$	371.47	0.448
	$4p\ ^4P^0 - 5s\ ^4P$	372.04	1.100
	$4s\ ^4P - 4p\ ^4S^0$	372.93	0.386
	$3d\ ^4D - 4p\ ^4D^0$	401.38	0.413
Ar III	$4p'\ ^3P^0 - 4d'\ ^3P^0$	248.89	0.216
	$4p'\ ^3P - 4d'\ ^3P^0$	250.44	0.316
	$4s\ ^5S^0 - 4p\ ^5P$	330.19	0.260
		331.12	0.240
	$4s'\ ^3D^0 - 4p'\ ^3F$	333.61	0.280
		334.47	0.230
		335.85	0.250

Table 1.
Measured Stark FWHM at T=22 500 K electron temperature and N=1.9 10^{23} m^{-3} electron density.

Acknowledgment

This research is a part of the project "Plasma Spectroscopy" supported by Ministry of Science and Technology of the Republic of Serbia.

References

Daviess J.T., Vaughan J.M., 1963 Aph.J. 137, 1302.
Djeniže S. et al., 1989, JQSRT 42, 429.
Djeniže S., Milosavljević V., Srećković A., 1998, JQSRT, TOM 59, 71.
Djeniže S., Bukvič S., Srećković A., Platiša M., 1996, J.Phys. B 29, 429.
Djeniže S., Bukvić S., Mišković D., 2000 (to be published)
Lesage A., Fuhr J., 1998, *Bibliography on Atomic Line Shapes and Shifts*, Supp.5 (April 1992 through December 1997) Publication de l'Observatoire de Paris.
Pellerin S., Musiol K., Chapelle J., 1997, JQSRT 57, 377.
Striganov R.A., Sventickii N.S., 1966, *Tablici Spectralnjih Linii*, Atomizdat, Moskva.
Wiese W.L., Smith M.W. Miles B.M., 1969, "*Atomic Transition Probabilities*" Vol. II., NSRDS-NBS 22 (DC.U.S.Government Printing Office, Washington).

Journal of Research in Physics Vol.28, No. 3, 239-242 (1999)

ON THE APPLICATION OF BALMER BETA LINE SHAPE FOR ELECTRON DENSITY DIAGNOSTICS IN THE RANGE $10^{20} - 10^{21}$ m^{-3}

M. IVKOVIĆ, N. KONJEVIĆ
Institute of Physics, 11081 Beograd, P. O. Box. 68
E-mail: ivkovic@atom.phy.bg.ac.yu

1. INTRODUCTION

The analysis of hydrogen Balmer beta (H_β = 486.13 nm) spectral line shape is one of the most common methods of electron density diagnostics from the beginning of seventies. Although, the laser interferometry method seems to provide the most reliable results at present, analysis of H_β line shapes is the easiest one and can be performed in every spectroscopic laboratory with satisfactory accuracy. In practice the most frequently used approaches are: the approximate experimental formulas and the comparison with tabulated data according to unified theory - VCS tables (Vidal,Cooper,Smith,1973), which is already carefully experimentally tested. In this work we present critical analysis of applications of this methods in case of relatively low electron concentrations (10^{20} - 10^{21} m^{-3}).

2. EXPERIMENTAL APPROXIMATE FORMULAS

On the basis on electron density (Ne) measurements via laser interferometry and determination of half – half widths (HWHM) under identical experimental conditions few experimental approximate formulas for dependence Ne = f (HWHM) are obtained (Wiesse et al, 1972, Kelleher, 1981). By application of these formulas on HWHM determinated from VCS tables at Ne = $1*10^{20}$ m^{-3} and Ne = $1*10^{21}$ m^{-3} for various temperatures, testing was performed. It should be stressed, that HWHM obtained by unified theory shows the best agreement with experimental data.

2.1 *Wiesse's formula*

From the measurements in electron density range 1.5 * 10^{22} - 10^{23} cm^{-3} and temperature range 9 000 – 14 000 K following approximate formula is determinated

$$Ne\ (cm^{-3}) = 10^{16} * (HWHM / 4.74)^{1.49}$$

i.e. according to (Helbig, 1998)

$$Ne\ (cm^{-3}) = 10^{16} * (FWHM / 9.4659)^{1.48983}$$

where HWHM is pure Stark halfwidth. Although HWHM very slowly depends on electron temperature Te, for Ne <$1*10^{21}$ m^{-3} and Te > 10 000 K errors become greater than 10%. Also, the main problem with application of this formula is complicated procedure of profile deconvolution at lower densities and consequently lower accuracy.

2.2. *Kelleher's formula*

From the measurements in Ne range 0.2 - 1.3 * 10^{22} m^{-3} and T from 10 000 to 20 000 K Kelleher obtained:

$$Ne\ (cm^{-3}) = 10^{16} * (W_S / 4.95)^{1.48}$$

where Ws - Stark halfwidths, W_D - Doppler halfwidths and Wi - instrumental halfwidths

$$W_S = (W_m^{1.4} - W_{D,i}^{1.4})^{1/1.4} \qquad W_{D,i} = (W_D^2 + W_i^2)^{0.5} \qquad W_D = 3.58 * 10^{-7} \lambda (T_g / M)^{0.5}$$

As one can see, the corrections due to instrumental and Doppler broadening in this formula are included. Unfortunately, validity range and origin of this correction is not known. This formula shows lower accuracy than Wiesse's under the same test conditions. Other authors (Czernichowski et all,1985) obtain similar conclusion. Namely, if a value of Ne obtained by Wiesse's formula instead of this one is used, all Kelleher's data (on shape of He I 447.1 nm spectral line from the same paper) are in accordance with papers published by other authors.

3. APPLICATIONS OF VCS TABLES

The VCS tables contain the normalized profiles $S(\Delta\alpha)$, from which one can obtain $S(\Delta\lambda)$ by

$$\Delta\lambda = F_0 \Delta * \alpha, \qquad S(\Delta\lambda) = S(\Delta\alpha) / F_0 \qquad \text{and} \qquad F_0 = 1.25 * 10^{-9} Ne^{2/3}.$$

where $\Delta\lambda$ is the wavelength perturbation of a line with respect to the unperturbed position of the line (in Å) and F_0 the normal field strength (in esu) due to electrons with density Ne (number per cm^{-3}).

3.1. *Graphic method*

From the obtained $S(\Delta\lambda)$ profiles, after determinations of halfwidths, the theoretical dependence of Ne on HWHM in log-log proportion for various temperatures are drawn. From such graphics for experimentally obtained halfwidths Ne can be obtained. This method is the easiest one, but one must have in mind that error of 7 % in determination of Ne requires determination of log(HWHM) with error less than 1%
(for example $\log (1.07*10^{21}) = 21.03$ with error of 0.14 %).

3.2. *Approximate formula Czernishowski – Chapelle*

On the basis of VCS tables the approximate formula (Czernichowski et all,1985) with accuracy of 5 % in the range $0.0316 < Ne[10^{22}\ m^{-3}] < 3.16$ and $5000 < Te[K] < 20000$ are obtained:

$$\log Ne = 22.578 + 1.478 \log W - 0.144 (\log W)^2 - 0.1265\ T$$

where W is FWHM of whole profile in nm, T is excitation temperature in K and Ne in m^{-3}. This formula has a 5% accuracy in the mentioned range, but at $1*10^{20}\ m^{-3}$ can give two times greater Ne, due to pronounce dependence on T. Also, applications is limited to the cases with equal gas and electron temperatures.

3.3. *Programs for comparison of whole profiles*

All published programs (to the authors' knowledge) on electron density determinations via comparison of whole H_β profiles are based on VCS tables. Let us present a brief description of published programs.

3.3.1. *Goode, Davor's EDFIT*

This program (Goode et al, 1984) is based on recalculations of tabulated VCS profiles to $S(\Delta\lambda)$, convolution with Doppler and instrumental profiles. The obtained profiles are normalized on unit intensity and sampled in equally spaced points 0.01nm apart till the 1% of intensity. Intermediate profiles are calculated by interpolation with polinoms. The comparison with experimental data sampled in the same wavelength points, by Ne interval halving algorithm and minimization of sum of square of residuals was performed. The exclusion of points in the center of the profile during the comparison is also included. The results obtained with this program show 2-3 times lower Ne than from H_β halfwidths which are not observed by the comparison of whole profiles by other authors (Thomsen et al, 1991). Also, the reasonable doubts (Chan,Montaser, 1989) that this program uses only profiles with Te=Tg=2500K and that has considerable software mistakes exist.

3.3.2. *Chan, Montaser's NE*

In this program (Chan,Montaser, 1989) intermediate profiles (for nontabulated Ne and Te) are obtained by cubic spline interpolation. Convolution of Doppler and instrumental profiles and area normalization are also performed. Same method as in 3.3.1. for the comparison of resulting profiles with experimental data are used. Authors point out the influence of Te and Tg on Ne determination and errors due to Lagrange polinoms interpolation of profiles.

3.3.3. *Kuraica, Konjević, Platiša, Pantelić FIT_SPC*

In this paper (Kuraica et al, 1992) $S(\Delta\lambda)$ is approximated with parabolic spline and intermediate profiles are obtained by Lagrange polinoms interpolation. This approach enables convolution of Stark and Doppler and instrumental profiles directly by convolution integral via erf functions instead of FFT. The profiles are normalized on unit intensity and superposition of additional profiles is enabled.

3.3.4. *Zhang et all. NNE*

This program (Zhang et al, 1994) is based on same principles as the 3.3.2. but written in C language instead of TURBO BASIC. Furthermore it has possibility to exclude some points in the center of the profile during the comparison with experimental data. Unfortunately authors neither supply as with program source nor explain the data entry.

3.3.5 *Starn et all*

In this case (Starn et al, 1995) normalization on unit intensity (for preventing of background intensity influence and owing to inability to record profile far from the center) was performed. The cubic spline interpolations of profiles and FFT convolution are also used. Determination of Ne via comparison of obtained theoretical profiles and experimental data by Fo instead of usual Ne interval halving is used. The exclusion of points in the center of the theoretical profile is also enabled. Unfortunately this program is written in LabVIEW program language for Machintosh and the author didn't respond to us so, we was unable to test it.

4. CONCLUSION

On the basis of this analysis for estimation of electron density from 10^{20} to 10^{21} m^{-3} we recommend the use of approximate formulas combination i.e. application of Kelleher's

formula for determination of Stark half-half widths and Wiesse's for Ne = f (HWHM) dependence.

The determination of electron density from the whole profiles based on VCS tables, in this concentration range exert systematic error due to inadequate description of central part of the profile caused by non inclusion of ion dynamics effect by unified theory (Kelleher et al, 1973, Cooper et al,1974). The exclusion of some points in the center of the profile at comparison with experimental points can lead to the error greater than 100% (Thomsen et al, 1991). Therefore new calculation and tabulation of hydrogen like profiles, which have to include the influence of ion motion effect are recommended (Griem, 1997). Naimely, tables based on the Model Microfield Method (Stehle, 1994) include this influence and give a better description of the central part of H_β profile than unified theory, but unfortunately the obtained halfwidths (according to author) are greater than experimentally observed and can be used only for estimations of electron densities. All this facts directed our further work towards writing a program for electron density determination based on tables obtained by Monte Carlo simulations.

References:

Chan, Montaser: 1989, *Spectrochim. Acta* **44B,** 175
Cooper, Smith,Vidal: 1974, *J.Phys.B: Atom.Molec.Phys.* 7, L101
Czernichowski Chapelle: 1985, *JQSRT* **33,** 427
Goode, Deavor: 1984, *Spectrochim. Acta* **39B,** 813
Griem: 1997, *Principles of Plasma Spectroscopy* Cambridge University Press
Helbig: 1998, private communcations
Kelleher; 1981, *JQSRT* **25,** 191
Kelleher,Wisse: 1973, *Phys.Rev.Lett.***31,** 1431
Kuraica, Konjević, Platiša,Pantelić: 1992, *Spectrochinica Acta* **47B,** 1173
Starn et all.: 1995, *Spectrochim. Acta* **50B,** 1147
Stehle: 1994, *Astron.Astrophys.Suppl.Ser.* **104,** 509
Thomsen, Helbig: 1991, *Spectochimica Acta* **46,** 1215
Vidal,Cooper,Smith: 1973, *Astrophys.J.Suppl. No.* 214 **25,** 37
Wiesse,Kelleher,Paquette: 1972, *Phys.Rev.A* **6,** 1132
Zhang et al.: 1994, *Spectrochim. Acta* **49B,** 817

Journal of Research in Physics Vol.28, No. 3, 243-246 (1999)

MEASURED STARK WIDTHS OF SINGLY IONIZED OXYGEN SPECTRAL LINES

V. Milosavljević and S. Djeniže
Faculty of Physics, University of Belgrade
P.O.B. 368, Serbia, Yugoslavia

1. INTRODUCTION

The knowledge of the OII spectral lines characteristics, like Stark width, is important for the determination of chemical abundance's of elements, and also for the estimation of the radiative transfer through stellar plasmas, as well as for opacity calculations. A number of experimental papers have dealt with Stark broadening of OII spectral lines (Platiša et al. 1975; Purić et al. 1988; Djeniže et al. 1991; Djeniže et al. 1998).

The aim of this work is to present measured Stark FWHM (full width at half maximum intensity, w) of two OII spectral lines that belong to 3s-3p and 3p-3d transitions. No experimental Stark FWHM data exist for these investigated spectral lines, to the knowledge of the authors. Measurements have been performed in the low pressure linear pulsed arc at $1.45 \cdot 10^{23}$ m^{-3} electron density and 38 000 K electron temperature

2. EXPERIMENT

The Modified version of the linear low pressure pulsed arc (Djeniže et al. 1998; Milosavljević & Djeniže 1998) has been used as a plasma source. A pulsed discharge driven in a quartz discharge tube of 5 mm i.d. and has an effective plasma length of 5.8 cm. The tube has end-on quartz windows. On the opposite side of the electrodes the glass tube was expanded in order to reduce erosion of the glass wall and also sputtering of the electrode material onto the quartz windows (Djeniže et al. 1998). The working gas was helium-nitrogen - oxygen mixture (90% He + 8% N_2 + 2% O_2) at 267 Pa filling pressure in flowing regime. Spectroscopic observation of isolated spectral lines was made end-on along the axis of the discharge tube. A capacitor of 8 μF was charged up to 4.5 kV. The line profiles were recorded by a shot-by-shot technique using a photomultiplier and a grating spectrograph system (Milosavljević et al. 1999). The exit slit (10 μm) of the spectrograph with the calibrated photomultiplier was micrometrically traversed along the spectral plane in small wavelength steps (0.0073 nm).

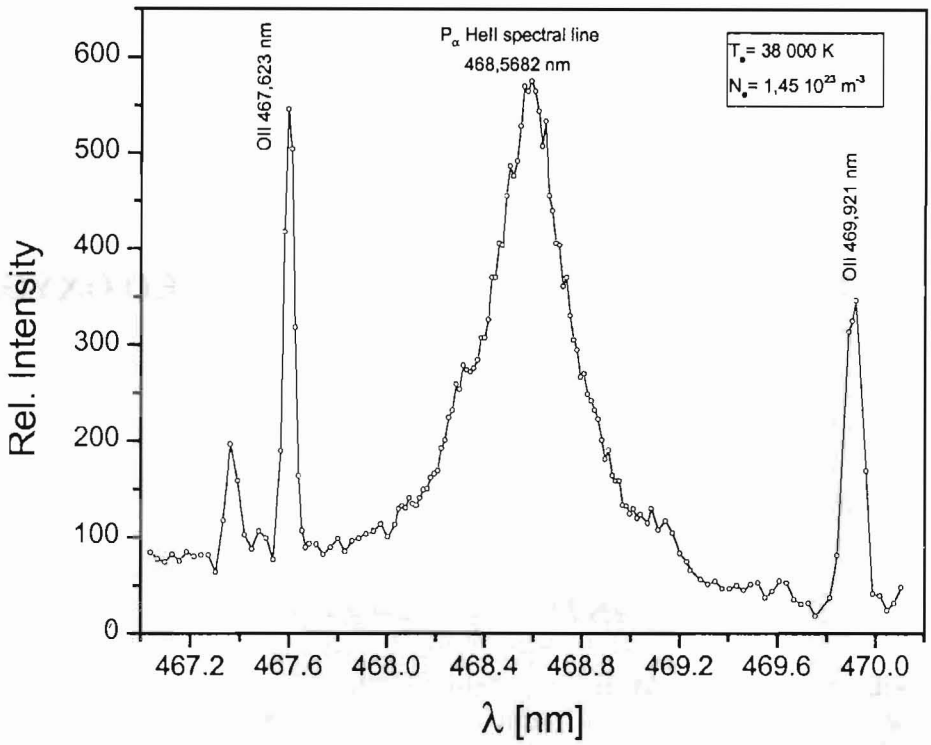

Recorded spectrum at 20 μs after the beginning of the discharge with the investigated OII lines.

The photomultiplier signal was digitized using oscilloscope, interfaced to a computer. Plasma reproducibility was monitored by the OII lines radiation and also by the discharge current (it was found to be within 6%). The measured profiles were of the Voigt type due to the convolution of the Lorentzian Stark and Gaussian profiles caused by Doppler and instrumental broadening. For electron density and temperature obtained in our experiment the Lorentzian fraction in the Voigt profile was dominant (over 80%). Van der Waals and resonance broadening were estimated to be smaller by more than an order of magnitude in comparison to Stark, Doppler and instrumental broadening. A standard deconvolution procedure (Davies & Vaughan, 1963) was used. The deconvolution procedure was computerized using the least squares algorithm. The Stark widths were measured with ±15% error. Great care was taken to minimize the influence of self-absorption on Stark width determinations. The opacity was checked by measuring line-intensity ratios within multiplet (No. 1). The values obtained were compared with calculated ratios of the products of the spontaneous emission probabilities and the corresponding statistical weights of the upper levels of the lines (Wiese et al. 1966). It turns out that these ratios differed by less than ±14%.

The plasma parameters were determined using standard diagnostic methods. The electron temperature (T) was determined from the rations of the relative intensities of the four N III spectral lines (409.74 nm; 410.34 nm; 463.42 nm and 464.06

nm) to the 463.054 nm N II spectral line with an estimated error of ±10 %. All the necessary atomic parameters were taken from Wiese et al. (1966). The electron density (N) decay was measured using a single wavelength He-Ne laser interferometer for the 632.8 nm transition and convenient Stark width of the P_α HeII line, with an estimated error of ±7%.

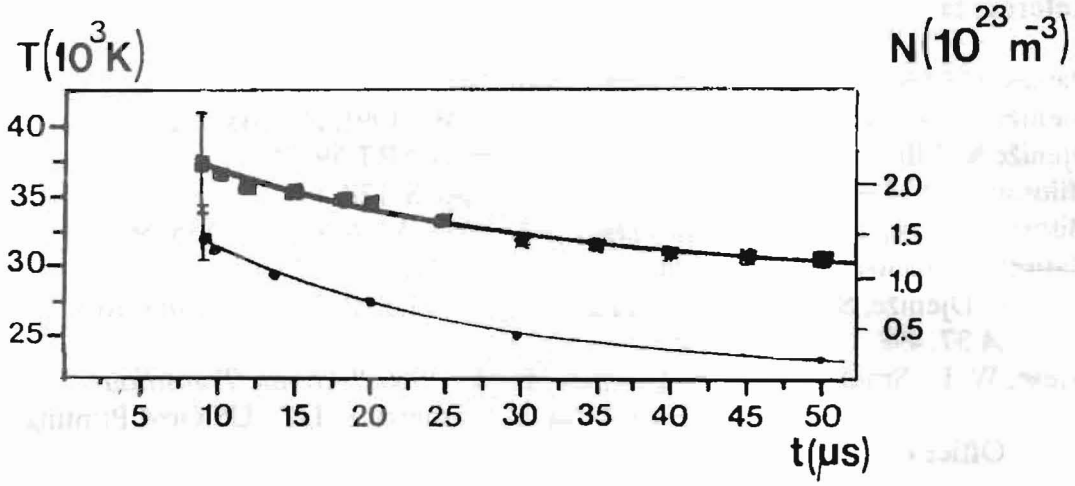

Temporal evolution of the electron temperature (T) ■, and electron density (N) •, with error bars in the decaying plasma.

3. RESULTS

The results of the measured w_m values (FWHM) at the $T=3.8\cdot10^4$ K electron temperature and $N= 1.45\cdot10^{23}$ m^{-3} electron density are given in the Table 1 together with transition arrays and multiplets.

Emitter	Transition	λ(nm)	w_m(nm)
OII	$3s^4P$-$3p^4D^0$ (1)	467.623	0.0514
	$3p^2D^0$-$3d^2F$ (25)	469.921	0.0555

Table 1

In turns out that our measured w_m values agree (within 25% accuracies) with experimental Stark widths data of other spectral lines that belong to multiplet No. 1 (Djenize et al. 1998 and references therein) and to multiplet No. 25 (Djeniže et al. 1991).

Acknowledgment

This research was supported by Ministry for Science and Technology of the Republic of Serbia.

References

Davies, J. T. and Vaughan, J. M. : 1963, *Astrophys. J.* 137, 1302.
Djeniže, S., Srećković, A., Labat, J. and Platiša, M. : 1991, *Z. Phys. D* 21, 295.
Djeniže S., Milosavljević V., Srećković A.: 1998, JQSRT 59, 71.
Milosavljevic V. and Djeniže S.: 1998, A&A Supp. S. 128, 197.
Milosavljevic V., Konjević R. and Djeniže S.: 1999, A&A Supp. S. 135, 565.
Platiša, M., Popović, M. and Konjević, N. : 1975, *A&A* 45, 325.
Purić, J., Djeniže, S., Srećković, A., Platiša, M. and Labat, J. : 1988, *Phys. Rev. A* 37, 498.
Wiese, W. L., Smith, M. W. and Glennon, B. M. : 1966, "*Atomic Transition Probabilities*", NSRDS NBS 4 Vol. 2 (Washington, DC : US Govt Printing Office).

Journal of Research in Physics Vol.28, No. 3, 247-250 (1999)

EXPERIMENTAL STARK SHIFTS OF SEVERAL Ar II SPECTRAL LINES

D. Mišković, A. Srećković, S. Bukvić, S. Djeniže
Faculty of Physics, University of Belgrade, P.O.B. 368, Serbia, Yugoslavia

1. INTRODUCTION

Only few papers deal with Stark shift (d) measurements of the singly ionized argon (Ar II) spectral lines (Konjević & Wiese 1990, and references therein). The aim of this paper is contribution to the knowledge of the Stark shift values at 22 500 K electron temperature and 1.9 x 10^{23} m^{-3} electron density. We have measured Stark shift values for four Ar II spectral lines that belong to four various tansitions. For the 471.4 nm Ar II spectral line measured values does not exist, to the knowledge of the authors. Our measured d values are compared with the existing experimental and theoretical data.

2. EXPERIMENT

The modified version of the linear low pressure pulsed arc (Djeniže et al 1989, Djeniže et al 1998) has been used as a plasma source. A pulsed discharge has been driven in a quartz discharge tube of 5 mm inner diameter and had an effective plasma length of 5.8 cm. The tube has end-on quartz windows. On the opposite side of the electrodes the glass tube was expanded in order to reduce sputtering of the electrode material onto the quartz windows. The working gas was argon and helium mixture (72% Ar + 28% He) at 130 Pa filling pressure in flowing regime. Spectroscopic observation of isolated spectral lines were made end-on along the axis of the discharge tube. A capacitor of 14 μF was charged up to 2.5 kV giving discharge current of up to 6.1 kA (determined using coil Rogovski). The line profiles were recorded by a shot-by-shot technique using a photomultiplier (EMI 9789 QB) and a grating spectrograph (Zeiss PGS-2, reciprocal linear dispersion 0.73 nm/mm in the first order) system. The exit slit (10 μm) of the spectrograph with the calibrated photomultiplier was micrometrically traversed along the spectral plane in small wavelength steps (0.0073 nm). The photomultiplier signal was digitized using oscilloscope, interfaced to a computer. A sample output, as example, is shown in Fig. 1.

The measured profiles were of the Voigt type due to convolution of the Lorentzian Stark and Gaussian profiles caused by Doppler and instrumental broadening. A standard deconvolution procedure (Davies & Vaughan 1963) was used to obtain the Stark width of the He II P-α spectral line. The procedure was computerized using the least square algorithm.

The Stark shifts were measured relative to the unshifted spectral lines emitted by the same plasma (Purić & Konjević 1972). The Stark shift of a spectral line can be measured experimentally by evaluating the position of the spectral line centre recorded at two various electron density values during the plasma decay. In principle, the method requires recording of the spectral line profile at the high electron density (N_1) that causes an appreciable shift and then, later, when the electron concentration

has dropped to the value (N_2) at least an order of magnitude lower. The difference of the line centre positions in the two cases is Δd, so that the shift d_1 at the higher electron density N_1 is:

$$d_1 = N_1 \Delta d / (N_1 - N_2).$$

In the case of our experiment the estimated error by the Stark shift determination was within ± 25%.

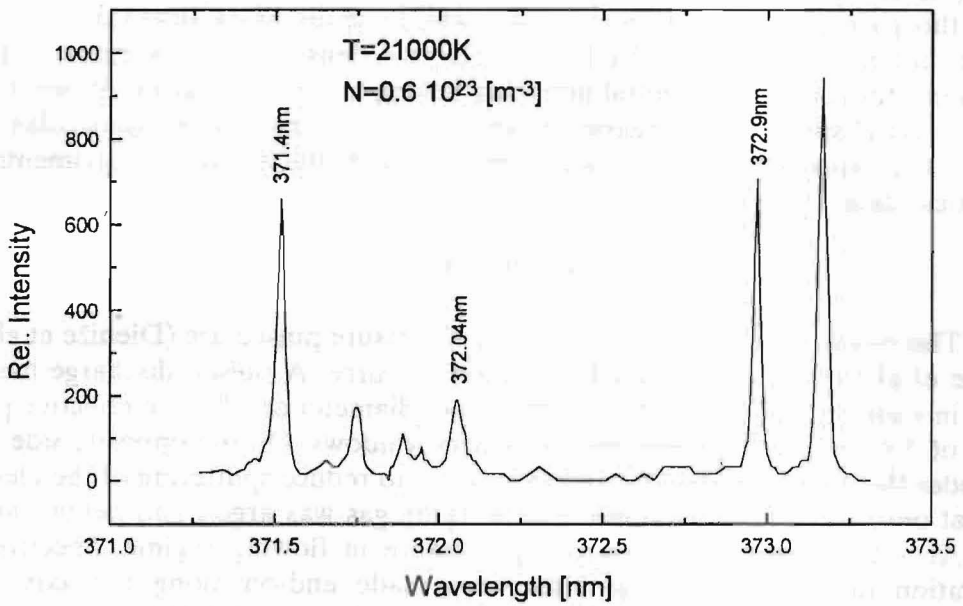

Fig. 1.
Recorded spectrum at 50th μs after beginning of the discharge with observed plasma parameters

The plasma parameters were determined using standard diagnostic methods. The electron temperature was determined from the Boltzmann-slope of seven Ar III spectral lines (330.2, 331.1, 335.9, 334.5, 333.6, 248.9 and 250.4 nm) within ± 10% accuracy. The necessary atomic data were used from Wiese et al. (1969). Electron density decay was obtained using the method of the laser interferometry with the 632.8 nm He-Ne laser line and, also, on the basis of the the Stark width of the convenient P-α (468.57 nm) spectral line from the He II spectrum within ± 7% accuracy.

3. RESULTS

Our results are presented in the Table 1 at T = 22 500 K electron temperature and N = 1.9 x 10^{23} m $^{-3}$ electron density, together with transition arrays and accuracy

(Acc.). The positive sift is toward the red.

Transition	Muttiplet	λ (nm)	d (nm)	Acc. (%)
3d–4p	$^4D - {}^2D^0$ (3)	371.47	0.005	20
4p–5s	$^4P^0 - {}^4P$ (42)	372.04	0.032	15
4s–4p	$^4P - {}^4S^0$ (10)	372.93	– 0.003	15
4p–4d	$^4D^0 - {}^4F$ (56)	357.66	0.013	25

Table 1.

4. DISCUSSION

In order to allow easy comparison among existing (measured and calculated) Stark shift values, we report in Fig. 2. variations of *d* with the electron temperatures for a given electron density equal to 10^{23} m^{-3}.

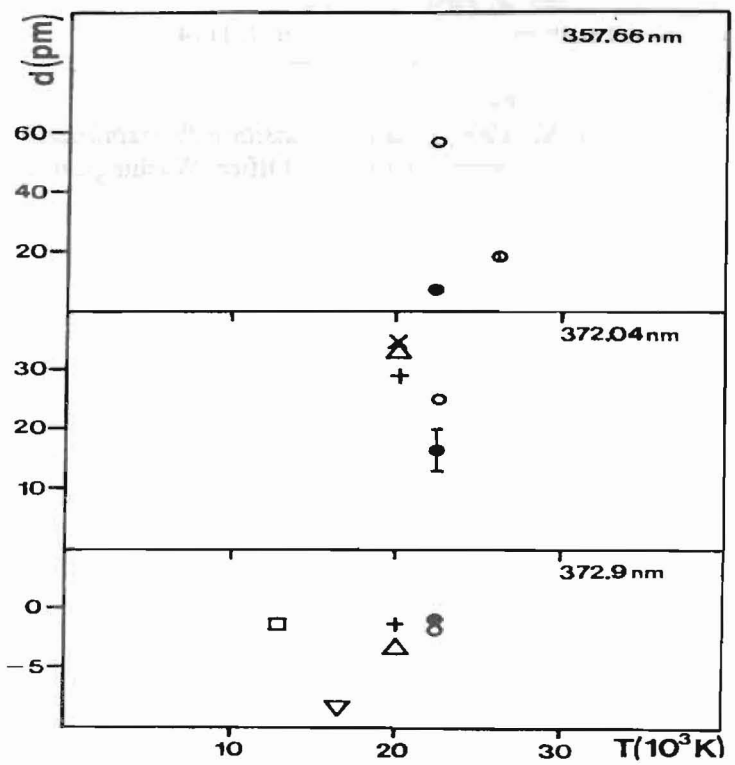

Fig. 2.

Stark shift (d) dependence on the electron temperature at 10^{23} electron density. Measured values: •, this work; 0, Aparicio et al. 1998; ±, Dzierzega & Musiol 1994; ϕ, Djeniže et al. 1989; ∇, Labat et al. 1974; Δ, Morris & Morris 1970. Theoretical values: +, Griem 1974 and x, Kršljanin & Dimitrijević 1989.

One can conclude that theoretical values exist only for the 372.04 nm and 372.93 nm spectral lines. It turns out that in the case of the 372.93 nm line the experimental and theoretical *d* data show mutual agreement in the vicinity of 21 000 K electron temperature. In the case of the other two spectral lines (372.04 nm and 357.6 nm) the existing *d* values show evident mutual scattering.

Acknowledgment: This research is a part of the project "Plasma Spectroscopy" supported by Ministry of the Science and Technology of the Republic of Serbia.

References

Aparicio J.A., Gigosos M.A., Gonzalez V.R., Perez C., dela Rosa M.I., Mar S.: 1998, *J. Phys. B*, 31, 1029.
Davies J.T., Vaughan J.M.: 1963, *Aph. J.*, 137, 1302.
Djeniže S., Malešević M., Srećković A., Milosavljević M., Purić J.: 1989, *JQSRT*, 42, 429.
Djeniže S., Milosavljević V., Srećković A.: 1998, *JQSRT*, 59, 71.
Dzierzega K., Musiol K.: 1994, *JQSRT*, 52, 747.
Griem H.R.:1974, *Spectral Line Broadening by Plasmas* (Academic Press, New York).
Konjević N., Wiese W.L.: 1990, *J. Phys. Chem. Ref. Data*, 19, No 6.
Kršljanin V., Dimitrijević M. S.: 1989, *Z. Phys. D*, 14, 273.
Labat J., Djeniže S., Ćirković Lj., Purić J.: 1974, *J. Phys. B*, 7, 1174.
Morris J.C., Morris, R.V.: 1970, *Report No ARL* 70-0038.
Purić J., Konjević N.: 1972, *Z. Phys.*, 249, 440.
Wiese W.L., Smith M.W., Miles B.M.: 1969, *Atomoc Transition Probabilities*, Vol II., NSRDS-NBS 22 (DC.U.S. Government Printing Office, Washington).

Journal of Research in Physics Vol. 28, No. 3, 251-254 (1999)

ON THE STARK BROADENING OF SOME Ar I SPECTRAL LINES

D. NIKOLIĆ, S. DJUROVIĆ, Z. MIJATOVIĆ, R. KOBILAROV AND N. KONJEVIĆ*
Institute of Physics, Trg Dositeja Obradovića 4, 21000 Novi Sad, Yugoslavia
**Institute of Physics, P.O.Box 68, 11080 Beograd, Yugoslavia*

1. INTRODUCTION

The investigation of the influence of Stark effect on the shape of neutral argon spectral lines has been extensive during the last three decades (Konjević and Roberts, 1976; Konjević et al., 1984), since argon is a widely available inert atomic gas which produce variety of favorable conditions for stable discharges. The determinations of quantitative spectroscopic data for argon, such as Stark broadening parameters (spectral line widths and shifts), are favorite subjects of plasma spectroscopists. In spite of these widely spread investigations, the convergence of the obtained results wasn't achieved. Namely, the different plasma sources and measurement techniques (which are sometimes quite complicated and laborious) showed, that the accuracy of 10% or better, hardly can be achieved. Moreover, even in the cases of similar experimental set-ups and methods, reported results of different authors may deviate by factors of two. In order to establish an experimental consistency within reported measurement techniques and among different experiments, obtained results are often compared with the most comprehensive theoretical predictions provided by (Griem, 1974). The several problems have been found as critical for all emission experiments, which are:

1) *Reliability of plasma source*. Ideally, the plasma source should be stationary and homogeneous. The most of the high-precision studies have been performed with stabilized arcs, as continuous plasma sources. In the case of the repetitive pulsed sources, significant reproducibility have to be provided. When the arc channel is observed side-on, reliable Abel inversion of recorded profiles should be used (see for example: Djurović,1998).

2) *Reliable plasma diagnostic approach*. The experimental conditions have to be chosen so that the plasma is approximately in a state of local thermodynamic equilibrium (LTE) and the checks for the existence of LTE have to be made repeatedly.

3) *Line intensity measurements*. The experimental techniques for spectral intensity recordings have been strongly developed during last decade with significant improvements of reliability and definition of recorded profiles (Djurović et al.,1997).

4) *Self-absorption* of spectral lines must be checked and eliminated if possible, otherwise recorded profiles must be corrected to this effect.

5) *Properly performed deconvolution* of experimental profiles. It is very important that all relevant broadening mechanisms are taken into account and represented in the form of mutually folded profiles. Parameter adjustments of such spectral line model should be performed by least-square fitting procedure (Nikolić et al., 1998).

If any of these problems is not properly handled in emission spectroscopy studies, noticeable uncertainties in the results may be introduced, which may lead to the considerable differences among reported results of various authors, as shown in Fig. 1. and Fig. 2. In these figures, experimental widths and shifts, for 12 neutral argon lines investigated in this work, are compared with theory (Griem, 1974) and other available experimental results. We suppose that all authors compared theirs result with the theoretical ones in the same manner. Noticeable scattering (for more than 200% in some cases) introduces confusion in this field and opens possibilities for new refined measurements of Stark broadening parameters of neutral argon lines in order to overcome problems listed above. In this experimental study we tried to solve these problems and to give new, more reliable results. The extended material is compiled in (Nikolić, 1998) and is available in limited number of copies.

2. RESULTS AND DISCUSSION

Theoretical Stark parameters for two of the investigated lines (419.10 nm, and 433.36 nm) do not exist, so they are not shown at Figs. 1 and 2. However, Ar I 419.10 nm spectral line is also experimentally investigated by Chapelle et al., 1967; some of the experimental papers deal with width and shift of Ar I 433.36 nm line: Musielok, 1994; Bues et al., 1969; Chapelle et al., 1967 and Gericke, 1961. There is no rule about overall agreement between any of the experiments. In some cases agreement is good, but in other cases disagreement is large. For example, the results of (Kusz and Mazur, 1996), are not shown on Figs.1 and 2, since the investigated ratios are larger then 3.00. The measured widths and shifts were corrected (up to 10%) on Van der Waals broadening effect as well as theoretical shifts (negligible for widths) on Debye shielding effect (from 11% to 19%).

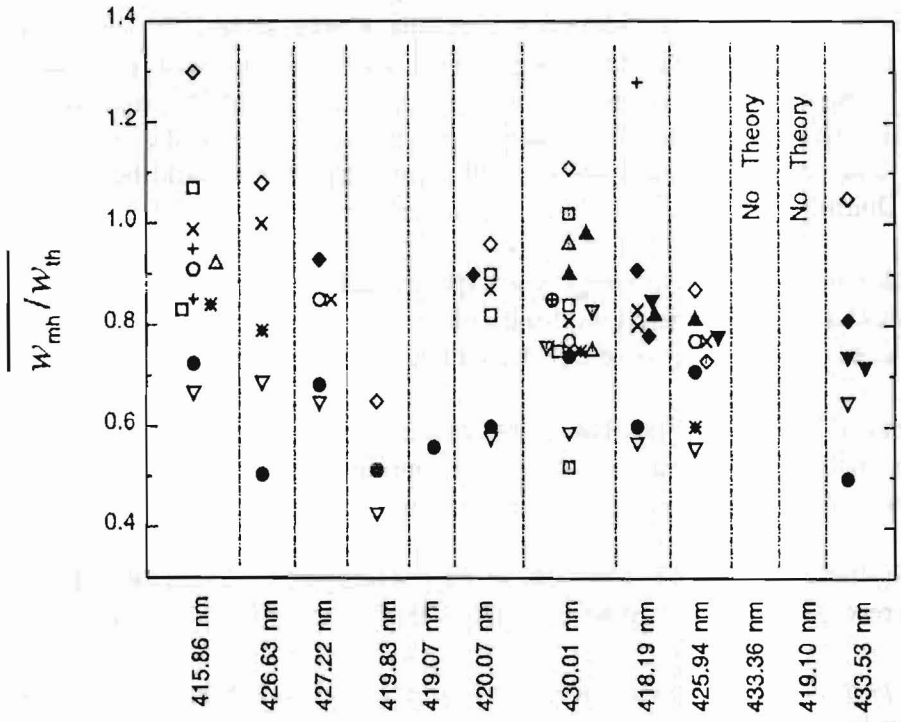

Fig. 1. The averaged ranges of compared measured (w_{mh}) and theoretical (w_{th}) Stark widths

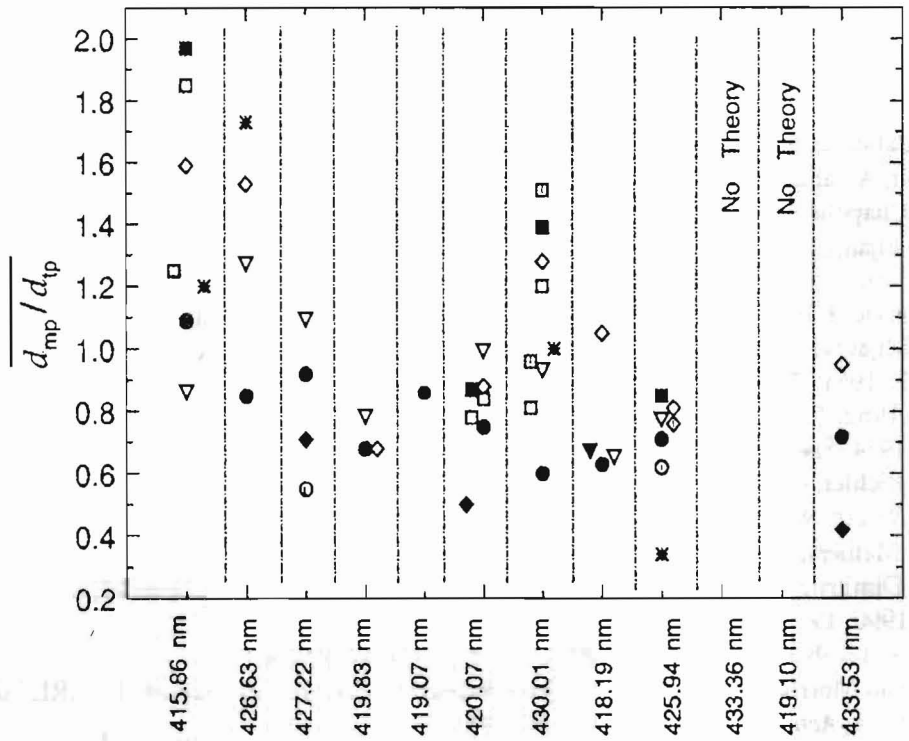

Fig. 2. The averaged ranges of compared measured (d_{mp}) and theoretical (d_{tp}) Stark shifts

The symbols, which make an appearance at given figures, represent various references used for comparing purposes and are listed below:

(●) This work;
(○) Jones et al., 1986;
(△) Jones et al., 1987;
(×) Musielok, 1994;
(✳) Powel, 1966;
(◇) Gericke, 1961;
(■) Morris and Morris, 1970;
(□) Griem, 1962;
(▽) Bues et al., 1969;
(+) Musielok et al., 1976;
(▽) Chernichowski and Chapelle,1983;
(⊙) Djeniže et al., 1995;
(◆) Chapelle et al., 1967;
(◬) Abbas et al., 1988;
(⊕) de Izarra et al., 1993;
(⊡) Queffelec and Girault, 1971;
(▲) Klein and Meiners,1977;
(▼) Schulz and Wende,1968;
(◈) Djurović et al., 1997;

The aim of this paper is to give new and reliable experimental data of Stark broadening parameters of Ar I lines and to point at necessity for new more reliable measurements. Attention was paid on precise spectral intensity recordings, wavelength measurements and procession of obtained data. The comparisons done in this work showed disagreement between other authors results as well as between experiments and theoretical predictions. Without numerous measurements of high precision, meaningful conclusions are not possible.

References

Abbas, A., Basha, T. S., and Abdel-Aal, Z. A.: 1988, *Jap. J. Appl. Phys.* **27**, 801
Bues, I., Haag, T., and Richter, J.: 1969, *Astron. & Astrophys.* **2**,249
Chapelle, J., Cabonne, Sy. A., Cabannes, F., and Blandin, J.: 1967, *J. Q. S. R. T.* **8**, 1201
Chernichowski, A., and Chapelle, J.: 1983, *Acta Phys. Pol. A* **63**, 67
de Izarra, C., Chapelle, J., Chernichowski, A., and Vallee, O.: 1993, *J. Q. S. R. T.* **49**, 433
Djeniže,S., Skuljan,Lj., and Konjević, R.:1995, *J. Q. S. R. T.* **54**, 581
Djurović, S.: 1998, *Contributed papers of 19th SPIG*, 329 (Ed. Konjević, N., Ćuk, M., and Videnović, I. R.), Faculty of Physics, University of Belgrade, Belgrade, Yugoslavia
Djurović, S., Mijatović, Z., Kobilarov, R., and Konjević, N.: 1997, *J. Q. S. R. T.* **57**, 695
Gericke, W. E.: 1961, *Z. Astrophys.* **53**, 68
Griem, H. R.: 1962, *Phys. Rev.* **128**, 515
Griem, H.R.: 1974, *Spectral Line Broadening by Plasmas*, Academic Press
Jones, D. W., Pichler, G., and Wiese, W. L.: 1987, *Phys. Rev. A* **35**, 2585
Jones, D. W., Wiese, W. L., and Woltz, L. A.: 1986, *Phys. Rev.* A **34**, 450
Klein, P., and Meiners, D.: 1977, *J. Q. S. R. T.* **17**, 197
Konjević, N., Dimitrijević,M.S., and Wiese,W.L.: 1984, *J. Phys. Chem. Ref. Data* **13**, 619; also: 1990, **19**, 1307
Konjević, N., and Roberts, J.R.: 1976, *J. Phys. Chem. Ref. Data* **5**, 209
Morris, J. C., and Morris, R. U.: 1970, *Aerospace Research Laboratories*, Report No. ARL 70-0038
Musielok, J.: 1994, *Acta Physica Polonica A* **86**, 315
Musielok, B., Musielok, J., and Wujec, T.: 1976, *Zesz. Nauk. Wyzsz. Szk. Pedag. Opolu, Fiz.* **17**, 63
Nikolić, D.: 1998, *MSc Thesis*, University of Belgrade, Belgrade (in Serbian)
Nikolić, D., Mijatović, Z., Kobilarov, R., Djurović, S., and Konjević, N.: 1998, *Contributed papers of 19th SPIG* , 191 Belgrade, Yugoslavia
Popenoe, C. H., and Shumaker Jr., J. B.: 1965, *J. of Research of NBS, Phys. and Chem.* A 69, 495
Powell, W. R.: 1966, *Ph. D. Thesis*, The John Hopkins University
Queffelec, J. L., and Girault, M.: 1971, *Rev. Phys. Appl.* **6**, 401
Schulz, P., and Wende, B.: 1968, *Zeitschrift für Physik* **208**, 116

Journal of Research in Physics Vol. 28, No. 3, 255-258 (1999)

EXPERIMENTAL STARK PARAMETERS FOR Ar I 426.63 nm AND Ar II 426.65 nm SPECTRAL LINES

D. NIKOLIĆ, S. DJUROVIĆ, Z. MIJATOVIĆ, R. KOBILAROV and N. KONJEVIĆ*
Institute of Physics, trg Dositeja Obradovića 4, 21000 Novi Sad, Yugoslavia
**Institute of Physics, P.O. Box 68, 11080 Belgrade, Yugoslavia*

1. INTRODUCTION

Large number of papers deals with shapes and shifts of plasma broadened argon lines (Konjević and Wiese, 1990 and references therein) and the reported results exhibit significant scattering. The results presented here are the part of an systematic and high precision experimental study of plasma broadened argon spectral lines. The Stark parameters of argon spectral lines emitted from wall-stabilized arc plasma can be found directly from recorded experimental profiles (Nikolić, 1998) whether they are isolated or overlapped. Experimental results are compared with theoretical predictions (Griem, 1974) in the range of electron number density $N_e \in (0.74, 2.9)\cdot 10^{22}$ m^{-3}. Such comparison exhibits discrepancy between measured and theoretical widths and shifts in the case of Ar I line, while theoretical data for Ar II line are not available.

2. EXPERIMENTAL

The emission plasma source is a wall-stabilized arc operated in argon at atmospheric pressure. For diagnostic purpose, the gas mixture containing 96% of argon and 4% of hydrogen enters the region between central part of the arc and electrode sections, and leave the arc through the outlets near electrodes with the flow rate of 0.03 l/min. The flow rate of the working gas (argon) was 3 l/min. The arc is operated at current of 30 A, supplied by an current-stabilized power supply with a 0.3% stability. The side-on observations were performed with a 1m monochromator equipped with a 1200 g/mm grating and 36000 step/rev stepping motor. The spectra are recorded by a data acquisition and processing system (Djurović et al., 1996). For the shift measurements, the emission from the Geissler tube at low-pressure argon discharge served as reference source of unshifted lines. The light from the arc plasma and from the reference source was alternatively focused onto the entrance slit of the monochromator by the means of the light chopper. An electron number density N_e in the range $(0.74, 2.9)\cdot 10^{22}$ m^{-3} is determined from the width of Balmer H_β line (Vidal et al.,1973) with overall uncertainty under 11%. As described in (White et al.,1958; Popenoe and Shumaker,1965), the electron temperature T_e in the range $(9300, 10800)$ K is obtained from plasma composition data with overall uncertainty under 5%.

3. RESULTS AND DISCUSSION

The Abel inversion procedure described in (Djurović, 1998) was applied on side-on recorded spectral line profiles. Modelling procedure (Nikolić, 1998) is used for obtaining the Stark electron widths and shifts, ion-broadening parameter as well as Stark full halfwidths (w_m). The spectral line profiles from the reference source were fitted to Gaussian profiles by least square method. The shift of plasma broadened lines is measured at the maximum (d_{mp})

of the extracted $j_{A,R}(x)$ profile and as electron shift d_e of extracted Lorentzian profile in the case of Ar II line . The experimental results of w_m, d_{mp} are represented in Table 1 along with available theoretical (semiclassical) (Griem, 1974) full halfwidths w_t and shifts d_{tp}.

Table 1. Measured and theoretical values for Stark widths and shifts

N_e (10^{22} m^{-3})	T_e (K)	Ar I 426.63 nm				Ar II 426.65 nm	
		w_m (0.1 nm)	w_m / w_t	d_{mp} (0.1 nm)	d_{mp} / d_{tp}	w_e (0.1 nm)	d_e (0.1 nm)
2.90	10760	0.280	0.45	0.177	0.80	0.262	0.179
2.82	10730	0.276	0.45	0.174	0.81	0.258	0.177
2.70	10700	0.267	0.46	0.166	0.80	0.250	0.174
2.46	10550	0.258	0.49	0.164	0.86	0.243	0.163
2.15	10400	0.231	0.50	0.142	0.84	0.214	0.151
1.90	10250	0.202	0.50	0.123	0.82	0.198	0.137
1.60	10050	0.189	0.56	0.116	0.90	0.179	0.122
1.40	9900	0.161	0.55	0.096	0.85	0.159	0.107
1.20	9720	0.146	0.58	0.089	0.91	0.133	0.096
0.98	9520	0.121	0.60	0.075	0.93	0.119	0.084
0.83	9400	0.112	0.66	0.064	0.93	0.099	0.068
0.74	9280	0.101	0.67	0.059	0.96	0.092	0.061

The measured widths and shifts are corrected for Van der Waals broadening (Griem, 1974), while resonance broadening effects are found negligible. The theoretical shifts are corrected for the Debye shielding effects (Griem, 1974). The error for both, halfwidth and shift measurements is estimated from under 8% to under 15% ranging from the highest to the lowest electron number densities. Figure 1 represents the temperature dependence of ratio of measured and theoretical shifts for Ar I 426.63 nm line. Weighted linear regression gives relatively weak temperature influence either for this work only (greater slope) or with the respect to all available results of other authors (smaller slope).

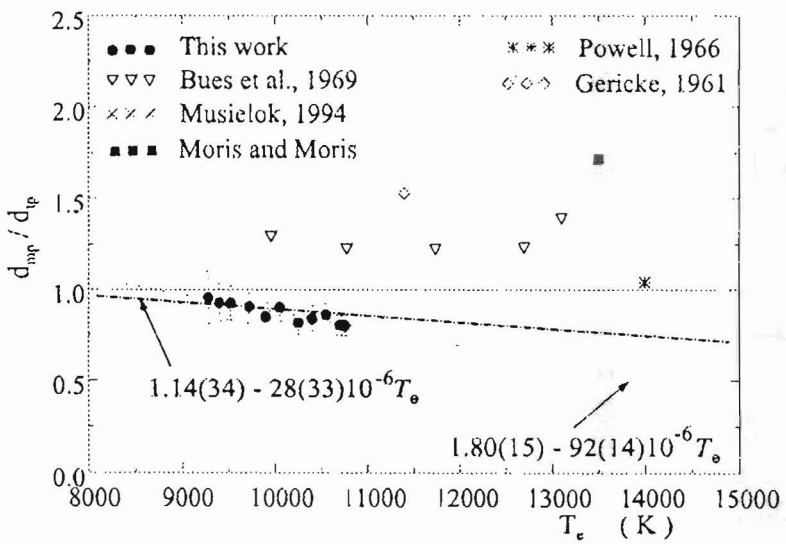

Fig. 1. Temperature dependence of measured to theoretical shifts ratio for Ar I 426.63 nm

Figure 2 gives the temperature dependence of ratio of measured and theoretical widths for Ar I 426.63 nm line. Weighted linear regression suggests relatively stronger (compared to shifts) temperature influence either for this work only (greater slope) or with the respect to all available results of other authors (smaller slope). According to (Nikolić, 1998), in the case of the Ar I 426.63 nm line, weighted mean for the d_{mp} / d_{tp} ratio is 0.85(2), while for w_m / w_t this value is 0.51(1).

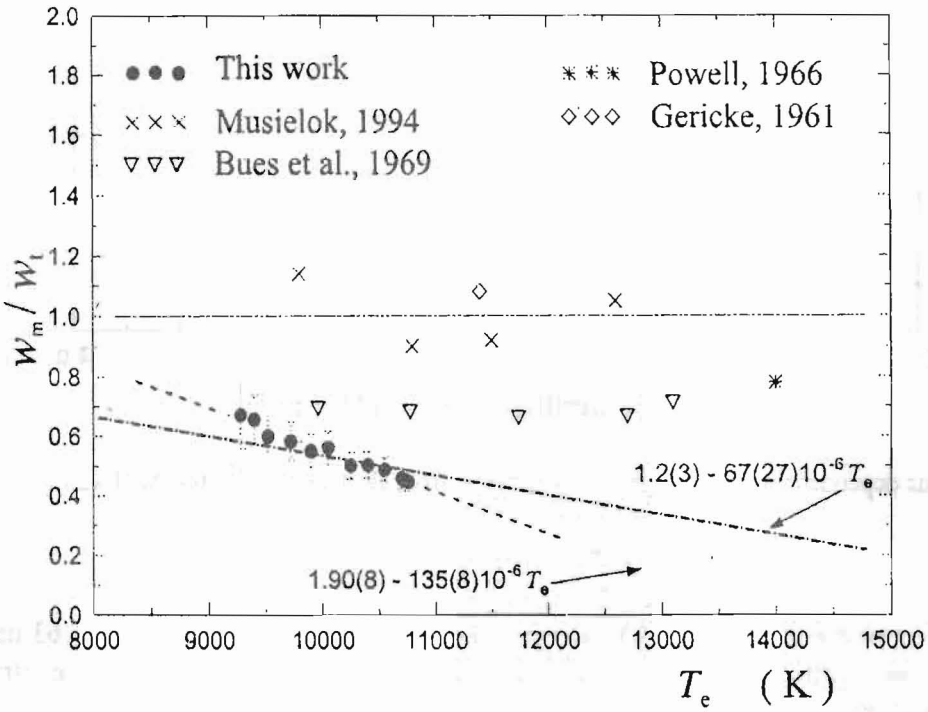

Fig. 2. Temperature dependence of measured to theoretical widths ratio for Ar I 426.63 nm

From the Figs. 1 and 2 it is obvious that results of the other authors are significantly scattered and systematically higher than values obtained in this work. Possible reason is due to overlapping of these close Ar I and Ar II spectral lines. The overlapping was detected from the fact that the red wing asymmetry of the recorded profile increases as electron number density decreases. Satisfactory fitting (Nikolić, 1998) of such experimental profiles is achieved only with the assumption of the existence of a close Ar II 426.65 nm line.

Figure 3 shows confirmed linear dependence of electron Stark widths and shifts from electron number density for Ar II 426.65 nm line. Due to lack of theoretical predictions (Griem, 1974), comparisons with the respect to the theory are not presented. Since the spectral lines of the single ionized atoms can be modelled with Voigt profiles (Griem, 1974), extracted Stark profile is of Lorentzian type, so the full measured halfwidth is: $w_m = 2 \cdot w_e$, while the measured shift at the maximum is $d_{mp} = d_e$.

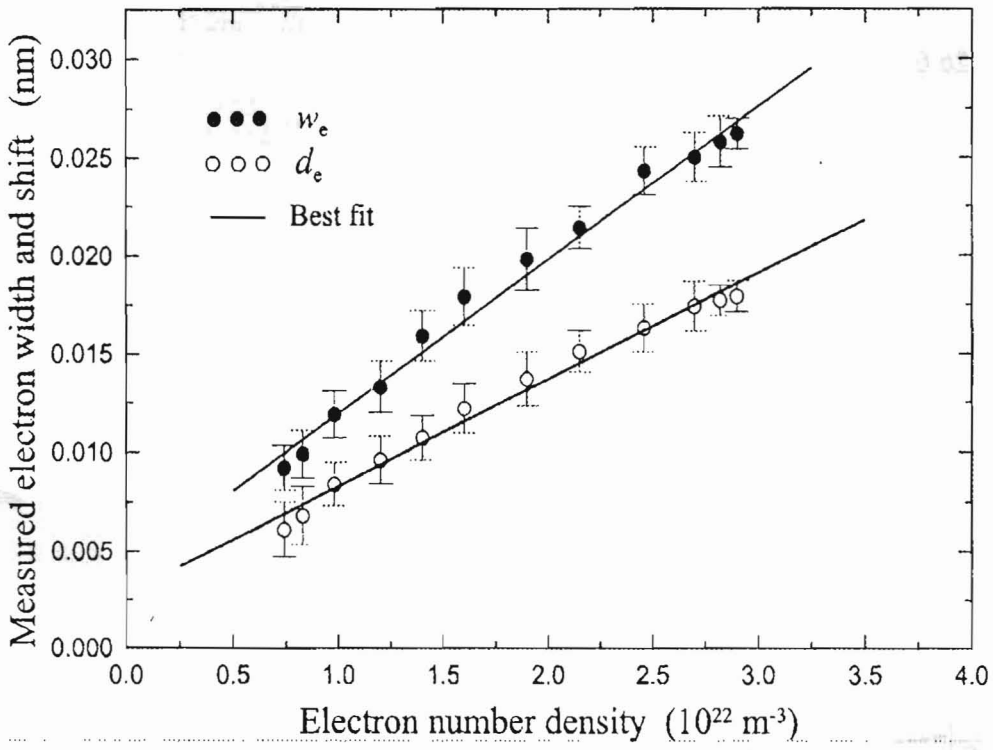

Fig. 3. Linear dependence of electron widths and shifts from electron density for Ar II 426.65 nm

The presence of Ar II 426.65 nm spectral line on the red wing of Ar I 426.63 nm line has to be taken into account, specially at high electron densities where the stronger overlapping effects can occurred.

References

Bues, I., Haag, T. and Richter, J.: 1969, *Astron. & Astrophys.* **2**, 249
Djurović, S.: 1998, *Contributed Papers of the 19th SPIG*, 329, Faculty of Physics, Belgrade
Djurović, S., Kobilarov, R., and Vujičić, B.: 1996, *Bull. Astron. Belgrade* **153**, 41
Gericke, W.E.: 1961, *Z. Astrophys.* **53**, 68
Konjević, N., and Wiese, W.L.: 1990, *J. Phys. Chem. Ref. Data*, **19**, 1307
Moris, J.C., and Moris, R.U.: *Aerospace Research Laboratories*, Report No. ARL 70-0038
Musielok, J.: 1994, *Acta Physica Polonica A* **86**, 315
Nikolić, D.: 1998, *Msc Thesis*, University of Belgrade, Belgrade.
Popenoe, C.H., Shumaker, J.B. Jr. : 1965, *J. of Research of NBS, Phys. and Chem. A* **69**, 495
Powel, W.R.: 1966, *Ph. D. Thesis*, The John Hopkins University
Vidal, C.R., Cooper, J., and Smith, E.W.: 1973, *Astrophys. J. Suppl. Ser.* **214**, 25
White, W.B., Jonson, S.M., and Dantzig, G.B.: 1958, *J. Chem. Phys.* **28**, 751

Journal of Research in Physics Vol. 28, No. 3, 259-261 (1999)

ION-BROADENING PARAMETER FOR C I 505.2 nm SPECTRAL LINE

D. NIKOLIĆ, Z. MIJATOVIĆ, S. DJUROVIĆ, R. KOBILAROV AND N. KONJEVIĆ*
Institute of Physics, Trg D. Obradovića 4, 21000 Novi Sad, Yugoslavia
**Faculty of Physics, P.O. Box 368, 11001 Belgrade, Yugoslavia*

1. INTRODUCTION

Usualy measured Stark parameters of plasma broadened neutral atom lines are the halfwidths and the shifts. Third, very important parameter - ion-broadening parameter A has been measured very rarely. There are only a few papers which reported measured values of A for Ar I, N I and C I spectral lines (Jones and Wiese, 1984; Jones et al, 1986 I; Jones et al, 1986 II; Nikolić et al, 1998). The importance of this parameter lies in the fact that it is the meausre of asimetry of the neutral spectral lines, so it's value influences widths and shifts of the lines. Approximate expressions for width and shift (at the peak of the profile) of neutral spectral lines are (Griem, 1974; Konjević and Roberts, 1974):

$$w = 2w_e[1 + 1.75 \cdot 10^{-4} N_e^{1/4} A(1 - 0.068 N_e^{1/6} T_e^{-1/2})] N_e \cdot 10^{-16} \quad (1)$$

$$d = [d_e \pm 2.00 \cdot 10^{-4} N_e^{1/4} A w_e (1 - 0.068 N_e^{1/6} T_e^{-1/2})] N_e \cdot 10^{-16} \quad (2)$$

where w_e and d_e are electron impact width and shift, respectively, N_e is the plasma electron density in cm^{-3} and T_e is the electron temperature. Parameter A depends on the electron density like:

$$A = A_N N_e^{1/4} \cdot 10^{-4} \ . \quad (3)$$

Experimentaly obtained values for widths and shifts have always been compared to the theoretical ones obtained from Eqs. (1) and (2). Value for A which enters Eqs. (1) and (2) is taken from corresponding theory (Bassalo et al. 1982, and Griem, 1974 for He I lines, and Griem, 1974 for other lines). As it can be seen from (1) and (2) such comparison can give wrong picture since values of A has not been checked. The methods for determination of A used by other authors (see references in Nikolic, 1999) are different. Here we will make comparison with the results obtained by Jones and Wiese (1984). Their method is based on fitting procedure of symetric Lorentzian to the experimental ones. The procedure applied in this work is based on fitting procedure of the theoretical profiles to the experimental ones. It has been applied earlier to several Ar I lines (Nikolić, 1998; Nikolić et al., 1998) while this is an application to the line of other element - carbon.

Pure Stark profile of broadened line is described by $j_{A,R}(x)$ function:

$$j_{A,R}(x) = \frac{1}{\pi} \int_0^\infty \frac{W_R(\beta)}{1 + (x - A^{4/3}\beta^2)^2} d\beta \quad (4)$$

where β is reduced electric plasma microfield and $W_R(\beta)$ is it's distribution.

2. EXPERIMENTAL

Spectral profiles of C I 505.2 nm line were recorded from the wall stabilized arc plasma. The detailed experimental procedure is described elsewhere (Mijatović et al., 1995). One example of recorded profile is presented in Fig. 1. As one can see from this

example, line profile is very well defined what is of great importance for the accuracy of fitting procedure.

3. FITTING PROCEDURE

This procedure is based on fitting the parameters of theoretical profile to the experimental one. In this case, the theoretical profile is the convolution of $j_{A,R}(x)$ (Eq. (4)) function and Gaussian arrising from Doppler and instrumental broadening. Details of this procedure could be found elsewhere (Nikolić et al., 1999; Nikolić et al., 2000). Solid line in Fig. 1 presents fitted profile. It could be seen that obtained function describes experimental profile satisfactorilly. Certain dissagreements exists at the parts of the line wings of the experimental profile.

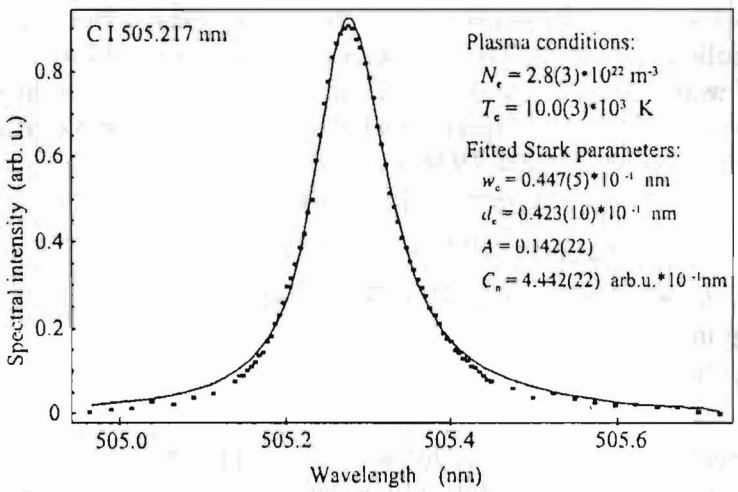

Fig. 1 An example of experimental and fitted profile.

4. RESULTS

One of the fiited parameter in above mentioned procedure is the ion-broadening parameter A. Obtained values of A for CI 505.2 nm at two electron densities are given in Table 1 together with the theoretical values A_G (Griem, 1974) and other experimental results A_{JWW} (Jones and Wiese, 1984). Graphically these results are presented in Fig. 2.

Table 1. Measured and theoretica values of A.

T (K)	N_e (10^{22} m^{-3})	$N_e^{1/4}$ (10^5 m$^{-3/4}$)	A	A_G	A_{JWW}
9700(290)	2.2(2)	3.85(9)	0.091(14)	0.07724	0.094(14)
9700(290)	2.2(2)	3.85(9)	0.116(18)	-	-
10000(300)	2.8(3)	4.11(9)	0.142(22)	0.08185	0.100(15)
10000(300)	2.8(3)	4.11(9)	0.158(24)	-	-
10000(300)	2.8(3)	4.11(9)	0.160(24)	-	-
10000	2.56	4	-	0.07617	0.097(15)

*Values were obtained at T=11600 K

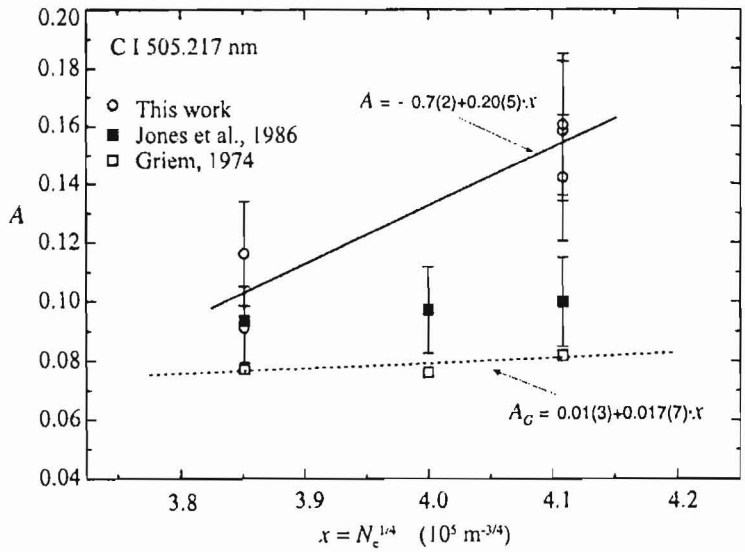

Fig. 2 Obtained values of a parameter A vs $N_e^{1/4}$

As it can be seen resultes obtained in this work are somewhat higher than other experimental and theoretical results. The error of parameter A determination is estimated to be about 15 % (Nikolić et al., 1998). The error is mainly caused by the scattering of the measured points of experimantal profiles. Dissagreement between results obtained in this work and results obtained by Jones end Wiese (1984) is significant (outside error limits).The reason for this could be found in different methods used for for the determinetion of A. In the future work, both methods should be applied to the same experimental profiles and in this way make comparison between them.

References

Bassalo J. M., Cattani M., and Walder V. S.: 1982, *JQSRT*, **28**, 75
Griem H. R.: 1974, *Spectral Line broadening by Plasmas*, Academic, New York.
Jones D. W., Pichler G. and Woltz L. A.: 1986, *Phys. Rev. A* **35**, 2585.
Jones D. W. and Wiese W. L.:1984, *Phys. Rev. A* **30**, 2602.
Jones D. W., Wiese W. L. and Woltz L. A.: 1986, *Phys. Rev. A* **34**, 450.
Konjević N. and Roberts J.R.: 1976, *J. Phys. Chem. Ref. Data*, **5**, 209.
Mijatović Z., Konjević N. Kobilarov R. and Djurović S.: 1995, *Phys. Rev. E* **51**, 613.
Nikolić D.: 1998, MSc Thesis, Faculty of Physics, University of Belgrade.
Nikolić D., Djurović S., Mijatović Z., Kobilarov R. and Konjević N.: 1998, *J. Res. Phys.*, **27**, 133.
Nikolić D. et al: 1999, *Invited Lecture at this Conference*
Nikolić D. et al: 2000, Accepted for publication in JQSRT

Journal of Research in Physics Vol. 28, No. 3, 263-266 (1999)

CHARACTERISTIC LINE PROFILE PARAMETERS OF HYDROGEN BALMER LINES IN AN EXTERNAL ELECTRIC FIELD

I. R. VIDENOVIĆ
Faculty of Physics, University of Belgrade, P.O.Box 368, 11000 Belgrade, Yugoslavia

1. INTRODUCTION

Several recently reported measurements of the electric field strength distribution in the cathode fall region of a glow discharge (Barbeau and Jolly, 1991; Ganguly and Garscadden, 1991; Donkó et al., 1994; Videnović et al., 1996; Kuraica et al., 1997) have employed the polarization-dependent Stark splitting coupled with Doppler broadening of hydrogen Balmer lines. In most of these studies, to determine local electric field strength the thorough theory of linear Stark effect is used. However, for some purposes the knowledge of line profile parameters only, e.g. the wavelength distance $\Delta\lambda_{pp}$ between most distinguished maximums (Kuraica et al., 1997) or the profile halfwidth $\Delta\lambda$ (Videnović et al., 1996), was good enough to obtain local electric field strength with sufficient accuracy. In this paper we extend the possibility of an ad-hoc local electric field and excited hydrogen atoms temperature determination to the usage of third characteristic profile parameter - the intensity ratio between the maximum and the center of the profile, I_{max}/I_c. This study is confined to the 0 – 20 kV/cm range of electric field strengths and 0.1 – 300 eV interval of excited hydrogen temperatures, which are the conditions that are shown to be typical for the cathode fall region of a glow discharge (see e.g. Videnović et al., 1996; Kuraica et al., 1997).

2. THEORY

Following either semiclassical or quantum mechanical theory of the linear Stark effect applied to the hydrogen and hydrogen-like emitter one obtains the known result that each energy level is splitted into equidistant sub-levels (Condon and Shortley, 1977). Therefore, the hydrogen spectral lines consist of numerous components which are polarized either linearly, parallel to the vector of external field $\vec{F}$ (π-components), or circularly, in the plane perpendicular to $\vec{F}$ (σ-components). The relative wavelength positions of these components are proportional to the electric field strength and form the characteristic symmetrical Stark patterns (Condon and Shortley, 1977). The fine structure splitting introduces the asymmetry in the Stark patterns of hydrogen lines. To calculate the eigenvectors and eigenvalues of the hydrogen atom, the perturbed Hamiltonian

$$H_n = H_{0n} + q\vec{F}\cdot\vec{R}_n \tag{1}$$

is used, where $\vec{F} = (0,0,F)$ is the perturbing electric field pointing along OZ axis, H_{0n} is the Hamiltonian of the hydrogen atom including the fine structure and $\vec{R}_n$ is the projection of the distance operator $\vec{R}$ on the space of the states with main quantum number n (no-quenching approximation). The eigenstates of the whole Hamiltonian H_n are defined by the relationship

$$H_n|v\rangle = E_v|v\rangle . \tag{2}$$

To carry out the numerical calculation, the basis of H_{0n} eigenstates $|n,j,l,m_j\rangle$ is used. The evolution operator of the group of states with main quantum number n for a given configuration of the static electric field $\vec{F}$ is given by:

$$U_n(t) = \exp\left(-\frac{i}{\hbar}H_n t\right) = \sum_\nu P_\nu \exp\left(-\frac{i}{\hbar}E_\nu t\right). \tag{3}$$

The intensities of the components of the transition $n \rightarrow n'$ are given by the relationship (Gigosos and González, 1998)

$$I_{nn'} = 2\,\mathrm{Re}\,\mathrm{tr}(\vec{d}_{n'n}\cdot U_n^+ \vec{d}_{nn'} U_{n'}), \tag{4}$$

where $\vec{d}_{nn'}$ is the nn' box of the atom dipole momentum operator that connects the group of states n with the n' one. Using (5), one obtains

$$I_{nn'} = 2\,\mathrm{Re}\sum_\nu\sum_{\nu'}\exp\left[-\frac{i}{\hbar}(E_\nu - E_{\nu'})t\right]\mathrm{tr}\,(\vec{d}_{n'n}\cdot P_\nu \vec{d}_{nn'} P_{n'}), \tag{5}$$

where P_ν is the projector on the subspace of states with eigenvalue E_ν. By using the Z component of the vector $\vec{d}_{nn'}$, the intensities of π transitions are obtained, while X and Y components yield the intensities of σ transitions. In the numerical modeling of Stark profiles of hydrogen lines we assumed that plasma broadening effects in the cathode fall region of a glow discharge may be neglected and to the each Stark component we have assigned a Gauss function only which takes into account the instrumental and Doppler broadening (see Videnović et al., 1996). The overall π or σ polarized profile are calculated as the superposition of all components polarized in the appropriate manner.

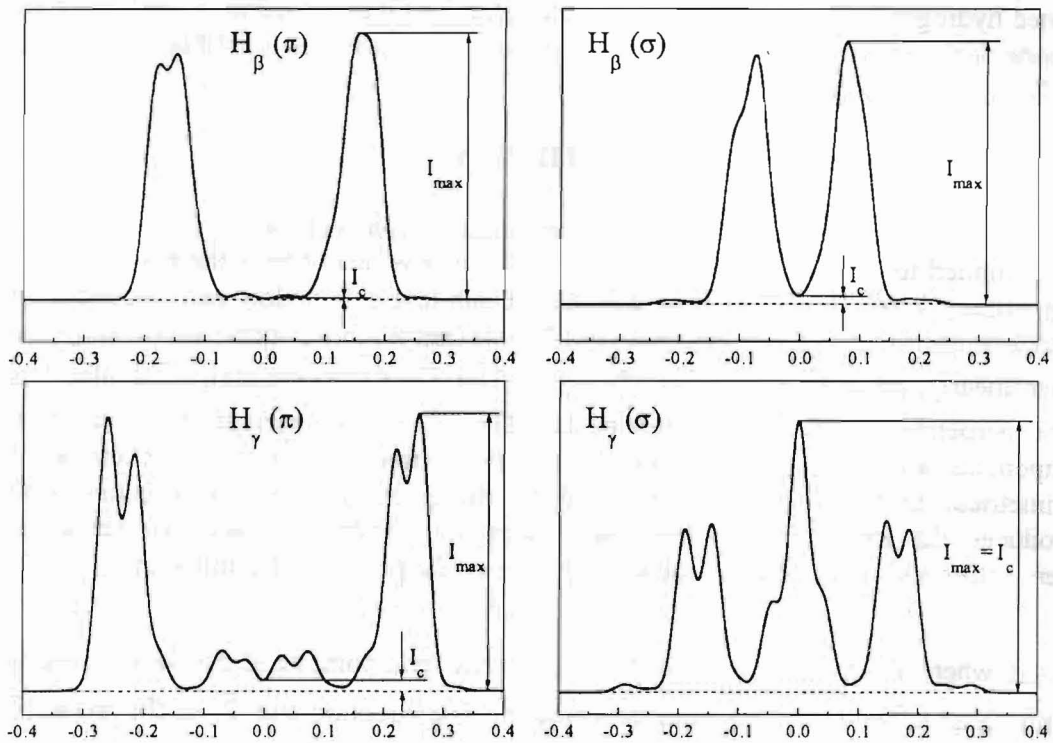

Fig. 1. Polarized Stark H_β and H_γ profiles, calculated upon the fine structure manifold, for the electric field strength of 12 kV/cm and the excited H-atoms temperature of 1 eV. On the abscissa axes relative wavelengths related to the unperturbed line (in nm) are given. Characteristic maximum I_{max} and central I_c intensities are defined also.

3. RESULTS AND DISCUSSION

The examples of the polarized profiles of the hydrogen Balmer H_β and H_γ lines, calculated following the fine structure manifold, for the electric field strength of 12 kV/cm and the excited hydrogen atoms temperature of 1 eV, are shown in Fig. 1. These conditions are selected as being of order typical for the cathode fall region of a glow discharge, see Videnović et al., 1996. For all profiles the intensities I_{max} and I_c. are defined. Obviously, for the $H_\gamma(\sigma)$ profile the ratio between these intensities is not applicable.

The temperature dependencies of the I_{max}/I_c ratio for the $H_\beta(\pi)$, $H_\beta(\sigma)$ and $H_\gamma(\pi)$ polarized profiles, at several electric field strengths in the range 0 – 20 kV/cm are shown in Figures 2, 3 and 4, respectively. For all profiles, with the temperature increase, the Stark splitting is overlapped with the Doppler broadening and profiles degenerate into single Gaussian, leading to the intensity ratio I_{max}/I_c value of 1.

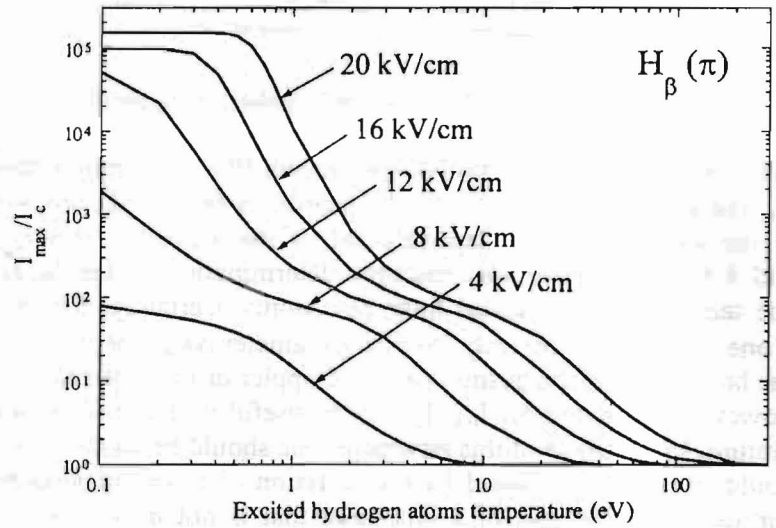

Fig. 2. Temperature dependencies of the intensity ratio I_{max}/I_c of the π-polarized H_β profile for several electric field strengths.

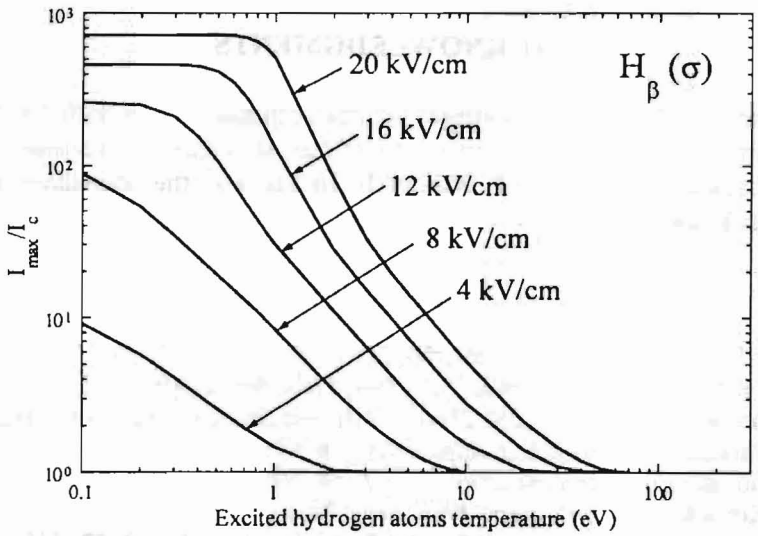

Fig. 3. Same as in Fig. 2, but for the σ-polarized H_β profile

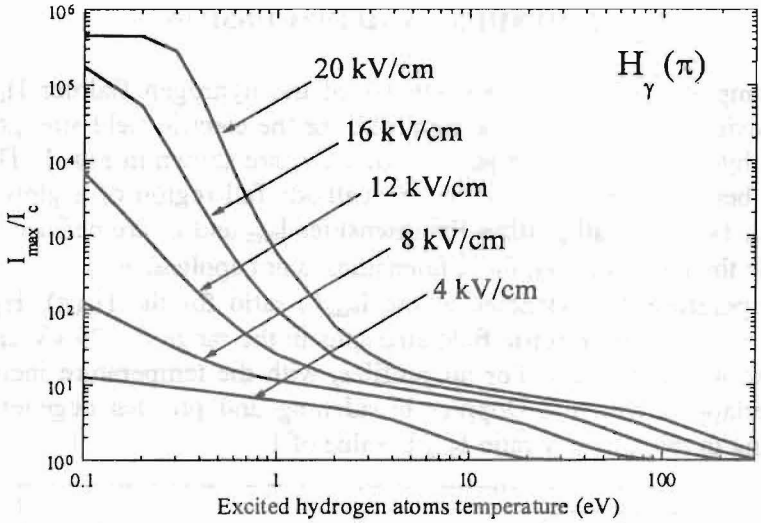

Fig. 4. Same as in Fig. 2, but for the π-polarized H_γ profile.

In conjunction with other line profile parameters (the wavelength distance between maximums $\Delta\lambda_{pp}$, see Kuraica et al., 1997, or the profile halfwidth $\Delta\lambda$, see Videnović et al., 1996) one may use the temperature dependencies of the intensity ratio I_{max}/I_c shown in figures 2, 3, and 4 for the ad-hoc spectroscopic determination of the local electric field intensity and the temperature of excited hydrogen atoms. Certainly, for the electric field determination, one should mostly rely to the parameter $\Delta\lambda_{pp}$, because it is the least dependent on the broadening mechanisms, such as Doppler or instrumental ones. For known electric field, however, the parameter I_{max}/I_c may be useful in determination of the excited H-atoms temperature. In the usage of this parameter one should be cautious, bearing in mind that its value could be strongly affected by the emission of so-called *field-free* lines – the lines that are emitted from the part of a discharge that is not under the influence of the external electric field (see e.g. Videnović et al., 1996; Kuraica and Konjević, 1997; Kuraica et al., 1997). These lines are detected at the central wavelength position, making the parameter I_{max}/I_c inapplicable.

ACKNOWLEDGMENTS

The author gratefully acknowledges private communication with Dr. Marco Antonio Gigosos who kindly provided the calculations of fine structure components and intensities. The valuable discussions with Prof. Nikola Konjević and the assistance of Mirjana M. Platiša are also acknowledged.

References

Barbeau C., Jolly J. : 1991, *Appl. Phys. Lett.*, **58**, 237.
Donkó Z., Rózsa K., Tobin R. C., Peard K. A. : 1994, *Phys. Rev. E*, **49**, 3283.
Condon E. U., Shortley G. H. : 1977, *The Theory of Atomic Spectra*, University Press, Cambridge.
Ganguly B. N., Garscadden A. : 1991, *J. Appl. Phys.*, **70**, 621.
Gigosos M. A., González M. A. : 1998, *Phys. Rev. E*, **58**, 4950.
Kuraica M. M., Konjević N. : 1997, *Appl. Phys. Lett.*, **70**, 1521.
Kuraica M. M., Konjević N., Videnović I. R. : 1997, *Spectrochim. Acta B*, **52**, 745.
Videnović I. R., Konjević N., Kuraica M. M. : 1996, *Spectrochim. Acta B*, **51**, 1707.

Journal of Research in Physics Vol. 28, No. 3, 267-269 (1999)

THE ASYMMETRY OF THE H_β LINE PROFILE

I. SAVIĆ, S. DJUROVIĆ, B. VUJIČIĆ, R. KOBILAROV
Institute of Physics, Trg Dositeja Obradovića 4, 21000 Novi Sad

1. INTRODUCTION

The profile of the Balmer H_β line is very important for plasma diagnostic purposes. It is well known that H_β spectral line profile emited from plasmas is asymmetric and red shifted (Wiese et al., 1972). Many experiments showed that H_β line has asymmetrical profile, especially in the intensity difference between blue and red peaks (Helbig and Nick, 1981; Mijatović et al., 1987; Halenka, 1988). Other experiments treated line widths (Wiese et al., 1972) or line wings (Bengtson and Chester, 1976) separately. The experimental results (Wiese et al., 1972; Mijatović et al., 1991) showed that H_β line has a red shift also. The most of theoretical calculations, see for example Kepple and Griem, (1968) and Vidal et al., (1973), give symmetrical and unshifted hydrogen line profiles. However, theoretical calculations developed by Demura (1974), give asymmetrical hydrogen line profiles.

In this work comparison between theoretical and experimental H_β line profile is given.

2. EXPERIMENT

The details of the experiment are given elsewhere (Mijatović, 1995). Briefly, the plasma source was magnetically driven T-tube 27 mm in diameter and supplied with a reflector. The T-tube was energized by using a 4 μF capacitor bank charged up to 20 kV. The filling gas was hydrogen at a pressure of 300 Pa. Spectroscopic observations of the plasma were made by 1m monochromator. The point of observation was 4 mm in front of the reflector. The photomultiplier signals were recorded by an oscilloscope equipped with a 35 mm camera. The H_β profiles was scanned at close intervals by using successive discharges over the wavelength range ± 30 nm from the line center.

The electron density of 2.92 10^{23} m^{-3} was determined from H_β halfwidth using Kepple and Griem, (1974) theory. Electron temperature of 21300 K was determined from line-to-continuum intensity ratio of the H_β line (Griem, 1964).

3. RESULTS AND DISCUSSION

Here we analyzed asymmetry of the Balmer H_β spectral line profile and compared the profile with theoretical ones (Griem, 1974; Demura, 1974) (Fig. 1). The experimental profiles are always asymmetrical what is illustrated in Fig. 1 on the 0.8, 0.7, 0.6, 0.5, 0.4, 0.3, 0.2 and 0.1 of the maximum of the H_β profile. Theoretical calculations performed by Griem, (1974) and Vidal et al., (1973) which were usually used for plasma diagnostic purposes give symmetrical profiles. These theoretical profiles are also considerable deeper

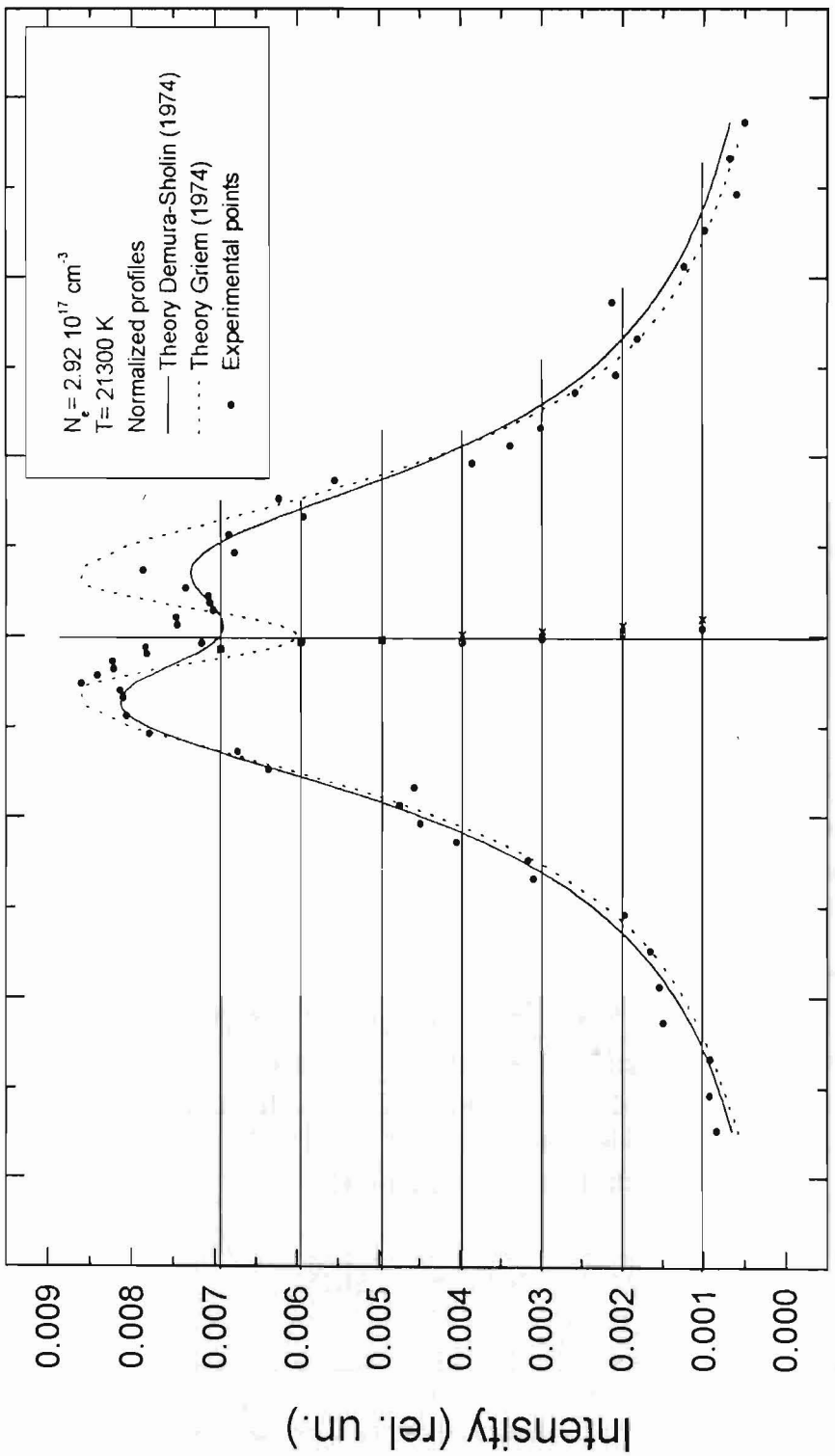

Figure 1. H_β Spectral line profile: theoretical (Griem 1974), (Demura 1974) and experimental profile.

on the line center then experimental profiles. The electron concentration is determined from the H_β halfwidth i. e. from comparison of experimental and theoretical (Griem, 1974; Vidal et al., 1973) halfwidths. In that case determination of the continuum level is very important, but it is difficult to perform it precisely. Uncertainty in continuum determination influences uncertainty in halfwidth determination. The better way for electron density determination should be halfwidth determination from fitting procedure. This is attempt to improve electron density determination.

Comparison of experimental and theoretical profiles calculated by Demura, (1974) shows better agreement then comparison with other theoretical profiles (Griem, 1974; Vidal et al., 1973). Theoretical profile (Demura, 1974) is asymmetrical and better describes peak intensities (Fig. 1).

From Fig. 1 one can see that line centers of the line width, measured on the different intensity positions, change the sign in halfwidth region in comparing with symmetrical line center (Griem, 1974; Vidal et al., 1973).

References

Bengtson, R. D. and Chester, G. R.: 1976, *Phys. Rev. A* **13**, 1762.
Demura, A. V. and Sholin, G. V.: 1974, *J. Quant. Spectrosc. Radiat. Transfer* **15**, 881.
Halenka, J.: 1988, *J. Quant. Spectrosc. Radiat. Transfer* **39**, 347.
Helbig, V. and Nick, K. P.: 1981, *J. Phys. B* **14**, 3573.
Griem, H. R.: 1964, *Plasma Spectroscopy*, McGraw-Hill, New York.
Griem, H. R.: 1974, *Spectral Line Broadening by Plasmas*, Academic Press, New York and London.
Kepple, P. and Griem, H. R.: 1968, *Phys. Rev.* **173**, 317.
Mijatović, Z., Pavlov, M. and Djurović, S.: 1987, *J. Quant. Spectrosc. Radiat. Transfer* **38**, 209.
Mijatović, Z., Pavlov, M. and Djurović, S.: 1991, *Phys. Rev. A* **43**, 6095.
Mijatović, Z., Djurović, S., Pavlov, M., Kobilarov, R. and Vujičić, B. T.: 1995, *Contrib. Plasma Phys.* **35**, 453.
Vidal, C. R., Cooper, J. and Smith, E. W.: 1973, *Astrophys. J. Suppl. Ser.* **25**, 37.
Wiese, W. L., Kelleher, D. E. and Paquette, D. R.: 1972, *Phys. Rev. A* **6**, 1132.

Journal of Research in Physics Vol. 28, No. 3, 271-273 (1999)

THE DECONVOLUTION OF SPECTRAL LINE PROFILES OBTAINED BY FABRY-PEROT INTERFEROMETER

B. KANTAR, N. M. ŠIŠOVIĆ AND M. PLATIŠA
Faculty of Physics, University of Belgrade, P.O. Box 368, 11001 Belgrade, Yugoslavia

1. INTRODUCTION

The Fabry-Perot interferometer is an instrument with high luminosity-resolution product and is widely used in optical spectroscopy. In addition, it is one of a few spectroscopic instruments for which analytic approximation to its apparatus function is known with a high accuracy. If the spectral source line shape is known, the shape observed by means of Fabry-Perot interferometer can be described as a convolution of spectral source line profile and its instrumental function. At the low perturbing gas pressure, the spectral source line shape is often approximated by well-known Voigt profile $I_V(\lambda)$ which is convolution of the Gaussian $I_D(\lambda)$ and Lorentzian $I_L(\lambda)$ distributions:

$$I_V(\lambda) = I_L(\lambda) \otimes I_D(\lambda) = \int_{-\infty}^{+\infty} d\lambda' I_L(\lambda - \lambda') I_D(\lambda')$$

If we assume that there is no correlation between collisional and Doppler broadening, then the line shape obtained by means of Fabry-Perot interferometer is a convolution of the Airy instrumental function and the Voigt profile. Following Balik (1966), this convolution can be given in an analytical form:

$$I(\lambda) = A\left\{\frac{1}{2} + \sum_{n=1}^{\infty} R^n \exp(-nL)\exp(-n^2 D^2/4)\cos\left[\frac{2\pi n}{\Delta\lambda_s}(\lambda - \lambda_o + \Delta)\right]\right\} \qquad (1)$$

where

$$D = \frac{\pi}{\Delta\lambda_s}\frac{\Delta\lambda_D}{\sqrt{\ln 2}} \; ; \; L = \frac{\pi}{\Delta\lambda_s}\Delta\lambda_L \qquad (2)$$

where: $\Delta\lambda_D$ and $\Delta\lambda_L$ are full halfwidths of Gaussian and Lorentzian fractions, respectively; $\Delta\lambda_s$ is free spectral range of Fabry-Perot interferometer; R is reflectivity of Fabry-Perot interferometer plates; Δ is the shift of the maximum with respect to the unperturbed wavelength λ_o; A is normalizing factor and I is normalized intensity.

The Gaussian fraction of Voigt profile gives the information about gas kinetic temperature of the discharge, while Lorentzian fraction describes the pressure broadening of the spectral line. In order to obtain parameters of the broadening (widths and shifts) it is necessary to apply deconvolution procedure to experimental line profiles.

Until recently, the graphical method for deconvolution of spectral line profiles scanned by piezoelectricaly driven Fabry-Perot interferometer from the relative widths (Platiša et al., 1983) is employed in our laboratory (Kuraica and Konjević, 1992; Šišović et al., 1995). However, we have found that its application is particularly difficult in case of overlapping lines.

In this paper we present a method for deconvolution of overlapping lines caused by two close spectral lines and/or by isotope components spectral lines of an inert gas. This deconvolution method uses software package MS Visual Studio 6.0. To optimize fitting

parameters values, Marquardt-Levenberg algorithm for χ^2 merit function minimisation is applied (Marquardt, 1963).

The method is tested on examples of atomic lines of natural neon. The model profiles match experimental data very well.

2. CALCULATIONS

Let assume that the measurements of line shapes are performed using natural neon which is mixture of ^{20}Ne (90.92%), ^{21}Ne (0.257%) and ^{22}Ne (8.823%) isotopes. In the good approximation the contribution of the ^{21}Ne isotope to the observed intensity can be omitted so that the overall shape is the superposition of two isotope components. The model function, which is fitted to the overall experimental shape, can be written as:

$$I(\lambda) = BL + A\sum_{k=1}^{2} a_k \left\{ \frac{1}{2} + \sum_{n=1}^{\infty} R^n \exp(-nL)\exp(-n^2 D^2/4)\cos\left[\frac{2n\pi}{\Delta\lambda_s}(\lambda - \lambda_0 + \Delta + d_k)\right]\right\} \quad (3)$$

where: BL is the base line value, a_k is the relative intensity of the k-th component of a line ($\Sigma a_k=1$), A is a normalizing factor independent of the wavelength λ, and R is reflectivity of Fabry-Perot interferometer plates. In Eq. (3): $L=(\pi\Delta\lambda_L)/(\Delta\lambda_s)$; $D=(\pi\Delta\lambda_D)/(\Delta\lambda_s(ln2)^{1/2})$; $\Delta\lambda_s$- the free spectral range of the Fabry-Perot interferometer; λ_o- the unperturbed wavelength of the line; Δ- the shift of the maximum with respect to the unperturbed wavelength λ_o; d_k- the isotope shift of the k-th component; $\Delta\lambda_D$ and $\Delta\lambda_L$ are full halfwidths of Gaussian and Lorentzian fractions of the measured profile, respectively. The number n determines accuracy of calculation as well as computing time, but its value can be set on 10, because the array given in Eq. (3) converges rapidly for values of R, D and L expected in laboratory conditions.

The parameters adjusted in fitting to the experimental profiles are: base line BL, normalizing factor A, reduced Doppler halfwidth D, reduced Lorentz halfwidth L and sum of shifts $\Delta+d_k$. The values of these parameters have to be initially estimated. The values for isotope shift d_k could be taken from the literature (Schöber, 1939) when available. The $\Delta\lambda_s$ value is determined by theory of ideal Fabry-Perot interferometer, while plates reflectivity R is given by the Fabry-Perot interferometer producer.

The minimization of χ^2 merit function must be proceed iteratively, because of nonlinear dependence of model function on fitting parameters. Therefore, Marquardt-Levenberg algorithm is used to optimize values of adjustable parameters during iterations. This algorithm is approved in practice and has became the standard of nonlinear least-square routine (Press et al., 1988). The applied iterative procedure is repeated until χ^2 value stops to decrease, fulfilling the condition that $\Delta\chi^2$ is less then initially entered best-fit value.

The estimated error in determination of adjustable parameters best-fit values is less then several percent.

As an illustration of application of described method, the deconvolution result for neutral atom neon line λ=585.25 nm (natural isotope mixture) is given in Fig.1.

One can see that the overall profile obtained by this method is in agreement with experimental one. In addition, the gas kinetic temperature of a hollow cathode discharge ($T_g=590K$), which is derived from reduced Gaussian halfwidth $\Delta\lambda_D$, corresponds to that one measured by thermocouple (Bukvić, 1984).

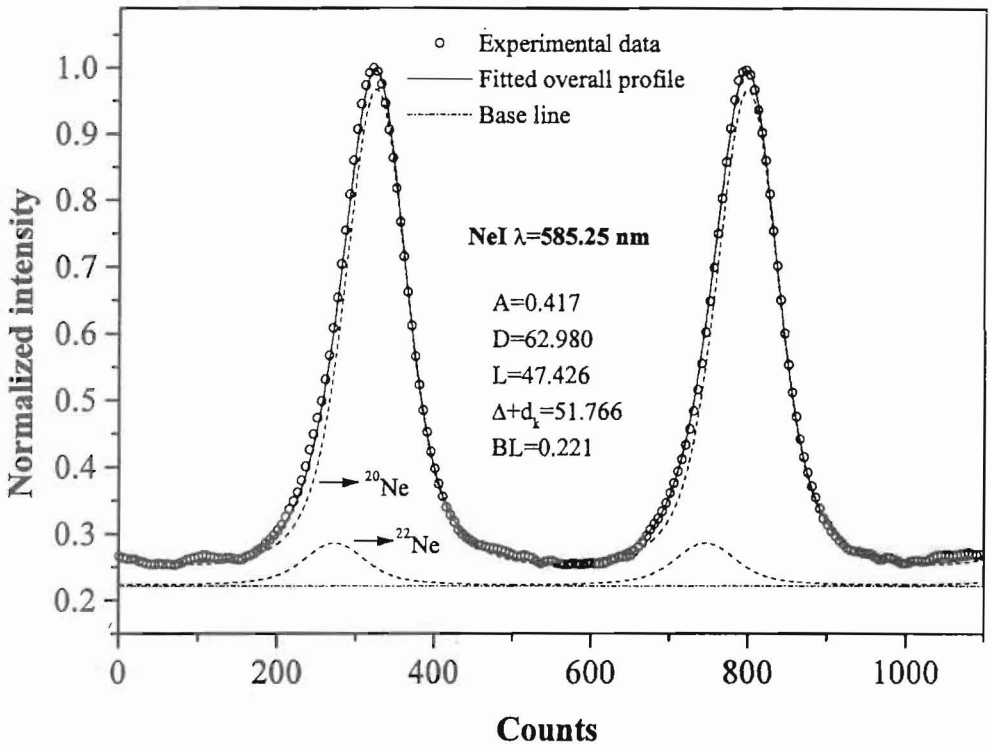

Fig. 1. An example of the deconvolution of atomic neon (natural mixture) spectral line λ=585.25 nm interferogram. The Fabry-Perot interferometer parameters: R=0.985; $\Delta\lambda_s$=473 counts (1count=$36*10^{-15}$ nm).

References

Balik, E.A.: 1966, *Appl. Opt.*, **5**, 170.

Bukvić S.: 1984, *M.Sc. Thesis*, Faculty of Physics, Belgrade.

Kuraica, M. and Konjević, N.: 1992, *Phys. Rev.*, **A46**, 1992, 4429.

Marquardt, D. W.:1963, *Journal of the Society for Industrial and Applied Mathematics*, **11**, 431.

Platiša, M., Konjević, R. and Bukvić, S.: 1983, *Opt. Las. Tech.*, **9**, 209.

Press, W. H., Flannery, B.P., Teukolsky, S.A. and Vetterling, W.T.: 1988, *Numerical recipes*, University Press, Cambridge.

Schöber, H.: 1939, *Phys. Zeitschr.*, **40**, 77.

Šišović, N., Videnović, I., Kuraica, M., Miljević, V. and Konjević, N.: 1995, *Pubs. Obs. Astron.*, **50**, 131.

Journal of Research in Physics Vol. 28, No. 3, 275-278 (1999)

SPATIAL DISTRIBUTION OF ROTATIONAL TEMPERATURE IN THE GRIMM-TYPE GLOW DISCHARGE

G. LJ. Majstorović, B. M. Obradović, M. M. Kuraica and N. Konjević

Faculty of Physics, University of Belgrade, 11001 Belgrade, P.O.Box 368, Yugoslavia

1. INTRODUCTION

Optical emission spectroscopy (OES) was used for determination of the rotational temperature from the spectra of nitrogen molecule. Relative rotational emission intensities are used to determine rotational temperatures under the assumption that the populations of molecular ions at the different energy levels follow a Boltzmann distribution. Here are followed classical papers (Boumans P.W.J.M,1966, Herzberg G., 1950) for the temperature determination.

We measured relative line intensities within R branch of even rotational quantum numbers of the First Negative System for (0-0) band in the Grimm type glow discharge. The spatial distribution of total intensity of whole band and rotational temperature of N_2^+ were determined. The results are presented at different pressures and currents.

2. EXPERIMENT

The experimental setup is presented schematically in Fig. 1. Our discharge source, a modified Grimm GD is laboratory made and described in detail elsewhere (M. Kuraica et al, 1992). Here, for completeness, minimum details will be given.

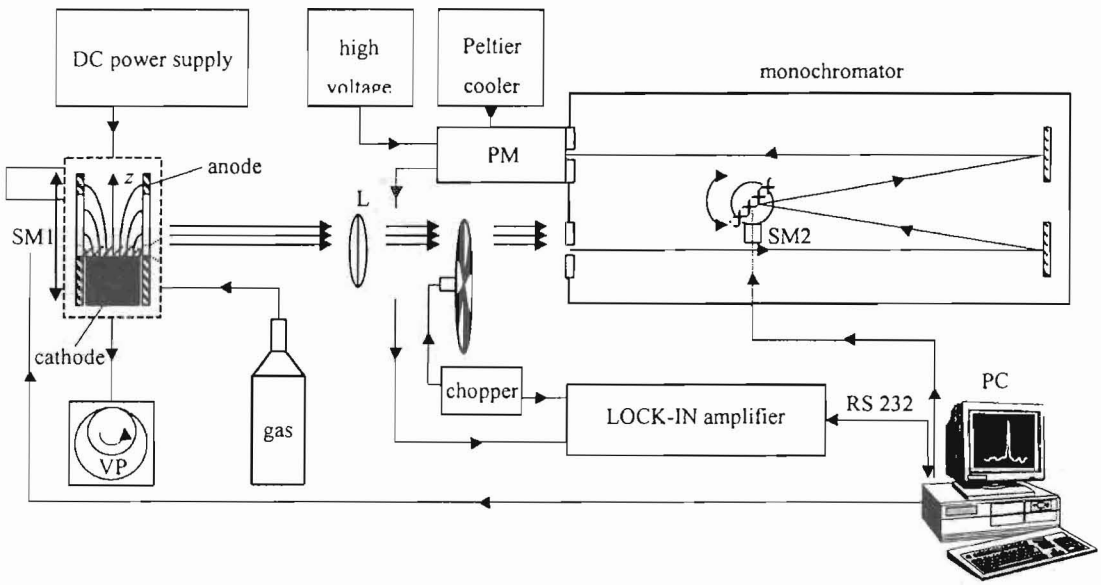

Fig. 1. Schematic diagram of the central part of Grimm GDS and experimental setup for side-on observations. Symbols: VP - vacuum pump, SM 1 and SM 2 - stepping motors L – lens, PM - photomultiplier.

The hollow anode 30 mm long with inner and outer diameters 8.00 mm and 13 mm, has a longitudinal slot (15 mm long and 1 mm wide) for side-on observations along the discharge axis. The water-cooled cathode holder has an exchangeable iron electrode, 18 mm long and 7.60 mm in diameter, which screws tightly into its holder to ensure good cooling. A gas flow of about 300 cm^3/min of nitrogen (99.995%) is sustained at variable pressure means of needle valve and a two-stage mechanical vacuum pump. To run the discharge a 0-2 kV, 0-100 mA current stabilized power supply is used. A ballast resistor of 10 kΩ is placed in series with the discharge and the power supply.

The radiation from the discharge source is focused with unity magnification (8 cm focal length achromat lens) onto the entrance slit of the scanning monochromator-photomultiplier system, see Fig. 1. For spectral line intensity axial distribution measurements, the discharge tube is translated in ≈0.1 mm steps by a stepping motor, so that the discharge image obtained through the observation slot is translated in the plane of the entrance slit (30 μm) of the monochromator. For the spectral recordings, 4 m Hilger and Watts Ebert type spectrometer with inverse dispersion of 0.242 nm/mm is used. All spectra are recorded with 30 μm entrance and exit slits, giving a Gaussian instrumental profile with 0.020 nm half-width. The monochromator is equipped with a stepping motor, which enables minimum wavelength change in steps of 0.0028 nm. For radiation detection, a photomultiplier with Peltier cooling is used. A lock-in signal amplification technique is employed. The entire experiment is controlled by a PC. The same computer is used for data acquisition.

3. RESULTS

In this paper are presented results of spatial distribution of whole line intensity and rotational temperature determination (as example Fig 3.) in the Grimm discharge with an iron cathode. The observation were performed side-on.

The method of determining a "rotational" temperature has been applied for the First Negative System of molecular ions N_2^+ which is $B^2\Sigma_u^+$-$X^2\Sigma_g^+$ transition, for 0-0 band degraded to shorter wavelengths (Fig 2.).

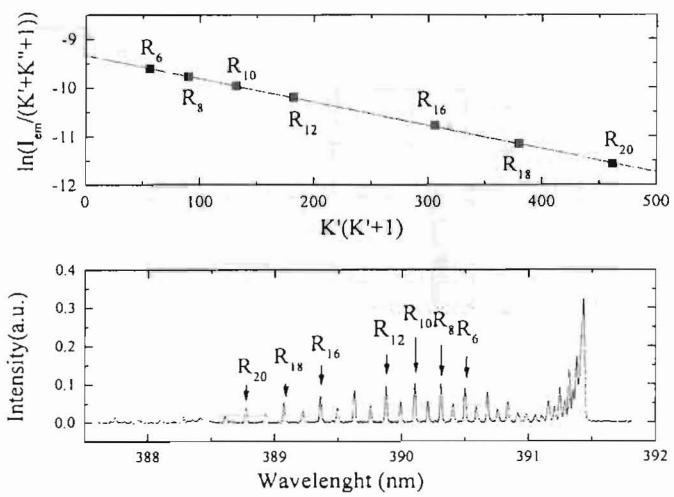

Fig.2. Example for emission spectra of the (0-0) band of the First Negative System of N_2^+ and a Boltzmann plot for lines R(6)-R(20) corresponding to a rotational temperature T_{rot}=620K.

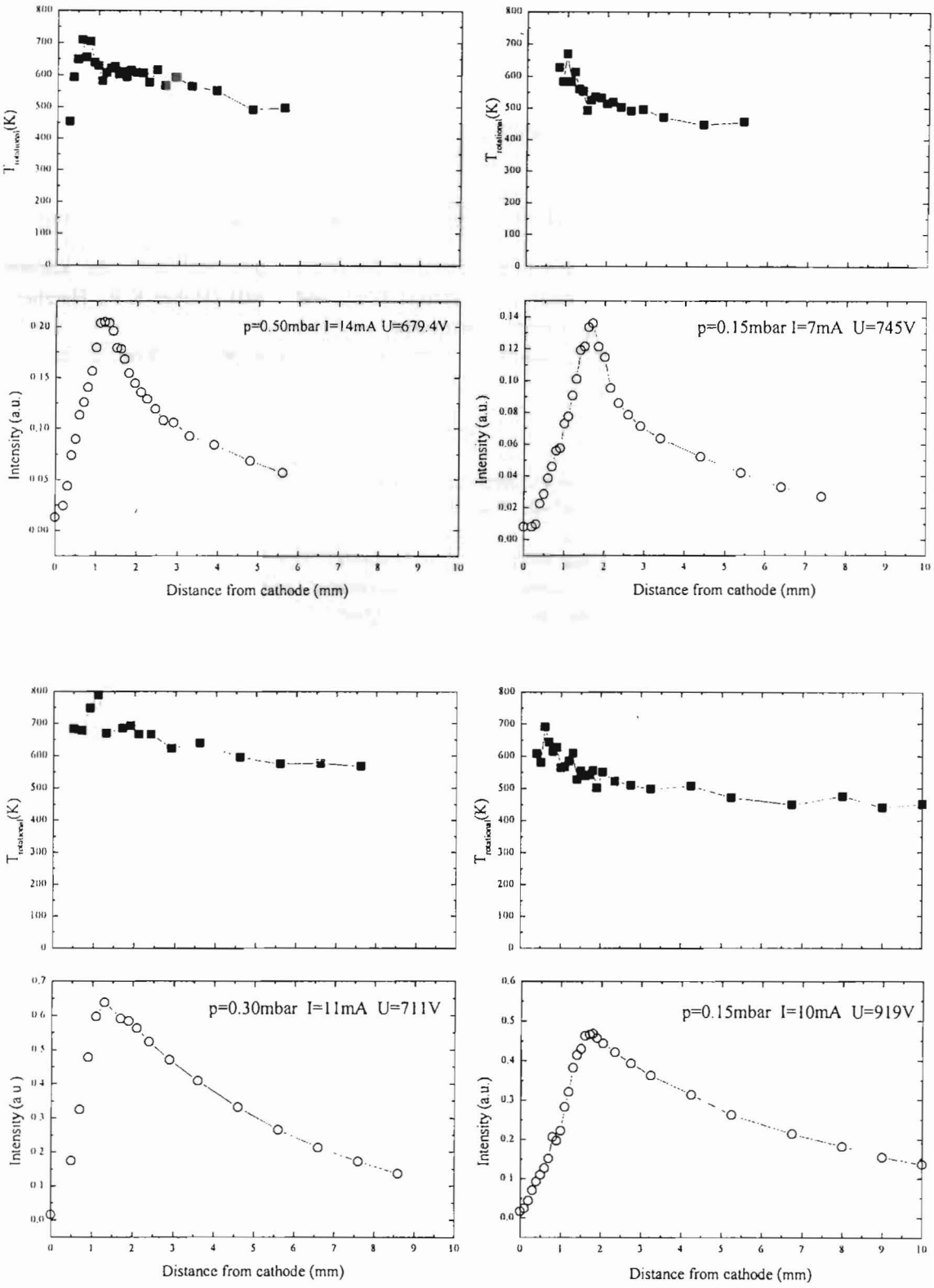

Fig.3. Spatial distributions of T_{rot} and whole band intensity for (0-0) band of the First Negative System of N_2^+ (391.44 nm) at different pressures and currents.

The variation of the intensity of the lines J_{em} in a rotational band as a function of quantum number J is given essentially by the thermal distribution of the rotation levels (Boumans P.W.J.M,1966, Herzberg G., 1950)

$$J_{em} = \frac{C_{em}\nu^4}{Q_r}(J' + J'' + 1)e^{-B_{v'}J'(J'+1)\frac{hc}{kT}}$$ where $\frac{C_{em}\nu^4}{Q_r}$ very nearly is constant.

By plotting $\ln\frac{J_{em}}{J' + J'' + 1}$ against J'(J'+1) a straight line with the slope $\frac{B_{v'}hc}{kT}$ is obtained. Relative intensities of R branch lines are measured from the band and with the known rotational constant of upper rotational states (from $B^2\Sigma_u$ and $\nu'=0$) (Huber K.P., Herzberg G.,1979) the temperature of the source were determined.

On the Fig.3. are presented results taken on three pressures and one of them is on two currents.

References

Boumans P.W.J.M : 1966, *Theory of Spectrochemical Excitation.*

Büger P.A., Alfy S. El., : 1975, Z. Naturfosh, **30a**, 466.

Büger P.A.: 1975, Z. Naturfosh **30a**, 216.

Herzberg G. : 1950 , *Spectra of Diatomic Molecules*,Van Nostrand, New York.

Huber K.P., Herzberg G.: 1979, IV. *Constants of diatomic molecules,* Van Nostrand, New York.

Kuraica M., Konjević N., Platiša M. and Pantelić D.: 1992, *Spectrochim. Acta B* **47**, 1173.

Journal of Research in Physics Vol. 28, No. 3, 279-282 (1999)

SPATIAL DISTRIBUTION OF VIBRATIONAL TEMPERATURE IN THE GRIMM-TYPE GLOW DISCHARGE

G. LJ. Majstorović, B. M. Obradović, M. M. Kuraica and N. Konjević

Faculty of Physics, University of Belgrade, 11001 Belgrade, P.O.Box 368, Yugoslavia

1. INTRODUCTION

Optical emission spectroscopy (OES) was used for determination of the vibrational temperature from the spectra of nitrogen molecule. Relative intensities of vibrational emission sequences are used to determine vibrational temperatures for the Second Positive System of molecular N_2 $C^3\Pi_u$-$B^3\Pi_g$ transition (Δv=-2 sequences).
The method that will be applied here is based on the assumption that the populations of moleculs at the different energy levels follow a Boltzmann distribution. We followed clasical papers (Herzberg G. ,1950) for determination.
We meassured relative band intensities of the Second Positive System in the Grimm type glow discharge. The spatial distribution of intensity of whole band and vibrational temperature of N_2 where determined. The results are presented at different pressures and currents.

2. EXPERIMENT

The experimental setup is presented schematically in Fig. 1. Our discharge source, a modified Grimm GD is laboratory made and described in detail elsewhere (M. Kuraica et al, 1992). Here, for completeness, minimum details will be given.

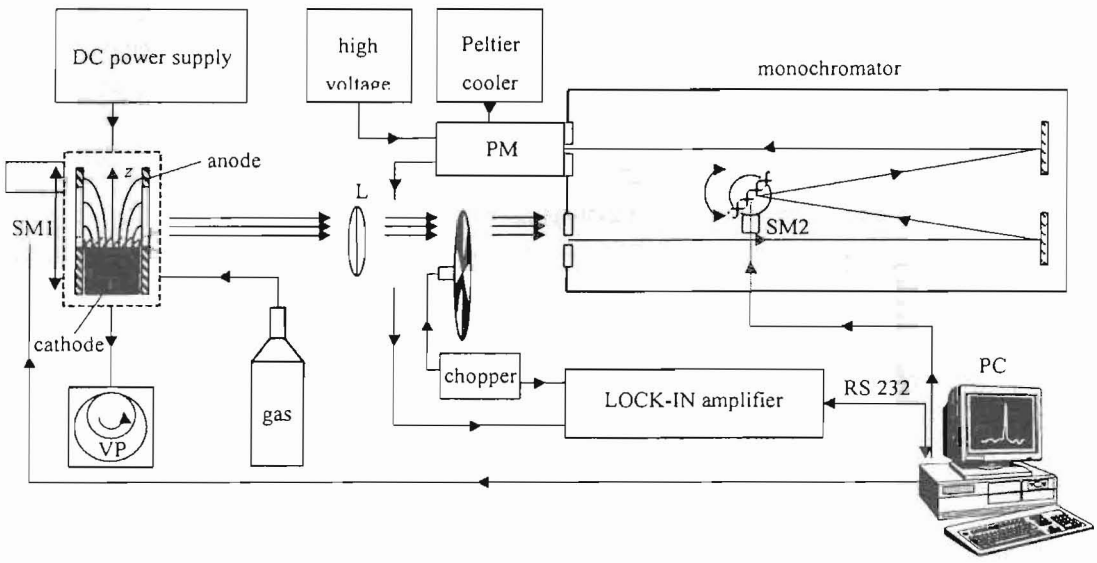

Fig. 1. Schematic diagram of the central part of Grimm GDS and experimental setup for side-on observations. Symbols: VP - vacuum pump, SM 1 and SM 2 - stepping motors L – lens, PM - photomultiplier.

The hollow anode 30 mm long with inner and outer diameters 8.00 mm and 13 mm, has a longitudinal slot (15 mm long and 1 mm wide) for side-on observations along the discharge axis. The water-cooled cathode holder has an exchangeable iron electrode, 18 mm long and 7.60 mm in diameter, which screws tightly into its holder to ensure good cooling. A gas flow of about 300 cm^3/min of nitrogen (99.995%) is sustained at variabile pressure means of needle valve and a two-stage mechanical vacuum pump. To run the discharge a 0-2 kV, 0-100 mA current stabilized power supply is used. A ballast resistor of 10 kΩ is placed in series with the discharge and the power supply.

The radiation from the discharge source is focused with unity magnification (8 cm focal length achromat lens) onto the entrance slit of the scanning monochromator-photomuliplier system, see Fig. 1. For spectral line intensity axial distribution measurements, the discharge tube is translated in ≈0.1 mm steps by a stepping motor, so that the discharge image obtained through the observation slot is translated in the plane of the entrance slit (30 μm) of the monochromator. For the spectral recordings, 4 m Hilger and Watts Ebert type spectrometer with inverse dispersion of 0.242 nm/mm is used. All spectra are recorded with 30 μm entrance and exit slits, giving a Gaussian instrumental profile with 0.020 nm half-width. The monochromator is equipped with a stepping motor, which enables minimum wavelength change in steps of 0.0028 nm. For radiation detection, a photomultiplier with Peltier cooling is used. A lock-in signal amplification technique is employed. the entire experiment is controled by a PC. The same computer is used for data acquisition.

3. RESULTS

In this paper are presented results of spatial distribution of whole band intensity and vibrational temperature determination (as example Fig. 3) in the Grimm discharge with an iron cathode. The observation were performed side-on.

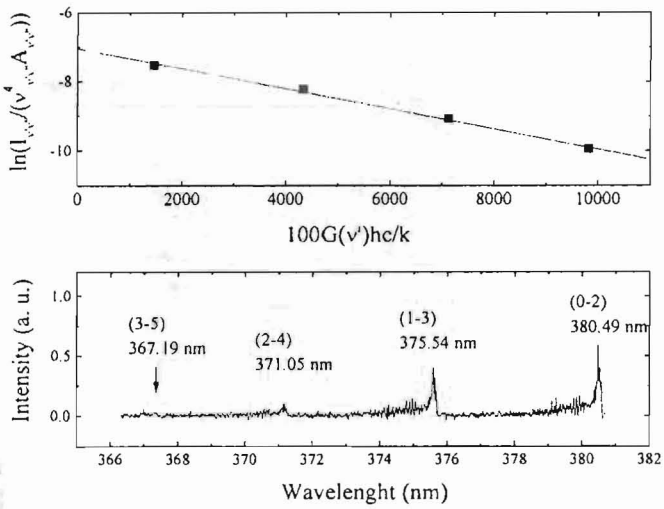

Fig. 2. Emission spectra of the Second Positive System of N_2, sequences (Δv=-2) and a Boltzmann plot with corresponding vibrational temperature T_{vib}=3400 K.

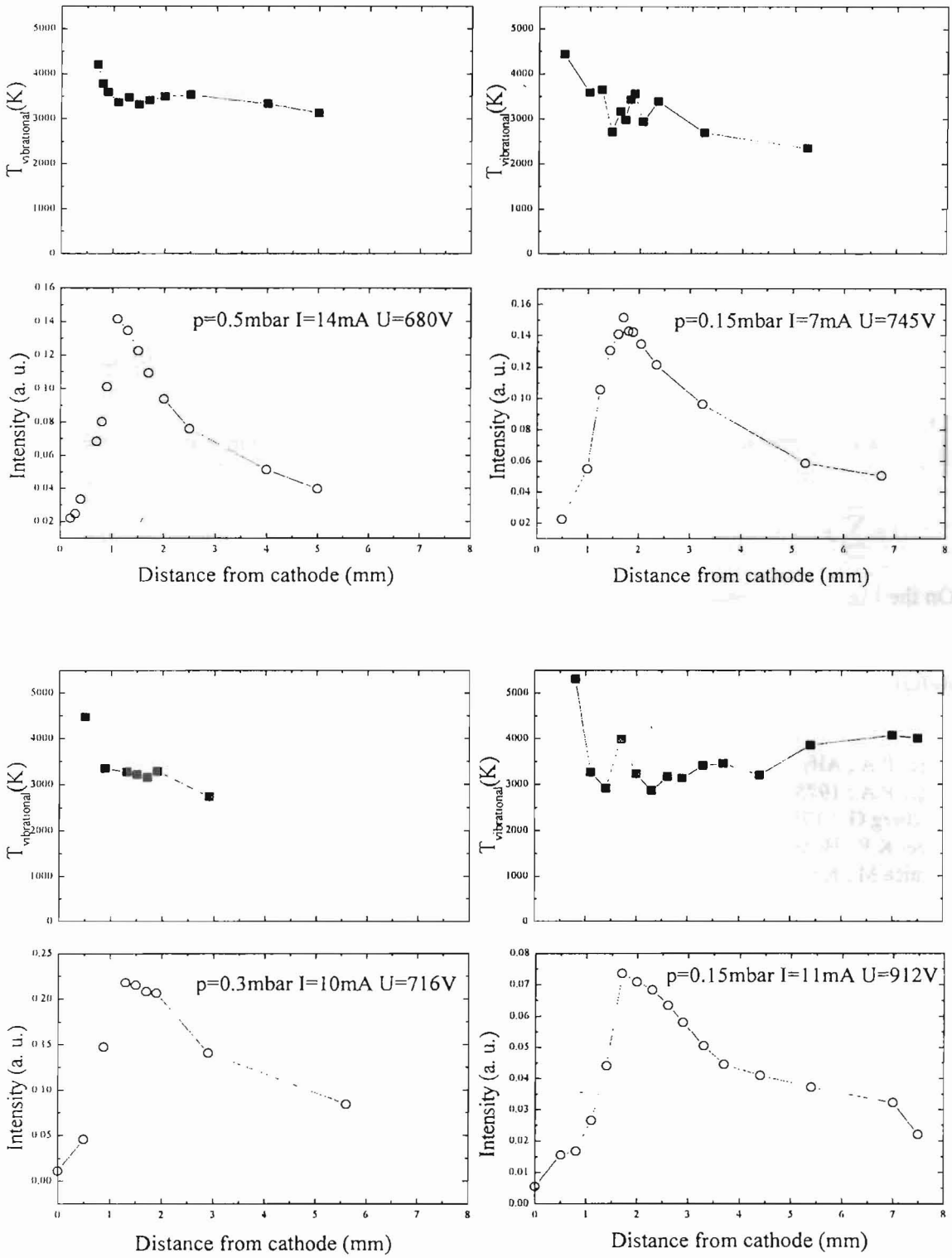

Fig. 3. Spatial distribution of T_{vib} and whole band intensity of the Second Positive System of N_2 sequences (Δv=-2), 380.49nm.

The method of determining a "vibrational" temperatures has been applied for the Second Positive Sistem of the N_2 molecule which is $C^3\Pi_u$-$B^3\Pi_g$ transition, for vibrational sequences (Δv=-2) : (0-2), (1-3), (2-4), (3-5) (Fig .2).

Relatively intensities of rotational-vibrational band is given (Herzberg G. ,1950 , Büger P.A., Alfy S. El., 1975, Büger P.A., 1975) as

$$I_{v'v''} = D \cdot \frac{N}{Q_v} \cdot e^{-\frac{G(v')\cdot hc}{kT}} \cdot \nu^4{}_{v'v''} \cdot A_{v'v''}$$

By plotting $\ln \frac{I_{v'v''}}{\nu^4{}_{v'v''} \cdot A_{v'v''}}$ against $100 \cdot G(v') \frac{h \cdot c}{k}$ a straight line is obtained whose slope is $\frac{1}{T_{vib}}$. G(v') is term velues for upper vibrational level (v') given with Dunham coefficients:

$G(v') = \sum_{i=1}^{n} y_{i0} (v + \frac{1}{2})^i$ in cm^{-1} as in (Laux C. O. and Kruger C. H. , 1992).

On the Fig.3 are presented results taken on three pressures and one of them is on two currents.

References

Büger P.A., Alfy S. El., : 1975, Z. Naturfosh, **30a**,466.
Büger P.A.: 1975, Z. Naturfosh **30a**, 216.
Herzberg G. : 1950 , *Spectra of Diatomic Molecules*, Van Nostrand, New York.
Huber K.P., Herzberg G.: 1979, IV. *Constants of diatomic molecules*, Van Nostrand, New York.
Kuraica M., Konjević N., Platiša M. and Pantelić D.: 1992, *Spectrochim. Acta B* **47**, 1173.
Laux C. O. and Kruger C. H. : 1992, *J. Quant. Spectrosc. Radiat. Transfer*, **48**, 9.
Lofthus A. and Krupenie P. H.: 1977, *J. Phys.Chem. Ref. Data*, **6**, 113.

Journal of Research in Physics Vol. 28, No. 3, 283-286 (1999)

SPECTROSCOPY STUDIE OF ATMOSPHERIC PRESSURE MICROWAVE INDUCED PLASMA

S.Jovićević, M.Ivković, Z.Pavlović, N.Konjević
Institute of Physics, 11080 Zemun, P.O. Box 68, Yugoslavia
E-mail:jovicevic @ atom.phy.bg.ac.yu

1. INTRODUCTION

The determination of electron number density (N_e) is important in diagnostic studies of plasmas used in analytical atomic emission (AAES) spectrometry. In these plasmas, gaseous species are partially ionized and the N_e values can be used to deduce the degree of ionization and the analytical characteristics of the plasmas. Several laboratory techniques have been applied for the determination of N_e: (a) Stark broadening; (b) Saha-Eggert ionization equilibrium; (c) absolute continuum intensity; (d) Langmuir probes. Among these techniques, Stark broadening is used most frequently in plasma spectrometry because the procedure is relatively simple, theoretical spectral line intensity profile is available for the emission line from H, He, and Ar, and most laboratories are equipped with optical instruments suitable for such kind of measurements. Additionally, the Stark broadening technique is applicable to plasmas where local thermal equilibrium (LTE) may not prevail.

In the present paper for characterization of plasma for spectrometric analyses, spatial distribution of atomic hydrogen line H_β at 486.13 nm for determination of electron number density, and the dependence of this parameter on operating condition have been investigated for the tangential flow MIP.

2. EXPERIMENT

The instrumental components and procedure in the present experiment, which were described elsewhere (Jovićević et all, 1996) are summarized in Table 1.

Table 1. Instrumental apparatus and components

Component	Specification
Microwave generator	2.45 GHz (AHF model: GMW 24 - 302 DR)
Microwave cavity	TEM_{010} Beenakker type (Beenakker, 1976) Van Dalen's modification (Van Dalen's et. all, 1978)
Discharge tube	tangential flow Al oxide (6 / 4 mm)
Nebulizer	right-angle pneumatic nebulizer (Meinhard TR30-C3)
Monochromator	0.5 m Ebert type (Jarrell Ash 82-025)
Photomultiplier	EMI 9659QB
Picoammeter	Keithley 414 S
Data acquisition	Boxcar averager (Stanford Research Systems SR 250)

In order to obtain the discharge which is temporally and spatially stable we exchange the single capillary discharge tube with so called "tangential flow torch" reported by Bollo-Kamara et. all (1981). Instead of quartz concentric tubes and thread insert, which are fused all together, we used alumna tubes separated by cooper wire. Windings of the wire are the same as coils of their threaded insert. Analyte sample gas goes through the inner tube, while the plasma support gas is introduced through the outer sleeve and exit from the cooper wire windings with a spiral trajectory. In such a manner, temporally and spatially stable discharge, separated from the walls, was obtained. Also the discharge wall etching and consequence memory effects are decreased and tube lifetime was prolonged. The wet and dry gases are obtained by system, which is similar to the one described by Veillon *et all* (1968). It consists of right angle pneumatic nebulizer, spray chamber in case of wet gases and additional evaporating chamber and modified Liebig-Graham condenser for obtaining dry gases. Other experimental conditions are presented in Table 2.

Table 2. Experimental conditions

	Sample gas	Support gas	Gas condition
1	$Ar + H_2O$	Ar	wet
2	$(Ar + 1.6\% H_2) + H_2O$	Ar	wet
3	$(Ar + 1.3\% H_2) + H_2O$	$Ar + 1.3\% H_2$	wet
4	$Ar + 1.6\% H_2$	$Ar + 1.6\% H_2$	pure
5	$Ar + 2.9\% H_2$	Ar	pure
6	$(Ar + 1.6\% H_2) + H_2O$	Ar	dry
7	$(Ar + 1.6\% H_2) + H_2O$	$Ar + 1.6\% H_2$	dry

For all presented side-on experiments, sample and support gas flow 20 ml/min and 200 ml/min respectively and forward microwave power of 80W are used. The two-axis movement of MIP for obtaining spatial distributions of various spectral lines shapes was enabled by the means of PC controlled x-y table.

3. RESULTS

The results of the electron number density obtained from spatial distribution of atomic hydrogen line H_β are presented. For the separation of contribution for different plasma layers and for obtaining the true radial plasma intensity distribution we used Abel inversion procedure as developed by Djurović *et all* (1996). Electron number density is determined from combinations of the approximate formulas i.e. application of Kelleher's (1981) formula for determination of Stark half-half widths and Wiesse's (Wiesse *et all*, 1972) dependence for Ne =f (Ws):

$$W_S = (W_m^{1.4} - W_{D,i}^{1.4})^{1/1.4} \qquad W_{D,i} = (W_D^2 + W_i^2)^{0.5} \qquad W_D = 3.58 * 10^{-7} \lambda (T_g / M)^{0.5}$$

where Ws - Stark halfwidths, W_D - Doppler halfwidths and Wi - instrumental halfwidths

$$Ne\ (cm^{-3}) = 10^{16} * (Ws / 4.74)^{1.49}$$

Typical obtained electron density spatial distribution is presented in Figure 1.

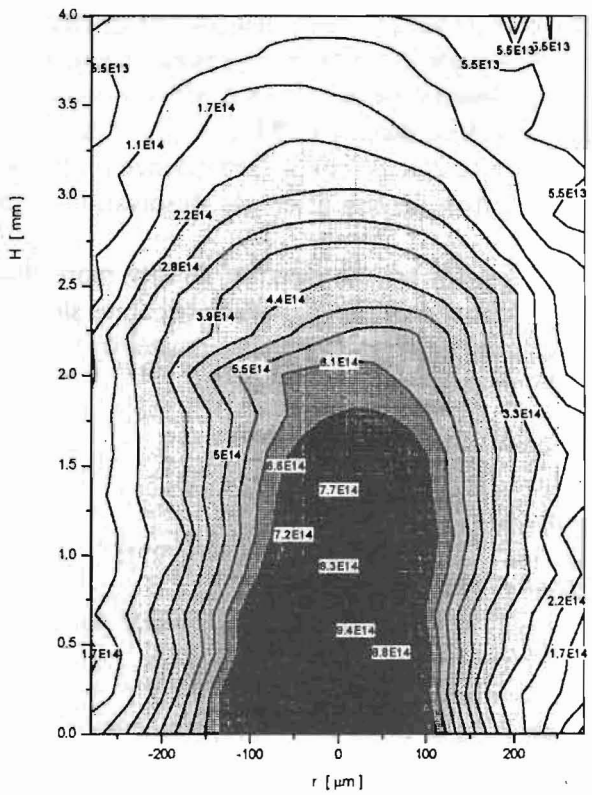

Figure 1. Electron density spatial distribution in case 1 (see Table 2.)

Electron density dependence on height in the middle of the discharge (x=0) in different cases is presented in Figure 2.

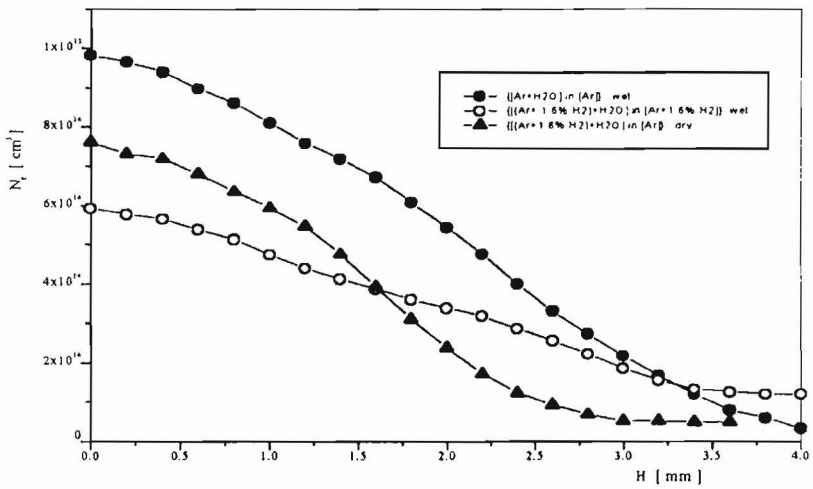

Figure 2. Electron density dependances on height in different cases

4. CONCLUSION

From performed measurements we conclude that maximum electron density ($1x10^{15}$ cm^{-3}) is obtained in wet Ar + H_2O sample gas with Ar as a support gas. If a 1.6% H_2 is added to sample gas, changes in electron density distribution are within experimental errors. Drying of sample gas lowers maximum electron density ($0.8x10^{15}cm^{-3}$), that becomes closer to the values obtained in pure gas mixture ($0.25x10^{15}cm^{-3}$). Dependence on height in all four cases is preserved. Lowering of the electron density after gas desolvation is observed by other authors (Pak et. all, 1994) too.

Adding of H_2 to support gas lowers the electron density more than desolvation (to $0.6x10^{15}cm^{-3}$), but also exchange spatial dependence, which becomes slower and broader (see Fig.2). This effect may be explained by large thermal conductivity of hydrogen plasma at elevated temperatures, caused by dissociation of molecules.

References

Beenakker C.I.M. 1976, *Spectrohimica Acta*, **31B**, 3.
Bollo-Kamara A., Codding E. G., 1981, *Spectrohimica Acta*, **36B**, 973.
Djurović S., Kelleher D. E., Roberts J. R., (to be published)
Jovićević S., Ivković M., Konjević N., 1996, *Publ.Obs.Astron.Belgrade*, **53**, 113.
Kelleher 1981,*JQSRT*, **25**, 191
Pak Y., S.R.Koirtyohann, 1994: Spectrohimica Acta **49B**, 593
Van Dalen J., de Lezenne Coulander P.A., de Galan L., 1978, *Spectrohimica Acta*, **33B**, 545.
Veillon C. Margoshes M. 1968, *Spectrohimica Acta*, **23B**, 553
Wiesse, Kelleher, Paquette, 1972, *Phys. Rev.***A 6**, 1132

Journal of Research in Physics Vol. 28, No. 3, 287-290 (1999)

ON THE STARK BROADENING OF AR VIII SPECTRAL LINES

MILAN S. DIMITRIJEVIĆ[1] AND SYLVIE SAHAL-BRECHOT[2]

[1] *Astronomical Observatory, Volgina 7, 11000 Belgrade, Yugoslavia*
E-mail mdimitrijevic@aob.bg.ac.yu

[2] *Observatoire de Paris, 92195 Meudon Cedex, France*
E-mail sahal@obspm.fr

Abstract. Within the semiclassical perturbation approach, we have considered electron-, proton-, and He III-impact line widths and shifts for 9 Ar VIII transitions, for perturber densities 10^{18} - 10^{22} cm^{-3} and temperatures T = 200,000 − 3,000,000 K.

1. INTRODUCTION

Stark broadening data for argon in different ionization stages are of interest for a number of problems in research of astrophysical, laboratory, laser produced and fusion plasmas, like *e.g.* plasma diagnostic and modelling. Stark broadening of Ar VIII spectral lines has been considered experimentaly (Hegazy *et al.* 1997) and theoreticaly (Purić *et al.* 1988, Hegazy *et al.* 1997, Djeniže and Srećković 1998, Konjević and Konjević 1998). In Hegazy *et al.* (1997) Stark broadening of 5f-6g and 5g-6h Ar VIII line profiles has been experimentaly investigated in gas-liner pinch. Obtained experimental results have been compared with the theoretical calculations performed in the same paper. These results has been discussed in Konjević and Konjević (1998). In Purić *et al.* (1988) and Djeniže *et al.* (1998), regularities and systematic trends have been used to estimate Ar VIII Stark broadening parameters. Moreover, Stark width for Ar VIII $4s^2S$-$4p^2P^o$ multiplet has been calculated in Djeniže *et al.* (1998) by using the symplified modified semiempirical approach (Dimitrijević and Konjević 1986).

As a continuation of our project (Dimitrijević 1996) to provide an as much as possible large set of reliable Stark broadening data for laboratory, laser produced, fusion and astrophysical plasma research, we have calculated within the semiclassical-perturbation formalism (sahal-Bréchot 1969ab, electron-, proton-, and ionized helium-impact line widths and shifts for 9 Ar VIII transitions.

2. RESULTS AND DISCUSSION

All relevant details concerning the obtained results and the calculation procedure will be published in Dimitrijević and Sahal–Bréchot (1999a). Here, we present only tables of Stark broadening parameters. Atomic energy levels needed for calculations have been taken from Bashkin and Stoner (1975). Our results for electron-, proton-, and He III-impact line widths and shifts for 9 Ar VIII transitions for perturber densities 10^{18}cm^{-3} – 10^{22}cm^{-3}, and the temperature range T = 200,000 – 3,000,000 K, will be published in Dimitrijević and Sahal-Bréchot (1999ab).

Table 1

Table 1. This table shows electron-, proton-, and He III-impact broadening parameters for Ar VIII for perturber density of 10^{18} cm^{-3} and temperatures from 200,000 up to 3,000,000 K. Transitions and corresponding wavelengths (in Å) are also given in the table. By dividing C by the corresponding full width at half maximum (Dimitrijević *et al.*, 1991), we obtain an estimate for the maximum perturber density for which the line may be treated as isolated and tabulated data may be used.

PERTURBER DENSITY = 1.E+18cm-3

PERTURBERS ARE :		ELECTRONS		PROTONS	
TRANSITION	T(K)	WIDTH(Å)	SHIFT(Å)	WIDTH(Å)	SHIFT(Å)
Ar VIII3S 3P	200000.	0.930E-02	-0.137E-03	0.150E-03	-0.973E-04
714.0 Å	500000.	0.614E-02	-0.156E-03	0.374E-03	-0.208E-03
C=0.71E+21	1000000.	0.464E-02	-0.149E-03	0.557E-03	-0.304E-03
	1500000.	0.400E-02	-0.149E-03	0.656E-03	-0.368E-03
	2000000.	0.362E-02	-0.145E-03	0.701E-03	-0.403E-03
	3000000.	0.317E-02	-0.141E-03	0.780E-03	-0.448E-03
Ar VIII3S 3P	200000.	0.899E-02	-0.130E-03	0.146E-03	-0.918E-04
700.4 Å	500000.	0.593E-02	-0.148E-03	0.362E-03	-0.197E-03
C=0.69E+21	1000000.	0.448E-02	-0.142E-03	0.538E-03	-0.288E-03
	1500000.	0.386E-02	-0.142E-03	0.633E-03	-0.349E-03
	2000000.	0.350E-02	-0.138E-03	0.675E-03	-0.382E-03
	3000000.	0.307E-02	-0.134E-03	0.750E-03	-0.425E-03
Ar VIII3S 4P	200000.	0.119E-02	0.977E-05	0.702E-04	0.100E-04
159.0 Å	500000.	0.815E-03	0.147E-04	0.112E-03	0.199E-04
C=0.13E+20	1000000.	0.638E-03	0.125E-04	0.131E-03	0.276E-04
	1500000.	0.562E-03	0.119E-04	0.140E-03	0.316E-04
	2000000.	0.516E-03	0.119E-04	0.148E-03	0.342E-04
	3000000.	0.462E-03	0.113E-04	0.158E-03	0.380E-04

Table 1 continued

PERTURBER DENSITY = 1.E+18cm-3

PERTURBERS ARE :		ELECTRONS		PROTONS	
TRANSITION	T(K)	WIDTH(Å)	SHIFT(Å)	WIDTH(Å)	SHIFT(Å)
Ar VIII4S 4P	200000.	0.210	-0.497E-02	0.106E-01	-0.586E-02
1887.0 Å	500000.	0.147	-0.561E-02	0.174E-01	-0.960E-02
C=0.19E+22	1000000.	0.117	-0.547E-02	0.209E-01	-0.120E-01
	1500000.	0.103	-0.527E-02	0.230E-01	-0.134E-01
	2000000.	0.952E-01	-0.512E-02	0.248E-01	-0.145E-01
	3000000.	0.852E-01	-0.447E-02	0.276E-01	-0.161E-01
Ar VIII3P 4S	200000.	0.161E-02	0.108E-03	0.535E-04	0.110E-03
229.4 Å	500000.	0.112E-02	0.130E-03	0.136E-03	0.176E-03
C=0.28E+20	1000000.	0.880E-03	0.122E-03	0.208E-03	0.216E-03
	1500000.	0.773E-03	0.118E-03	0.243E-03	0.239E-03
	2000000.	0.708E-03	0.115E-03	0.269E-03	0.257E-03
	3000000.	0.628E-03	0.104E-03	0.314E-03	0.282E-03
Ar VIII3P 4S	200000.	0.164E-02	0.110E-03	0.542E-04	0.111E-03
230.9 Å	500000.	0.114E-02	0.131E-03	0.137E-03	0.178E-03
C=0.28E+20	1000000.	0.893E-03	0.124E-03	0.211E-03	0.219E-03
	1500000.	0.784E-03	0.119E-03	0.245E-03	0.242E-03
	2000000.	0.718E-03	0.117E-03	0.272E-03	0.260E-03
	3000000.	0.637E-03	0.105E-03	0.318E-03	0.285E-03
Ar VIII3P 3D	200000.	0.573E-02	-0.637E-04	0.148E-03	-0.359E-04
519.2 Å	500000.	0.379E-02	-0.616E-04	0.314E-03	-0.798E-04
C=0.38E+21	1000000.	0.287E-02	-0.816E-04	0.438E-03	-0.120E-03
	2000000.	0.225E-02	-0.711E-04	0.513E-03	-0.165E-03
	3000000.	0.198E-02	-0.682E-04	0.551E-03	-0.183E-03
Ar VIII3P 3D	200000.	0.591E-02	-0.665E-04	0.153E-03	-0.379E-04
526.6 Å	500000.	0.391E-02	-0.648E-04	0.324E-03	-0.841E-04
C=0.40E+21	1000000.	0.296E-02	-0.849E-04	0.453E-03	-0.127E-03
	1500000.	0.255E-02	-0.727E-04	0.498E-03	-0.154E-03
	2000000.	0.232E-02	-0.741E-04	0.530E-03	-0.173E-03
	3000000.	0.204E-02	-0.711E-04	0.569E-03	-0.192E-03
Ar VIII3D 4P	200000.	0.547E-02	0.102E-03	0.346E-03	0.785E-04
337.6 Å	500000.	0.376E-02	0.127E-03	0.547E-03	0.141E-03
C=0.60E+20	1000000.	0.295E-02	0.124E-03	0.636E-03	0.194E-03
	1500000.	0.260E-02	0.116E-03	0.683E-03	0.215E-03
	2000000.	0.239E-02	0.116E-03	0.721E-03	0.233E-03
	3000000.	0.214E-02	0.111E-03	0.770E-03	0.258E-03

As a sample of our results, the Stark broadening parameters for Ar VIII spectral lines broadened by electron and proton impacts, for a perturber density of 10^{18} cm^{-3},

are shown in Table 1. We also specify a parameter C (Dimitrijević and Sahal–Bréchot 1984), which gives an estimate for the maximum perturber density for which the line may be treated as isolated when it is divided by the corresponding full width at half maximum. For each value given in Table 1, the collision volume (V) multiplied by the perturber density (N) is much less than one and the impact approximation is valid (Sahal–Bréchot, 1969ab).

There is not an enough complete set of reliable atomic data to perform an adequate semiclassical perturbation calculation of the Stark broadening of Ar VIII 5f-6g and 5g-6h line profiles, experimentaly and theoreticaly investigated in Hegazy *et al.* (1997). This is similar for Ar VIII 4p-4d and 4p-5s Stark widths estimated on the basis of regularities and systematic trends in Djeniže *et al.* (1998). In Purić *et al.* (1988), full Stark width at half maximum (W) for $4s^2S$-$4p^2P^o$ multiplet has been estimated on the basis of the regular dependence on the upper level ionization potential to be 0.0244 Å at the temperature T=80,000 K and for an electron density of $10^{17}cm^{-3}$. For the same multiplet and electron density, W=0.018Å has been obtained in Djeniže *et al.* (1998) on the basis of established regularities along the argon isonuclear sequence, for T=150,000 K. Our result for T=200,000 K is 0.0210Å which is a good agreement.

The new experimental data will be very useful for further development and rafinement of the theory of multicharged ion lines and for the investigation of regularities and systematic trends.

References

Bashkin, S., Stoner, J. O. Jr. : 1978, Atomic Energy Levels and Grotrian Diagrams, Vol. 2, North Holland, Amsterdam.

Dimitrijević, M. S., Konjević, N. : 1986, *Astron. Astrophys.*, **163**, 297 .

Dimitrijević, M.S., and Sahal-Bréchot, S. : 1984, *JQSRT* **31**, 301.

Dimitrijević M.S. and Sahal-Bréchot, S. : 1999a, *Zh. Prikl. Spektrosk.* submitted.

Dimitrijević, M. S., and Sahal–Bréchot, S. : 1999b, *Serb. Astron. J.*, **159**, in press.

Djeniže, S., Srećković, A. : 1998, *Serb. Astron. J.*, **157**, 25.

Griem, H. R. : 1974, Spectral Line Broadening by Plasmas, Academic Press, New York.

Hegazy, H., Büscher, S., Kunze, H. J., Wrubel, Th. : 1997, *J. Quant. Spectrosc. Radiat. Transfer*, **58**, 627.

Konjević, R., Konjević, N. : 1998, 19^{th} SPIG, Zlatibor 1998, Contributed papers, Faculty of Physics, Belgrade, p. 373.

Purić, J., Djeniže, S., Srećković, A., Ćuk, M., Labat, J., Platiša, M. : 1988, *Z. Phys. D*, **8**, 343.

Sahal-Bréchot, S. : 1969a, *Astron. Astrophys.* **1**, 91.

Sahal-Bréchot, S. : 1969b, *Astron. Astrophys.* **2**, 322.

Journal of Research in Physics Vol. 28, No. 3, 291-294 (1999)

ON THE STARK BROADENING OF NEUTRAL SILVER SPECTRAL LINES

MILAN S. DIMITRIJEVIĆ[1] AND SYLVIE SAHAL-BRECHOT[2]

[1] *Astronomical Observatory, Volgina 7, 11050 Belgrade, Yugoslavia*
E-mail mdimitrijevic@aob.aob.bg.ac.yu

[2] *Observatoire de Paris, 92195 Meudon Cedex, France*
E-mail sahal@obspm.fr

Abstract. Within the semiclassical perturbation approach, we have calculated electron-, proton-, and ionized helium-impact line widths and shifts for 48 Ag I lines, for perturber densities $10^{12} - 10^{19}$ cm^{-3} and temperatures T = 2,500 − 50,000 K.

1. INTRODUCTION

Stark broadening contribution to neutral silver spectral line shapes has been considered experimentaly (Holtsmark and Trumpy 1925, Kitaeva 1956) and theoreticaly (Kitaeva 1956, Pichler 1972). In Pichler (1972) quadratic Stark broadening constants of neutral silver spectral lines, calculated in the Coulomb approximation, have been determined. Our objective here, is to continue efforts to provide to plasma physicists and astrophysicists Stark broadening parameters needed for investigation and modelling of various plasmas (see Dimitrijević and Sahal - Bréchot 1984, Dimitrijević 1996, and references therein). In this contribution, a part of our results for electron-, proton-, and ionized helium-impact line widths and shifts for 48 Ag I spectral lines is presented.

2. RESULTS AND DISCUSSION

A summary of the formalism is given e. g. in Dimitrijević and Sahal-Bréchot 1984. Energy levels have been taken from Moore (1971).

Our results for 48 neutral silver spectral lines as a function of the perturber density and temperature will be published in Dimitrijević and Sahal-Bréchot (1999).

As a sample of our results, the Stark broadening parameters for Ag I spectral lines broadened by electron and proton impacts, for a perturber density of 10^{16} cm^{-3}, are shown in Table 1.

The existing experimental data (Holtsmark and Trumpy 1925, Kitaeva 1956) are not included in the review of critically selected experimental Stark broadening data

(Konjević and Roberts 1976). In order to make a comparison of theory with reliable experimental data, the results of corresponding experiments to determine the Stark broadening of Ag I lines will be of interest for further development and rafinement of the theory.

Table 1

This table shows electron- and proton-impact broadening full half-widths (FWHM) and shifts for Ag I for a perturber density of 10^{16} cm^{-3} and temperatures from 2,500 up to 50,000 K. By deviding C with the full linewidth, we obtain an estimate for the maximum perturber density for which the line may be treated as isolated and tabulated data may be used (Dimitrijević and Sahal-Bréchot 1984). For each value given in Table 1, the collision volume (V) multiplied by the perturber density (N) is much less than one and the impact approximation is valid (Sahal–Bréchot, 1969ab). Values for NV $>$ 0.5 are not given and values for 0.1 $<$ NV $\leq$ 0.5 are denoted by an asterisk.

PERTURBER DENSITY = 1.E+16cm-3

PERTURBERS ARE :		ELECTRONS		PROTONS	
TRANSITION	T(K)	WIDTH(Å)	SHIFT(Å)	WIDTH(Å)	SHIFT(Å)
AgI 5S - 5P	2500.	0.375E-02	0.179E-02	0.227E-02	0.482E-03
0.5 0.5	5000.	0.422E-02	0.208E-02	0.228E-02	0.548E-03
3383.9 Å	10000.	0.443E-02	0.225E-02	0.229E-02	0.622E-03
C= 0.15E+20	20000.	0.500E-02	0.218E-02	0.231E-02	0.700E-03
	30000.	0.567E-02	0.183E-02	0.232E-02	0.751E-03
	50000.	0.691E-02	0.142E-02	0.234E-02	0.819E-03
AgI 5S - 5P	2500.	0.385E-02	0.199E-02	0.230E-02	0.555E-03
1.5 0.5	5000.	0.437E-02	0.243E-02	0.232E-02	0.632E-03
3281.6 Å	10000.	0.465E-02	0.275E-02	0.233E-02	0.717E-03
C= 0.13E+20	20000.	0.523E-02	0.275E-02	0.235E-02	0.809E-03
	30000.	0.589E-02	0.240E-02	0.237E-02	0.867E-03
	50000.	0.707E-02	0.191E-02	0.239E-02	0.946E-03
AgI 5S - 6P	2500.	0.459E-01	0.312E-01	*0.116E-01	*0.723E-02
0.5 0.5	5000.	0.493E-01	0.303E-01	*0.128E-01	*0.912E-02
2070.5 Å	10000.	0.521E-01	0.268E-01	0.141E-01	0.110E-01
C= 0.19E+18	20000.	0.529E-01	0.221E-01	0.157E-01	0.128E-01
	30000.	0.525E-01	0.190E-01	0.168E-01	0.139E-01
	50000.	0.518E-01	0.149E-01	0.183E-01	0.154E-01
AgI 6S - 6P	2500.	3.07	1.94	*0.787	*0.490
0.5 0.5	5000.	3.34	1.67	*0.867	*0.616
17417.9 Å	10000.	3.73	1.23	0.957	0.738
C= 0.14E+20	20000.	4.02	0.900	1.06	0.861
	30000.	4.12	0.690	1.13	0.936
	50000.	4.23	0.453	1.24	1.03

Table 1 continued

PERTURBER DENSITY = 1.E+16cm-3

PERTURBERS ARE :		ELECTRONS		PROTONS	
TRANSITION	T(K)	WIDTH(Å)	SHIFT(Å)	WIDTH(Å)	SHIFT(Å)
AgI 6S - 6P	2500.	3.90	2.22	*0.992	*0.617
1.5 0.5	5000.	4.21	1.75	*1.11	*0.799
16821.9 Å	10000.	4.44	1.32	*1.24	*0.973
C= 0.69E+19	20000.	4.49	0.877	1.40	1.15
	30000.	4.50	0.630	1.50	1.25
	50000.	4.50	0.384	1.67	1.38
AgI 5P - 6S	2500.	0.113	0.796E-01	0.265E-01	0.207E-01
0.5 0.5	5000.	0.132	0.954E-01	0.292E-01	0.242E-01
7689.9 Å	10000.	0.148	0.115	0.324E-01	0.279E-01
C= 0.34E+20	20000.	0.159	0.120	0.360E-01	0.318E-01
	30000.	0.170	0.121	0.383E-01	0.343E-01
	50000.	0.181	0.106	0.415E-01	0.376E-01
AgI 5P - 6S	2500.	0.129	0.914E-01	0.308E-01	0.237E-01
0.5 1.5	5000.	0.151	0.112	0.339E-01	0.278E-01
8275.8 Å	10000.	0.169	0.132	0.375E-01	0.320E-01
C= 0.39E+20	20000.	0.183	0.137	0.416E-01	0.365E-01
	30000.	0.197	0.138	0.443E-01	0.393E-01
	50000.	0.211	0.119	0.479E-01	0.431E-01
AgI 5P - 7S	2500.	0.163	0.113	0.348E-01	0.258E-01
0.5 0.5	5000.	0.190	0.137	0.391E-01	0.319E-01
4477.3 Å	10000.	0.209	0.162	0.439E-01	0.379E-01
C= 0.43E+19	20000.	0.226	0.152	0.492E-01	0.440E-01
	30000.	0.239	0.147	0.526E-01	0.477E-01
	50000.	0.262	0.125	0.573E-01	0.526E-01
AgI 5P - 7S	2500.	0.177	0.121	0.379E-01	0.281E-01
0.5 1.5	5000.	0.206	0.148	0.425E-01	0.347E-01
4669.8 Å	10000.	0.230	0.172	0.477E-01	0.412E-01
C= 0.47E+19	20000.	0.246	0.164	0.535E-01	0.478E-01
	30000.	0.260	0.159	0.572E-01	0.518E-01
	50000.	0.285	0.134	0.623E-01	0.571E-01
AgI 5P - 8S	2500.	0.346	0.226	*0.709E-01	*0.434E-01
0.5 0.5	5000.	0.398	0.274	*0.800E-01	*0.587E-01
3841.8 Å	10000.	0.438	0.298	*0.899E-01	*0.730E-01
C= 0.15E+19	20000.	0.497	0.287	*0.101	*0.870E-01
	30000.	0.533	0.252	*0.108	*0.952E-01
	50000.	0.603	0.215	0.118	0.106

Table 1 continued

PERTURBER DENSITY = 1.E+16cm-3

PERTURBERS ARE :		ELECTRONS		PROTONS	
TRANSITION	T(K)	WIDTH(Å)	SHIFT(Å)	WIDTH(Å)	SHIFT(Å)
AgI 5P - 8S	2500.	0.372	0.243	*0.762E-01	*0.466E-01
0.5 1.5	5000.	0.428	0.302	*0.860E-01	*0.631E-01
3982.7 Å	10000.	0.470	0.319	*0.966E-01	*0.784E-01
C= 0.16E+19	20000.	0.531	0.308	*0.108	*0.934E-01
	30000.	0.573	0.270	*0.116	*0.102
	50000.	0.649	0.231	0.126	0.114
AgI 6P - 7S	2500.	8.95	-0.462	*1.41	-0.745
0.5 0.5	5000.	11.8	0.868	1.50	-0.905
27858.3 Å	10000.	14.0	2.09	1.61	-1.06
C= 0.35E+20	20000.	16.0	2.84	1.75	-1.23
	30000.	17.0	2.68	1.86	-1.33
	50000.	18.3	2.39	2.02	-1.46
AgI 6P - 7S	2500.	14.2	-1.73	*2.44	-1.52
0.5 1.5	5000.	17.1	0.652E-01	*2.71	-1.92
29531.5 Å	10000.	19.0	1.96	3.01	-2.31
C= 0.21E+20	20000.	20.5	3.08	3.38	-2.70
	30000.	21.3	3.00	3.65	-2.93
	50000.	22.4	2.92	4.08	-3.24

References

Dimitrijević, M. S. : 1996, *Zh. Prikl. Spektrosk.* **63**, 810.
Dimitrijević, M.S., and Sahal-Bréchot, S. : 1984, *JQSRT* **31**, 301.
Dimitrijević M.S. and Sahal-Bréchot, S. : 1999, *Atomic Data and Nuclear Data Tables* submitted.
Holtsmark, J., Trumpy, B. : 1925, *Z. Phys.* **31**, 803.
Kitaeva, V. F. : 1956, *Tr. Fiz. Inst. Acad. Nauk SSSR* **11**, 3.
Konjević, N., Roberts, J. R. : 1976, *J. Phys. Chem. Ref. Data* **5**, 209.
Moore, C. E. : 1971, *Atomic Energy Levels III*, NSRDS-NBS 35, Washington.
Pichler, G. : 1972, *Fizika* **4**, 235.
Sahal-Bréchot, S. : 1969a, *Astron.Astrophys.* **1**, 91.
Sahal-Bréchot, S. : 1969b, *Astron.Astrophys.* **2**, 322.

Journal of Research in Physics Vol. 28, No. 3, 295-298 (1999)

ON THE STARK BROADENING OF NEUTRAL CALCIUM LINES

MILAN S. DIMITRIJEVIĆ[1] AND SYLVIE SAHAL-BRECHOT[2]
[1] *Astronomical Observatory, Volgina 7, 11050 Belgrade, Yugoslavia*
E-mail mdimitrijevic@aob.aob.bg.ac.yu

[2] *Observatoire de Paris, 92195 Meudon Cedex, France*
E-mail sahal@obspm.fr

Abstract. Using a semiclassical approach, we have calculated electron-, proton-, He II-, Mg II-, Si II-, and Fe II-impact line widths and shifts for 189 neutral calcium lines, as a function of temperature and perturber density. Perturbers selected here, are the main perturbers in solar and stellar atmospheres.

1. INTRODUCTION

Neutral calcium lines are very important for stellar spectra synthesis and stellar plasma analysis due to cosmical abundance of this element. Stark broadening parameters of Ca I are important as well for laboratory plasma diagnostics, modelling and investigation. In order to complete as much as possible Stark broadening data needed for astrophysical and laboratory plasma research and stellar opacities calculations, we have published in a series of papers, results of large scale calculations of Stark broadening parameters for a number of spectral lines of various emitters (Dimitrijević, 1996, 1997 and references therein). Our calculations have been performed within the semiclassical - perturbation formalism (Sahal-Bréchot, 1969ab), for transitions when a sufficiently complete set of reliable atomic data exist and the good accuracy of obtained results is expected.

Up to now, Stark broadening parameters for 79 He I, 62 Na, 51 K, 61 Li, 25 Al, 24 Rb, 3 Pd, 19 Be, 270 Mg, 31 Se, 33 Sr, 14 Ba, 28 Ca II, 30 Be II, 29 Li II, 66 Mg II, 64 Ba II, 19 Si II, 3 Fe II, 2 Ni II, 12 B III, 23 Al III, 10 Sc III, 27 Be III, 32 Y III, 20 In III, 2 Tl III, 10 Ti IV, 39 Si IV, 90 C IV, 5 O IV, 114 P IV, 2 Pb IV, 19 O V, 30 N V, 25 C V, 51 P V, 34 S V, 26 V V, 30 O VI, 21 S VI, 2 F VI, 14 O VII, 10 FVII, 10 Cl VII, 20 Ne VIII, 4 K VIII, 6 Kr VIII, 4 Ca IX, 30 K IX, 8 Na IX, 57 Na X, 48 Ca X, 4 Sc X, 7 Al XI, 4 Si XI, 18 Mg XI, 4 Ti XI, 10 Sc XI, 9 Si XII, 27 Ti XII, 61 Si XIII and 33 V XIII multiplets become available.

Data for particular lines of F I, B II, C III, N IV, Ar II, Ga II, Ga III, Cl I, Br I, I I, Cu I, Hg II, N III, F V and S IV also exist.

In order to continue our project to provide to physicists and astrophysicists an as much as possible complete set of needed reliable Stark broadening data, we have

calculated within the semiclassical-perturbation formalism, electron-, proton-, He II-, Mg II-. Si II-, and Fe II - impact line widths and shifts for 189 neutral calcium lines, as a function of temperature and perturber density. Perturbers selected here, are the main perturbers in solar and stellar atmospheres.

2. RESULTS AND DISCUSSION

A summary of the formalism has been published several times (see e. g. Dimitrijević and Sahal-Bréchot 1984). Energy levels have been taken from Sugar and Corliss (1979). .

Our results for 189 Ca I multiplets as a function of the perturber density and temperature and the comparison with available experimental and theoretical data will be published in Dimitrijević and Sahal-Bréchot (1999a,b).

Table 1

This table shows electron- and proton-impact broadening full half-widths (FWHM) and shifts for Ca I for a perturber density of 10^{16} cm^{-3} and temperatures from 2,500 up to 50,000 K. By deviding C with the full linewidth, we obtain an estimate for the maximum perturber density for which the line may be treated as isolated and tabulated data may be used (Dimitrijević and Sahal-Bréchot 1984). For each value given in Table 1, the collision volume (V) multiplied by the perturber density (N) is much less than one and the impact approximation is valid (Sahal–Bréchot, 1969ab). Values for NV > 0.5 are not given and values for $0.1 <$ NV ≤ 0.5 are denoted by an asterisk.

PERTURBER DENSITY = 1.E+16cm-3

PERTURBERS ARE :		ELECTRONS		PROTONS	
TRANSITION	T(K)	WIDTH(Å)	SHIFT(Å)	WIDTH(Å)	SHIFT(Å)
4S - 4P	2500.	0.103E-01	0.578E-02	0.581E-02	0.155E-02
4227.9 Å	5000.	0.115E-01	0.665E-02	0.587E-02	0.178E-02
C= 0.17E+20	10000.	0.124E-01	0.795E-02	0.592E-02	0.202E-02
Singlet	20000.	0.143E-01	0.807E-02	0.600E-02	0.229E-02
	30000.	0.162E-01	0.724E-02	0.605E-02	0.245E-02
	50000.	0.193E-01	0.585E-02	0.613E-02	0.268E-02
4S - 5P	2500.	0.672E-01	0.474E-01	*0.180E-01	*0.110E-01
2722.5 Å	5000.	0.726E-01	0.456E-01	*0.197E-01	*0.137E-01
C= 0.42E+18	10000.	0.798E-01	0.364E-01	0.216E-01	0.163E-01
Singlet	20000.	0.864E-01	0.289E-01	0.238E-01	0.190E-01
	30000.	0.878E-01	0.245E-01	0.254E-01	0.206E-01
	50000.	0.887E-01	0.185E-01	0.276E-01	0.228E-01

Table 1 continued

PERTURBER DENSITY = 1.E+16cm-3

PERTURBERS ARE :		ELECTRONS		PROTONS	
TRANSITION	T(K)	WIDTH(Å)	SHIFT(Å)	WIDTH(Å)	SHIFT(Å)
5S - 5P	2500.	7.36	3.52	* 1.85	* 1.07
29288.1 Å	5000.	9.21	2.15	2.00	1.32
C= 0.49E+20	10000.	11.4	0.952	2.17	1.57
Singlet	20000.	12.7	0.146	2.38	1.82
	30000.	13.4	-0.315	2.52	1.97
	50000.	14.0	-0.477	2.73	2.17
5S - 6P	2500.	1.82	0.810	*0.616	*0.172
11959.2 Å	5000.	2.24	0.884	*0.644	*0.212
C= 0.14E+20	10000.	2.83	0.902	*0.661	*0.251
Singlet	20000.	3.54	0.705	0.676	0.291
	30000.	3.99	0.624	0.686	0.315
	50000.	4.49	0.565	0.700	0.347
4P - 5S	2500.	0.363	0.219	0.826E-01	0.581E-01
12678.8 Å	5000.	0.407	0.275	0.897E-01	0.680E-01
C= 0.83E+20	10000.	0.441	0.325	0.979E-01	0.784E-01
Singlet	20000.	0.496	0.321	0.107	0.894E-01
	30000.	0.535	0.290	0.113	0.963E-01
	50000.	0.618	0.241	0.122	0.106
4P - 4D	2500.	0.394	-0.172	0.873E-01	-0.537E-01
7328.2 Å	5000.	0.428	-0.111	0.948E-01	-0.654E-01
C= 0.30E+19	10000.	0.466	-0.625E-01	0.103	-0.770E-01
Singlet	20000.	0.475	-0.263E-01	0.114	-0.889E-01
	30000.	0.481	-0.437E-02	0.121	-0.962E-01
	50000.	0.488	0.320E-02	0.132	-0.106
4P - 5D	2500.	0.460	-0.241	*0.134	*-0.540E-01
5190.3 Å	5000.	0.511	-0.225	*0.143	*-0.693E-01
C= 0.16E+19	10000.	0.581	-0.164	*0.151	*-0.838E-01
Singlet	20000.	0.697	-0.119	*0.160	*-0.984E-01
	30000.	0.758	-0.105	0.166	-0.107
	50000.	0.825	-0.808E-01	0.175	-0.119
5S - 5P	2500.	2.24	1.53	0.704	0.360
19897.4 Å	5000.	2.64	1.49	0.746	0.436
C= 0.47E+20	10000.	3.13	1.05	0.791	0.511
Triplet	20000.	3.93	0.687	0.844	0.590
	30000.	4.34	0.593	0.879	0.638
	50000.	4.72	0.388	0.929	0.702

4P - 5S	2500.	0.820E-01	0.652E-01	0.208E-01	0.168E-01
6143.9 Å	5000.	0.983E-01	0.777E-01	0.232E-01	0.198E-01
C= 0.19E+20	10000.	0.114	0.925E-01	0.259E-01	0.229E-01
Triplet	20000.	0.124	0.993E-01	0.290E-01	0.262E-01
	30000.	0.130	0.100	0.309E-01	0.282E-01
	50000.	0.136	0.912E-01	0.336E-01	0.309E-01
4P - 6S	2500.	0.146	0.104	*0.326E-01	*0.237E-01
3966.5 Å	5000.	0.172	0.127	0.367E-01	0.296E-01
C= 0.32E+19	10000.	0.190	0.149	0.411E-01	0.353E-01
Triplet	20000.	0.202	0.150	0.462E-01	0.411E-01
	30000.	0.211	0.143	0.494E-01	0.447E-01
	50000.	0.222	0.121	0.538E-01	0.493E-01
4P - 4D	2500.	0.943E-01	-0.316E-01	0.244E-01	-0.998E-02
4446.3 Å	5000.	0.106	-0.174E-01	0.252E-01	-0.118E-01
C= 0.23E+19	10000.	0.126	-0.237E-02	0.261E-01	-0.137E-01
Triplet	20000.	0.141	0.108E-01	0.273E-01	-0.157E-01
	30000.	0.149	0.137E-01	0.281E-01	-0.169E-01
	50000.	0.157	0.164E-01	0.294E-01	-0.185E-01

As a sample of our results, the Stark broadening parameters for Ca I spectral lines broadened by electron and proton impacts, for a perturber density of 10^{16} cm^{-3}, are shown in Table 1.

References

Dimitrijević, M. S. : 1996, *Zh. Prikl. Spektrosk.* **63**, 810.
Dimitrijević, M. S. : 1997, *Astrophys. Space Sci.* **252**, 415.
Dimitrijević, M.S., and Sahal-Bréchot, S. : 1984, *JQSRT* **31**, 301.
Dimitrijević M.S. and Sahal-Bréchot, S. : 1999a, *Astron. Astrophys. Suppl. Series* submitted.
Dimitrijević M.S. and Sahal-Bréchot, S. : 1999b, *Serb. Astron. J.* **160**, in press.
Sahal-Bréchot, S. : 1969a, *Astron.Astrophys.* **1**, 91.
Sahal-Bréchot, S. : 1969b, *Astron.Astrophys.* **2**, 322.
Sugar, J. and Corlis, C. : 1979, *J. Phys. Chem. Ref. Data* **8**, 865.

Journal of Research in Physics Vol. 28, No. 3, 299-302 (1999)

THE ELECTRON-IMPACT BROADENING PARAMETERS FOR ASTROPHYSICALLY IMPORTANT LINES IN Co II SPECTRA

D. TANKOSIĆ, L. Č. POPOVIĆ, M. S. DIMITRIJEVIĆ
Astronomical Observatory, Volgina 7, 11000 Belgrade, Yugoslavia

1. INTRODUCTION

The spectral lines for singly ionized cobalt are present in stellar spectra, as e.g. in Hg-Mn star spectra (Bolcal and Didelon, 1987). The abundance of cobalt is derived by fitting-synthesis analysis of co-added high-resolution *International Ultraviolet Explorer (IUE) spectra*. The investigation of cobalt abundance in Hg-Mn stars shows that the most of the Hg-Mn stars are evidently largely cobalt-deficient ([Co/H]≤ -2dex), but exceptions for mildly cobalt-rich stars, νCnc and φHer, and cobalt-normal stars 87 Psc and 36 Lyn are notable (Smith and Dworetsky, 1993). Also, in hot star atmospheres Stark broadening mechanism is the main pressure broadening mechanism (Dimitrijević, 1989). Consequently, in order to investigate and modeling the Hg-Mn star and other type of hot star atmospheres, the Stark broadening parameters for Co II spectral lines are needed.

There is not measured Stark broadening parameters for Co II lines. However for the resonant $3d^8\ ^3F\text{-}3d^7 4p\ ^3G^0$ (λ=2058.9Å) Co II line the Stark broadening data have been estimated based on regularities and systematic trends by Lakićević (1983).

In order to provide to astrophysicist the needed data, we have calculated Stark broadening parameters for 12 Co II spectral lines, from the $a^5F\text{-}z^5G^0$ multiplet. Calculations were performed by using the modified semiempirical approach (Dimitrijević and Konjević, 1980; Dimitrijević and Konjević, 1981; Popović and Dimitrijević, 1996). Also, considering that Co II (λ=2307.85Å) line has been used for cobalt abundance determination (see e.g. Smith and Dworetsky, 1993) in HgMn stars, we have tested the influence of Stark mechanism on width of this line in layers of A type stars, as well as DA and DB white dwarfs. This has been done with the help of Kurucz's model atmospheres (Kurucz, 1979) of an A type star (T_{eff}=10000K, logg=4), and with Wickramasinghe's models of DA (T_{eff}=10000K, logg=6) and DB (T_{eff}=15000K, logg=7) white dwarf atmospheres (Wickramasinghe, 1972).

2. RESULTS AND DISCUSSION

As an example of our results, we present here the electron-impact broadening parameters for $a^5F_4 - z^5G^0_5$ Co II line as a function of temperature, calculated by using the modified semiempirical approach. The energy levels were taken from Pickering et al (1998). Oscillator strength data have been calculated by using the Bates-Damgaard method (Bates and Damgaard, 1949).

In Table 1, Stark widths and shifts for $a^5F_4 - z^5G^0_5$ Co II spectral line, for an electron density of $10^{23}m^{-3}$ and temperature range 5000-50000K, are shown. The configuration mixing has been taken into account in calculation.

It is no possible to compare our data with other, since experimental data do not exist and we have not calculated Stark broadening data for the line treated by Lakićević (1983).

We have considered the influence of the Stark broadening mechanism on Co II (λ=2307.85 Å) line in stellar plasma, by using the Kurucz's model atmospheres of an A type star (T_{eff}=10000K, log g=4), and with Wickramasinghe's models of DA (T_{eff}=10000K, log g=6) and DB (T_{eff}=15000K, log g=7) white dwarf atmospheres. The results of our investigation are presented in Table 2 and Figs. 1 and 2.

Thermal Doppler and Stark widths as functions of optical depth, for the considered Co II line, are compared in Figs.1. and 2. for an A type star and DA and DB white dwarf, respectively. As one can see from Fig. 1, in photospheric layers of hot A type stars the Stark line width is one order of magnitude larger than thermal Doppler one. In higher layers of stellar atmospheres (τ≈-4) however, the thermal Doppler mechanism is more important. In Fig. 2 one can see, that in the case of DA and DB white dwarf atmospheres Stark broadening mechanism is important in all atmospheric layers, especially in deeper layers, where the Stark width is two or three orders of magnitude larger than the thermal Doppler width.

Table 1. Stark (full) widths and shifts for the Co II λ=2307.85Å spectral line. The electron density is $10^{23}m^{-3}$.

Transition	T(K)	Stark FWHM (Å)	d(Å)
$a^5F_4 - z^5G^0_5$ λ=2307.85 Å	5000	0.751E-01	-0.182E-01
	10000	0.524E-01	-0.130E-01
	20000	0.363E-01	-0.928E-02
	30000	0.293E-01	-0.768E-02
	40000	0.253E-01	-0.675E-02
	50000	0.227E-01	-0.608E-02

Table 2. Thermal Doppler and Stark full widths for the Co II λ=2307.85Å line as a function of optical depth for a DA white dwarf model (T_{eff}=10000K, log g=6).

τ	T(K)	log(p_e)	Stark FWHM (Å)	Thermal Doppler FWHM (Å)
0.00	7009	1.068	0.762E-04	0.342E-03
0.05	8034	2.599	0.210E-02	0.366E-03
1.25	11501	4.211	0.498E-01	0.438E-03
2.00	12474	4.413	0.701E-01	0.457E-03
6.00	14914	4.657	0.935E-01	0.499E-03
10.00	16102	4.716	0.953E-01	0.519E-03

Table 3. Thermal Doppler and Stark full widths for the Co II λ=2307.85Å line as a function of optical depth for a DB white dwarf model (T_{eff}=15000K, log g=7).

τ	T(K)	log(p_e)	Stark FWHM (Å)	Thermal Doppler FWHM (Å)
0.00	8998	2.465	0.130E-02	0.388E-03
0.05	9158	3.815	0.253E-01	0.406E-03
1.25	13859	4.877	0.173	0.481E-03
2.00	14847	5.062	0.239	0.498E-03
6.00	18222	5.699	0.758	0.552E-03
10.00	19934	6.000	1.320	0.577E-03

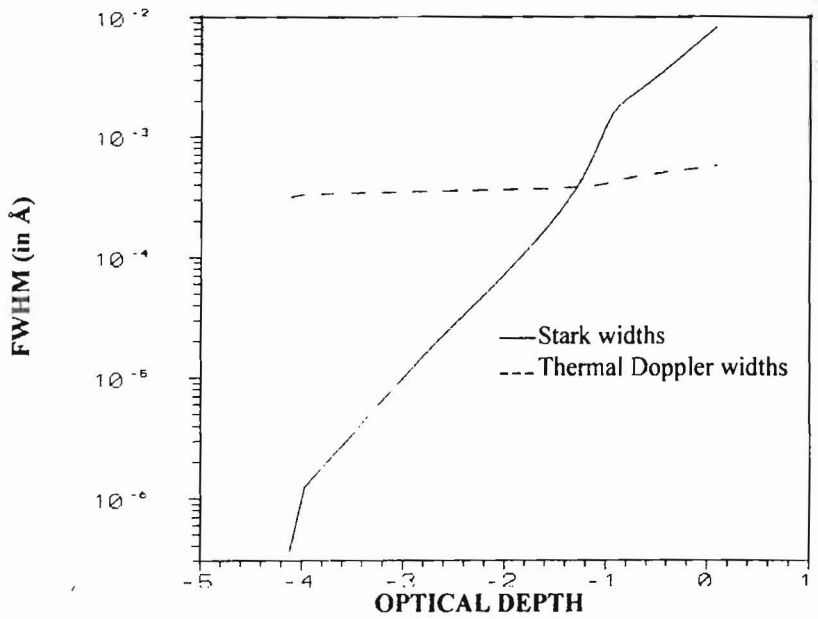

Fig. 1. Thermal Doppler and Stark full widths for the Co II λ=2307.85 Å line as functions of optical depth for an A type star (T_{eff}=10000K, log g=4).

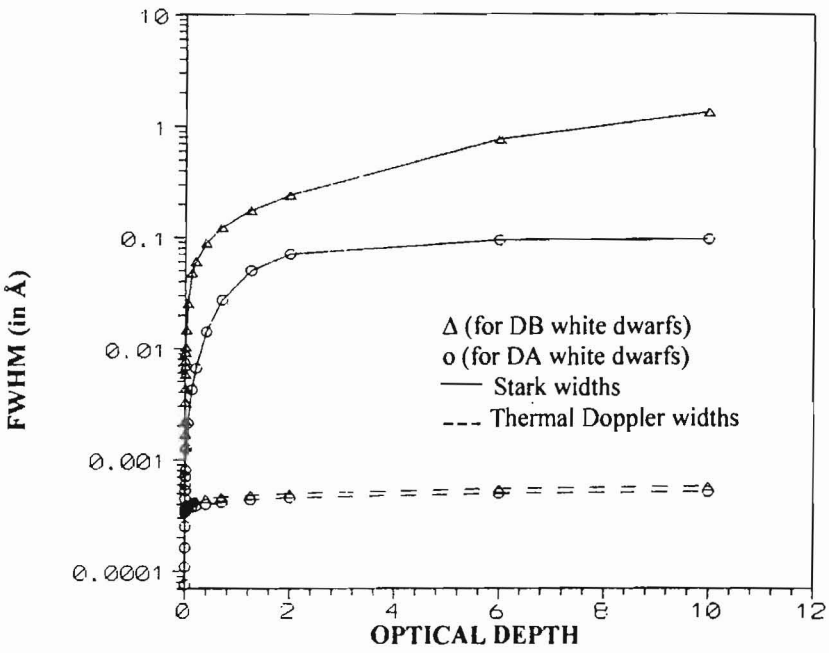

Fig. 2. Thermal Doppler and Stark full widths for the Co II λ=2307.85 Å line as functions of optical depth for DA (T_{eff}=10000K, log g=6) and DB (T_{eff}=15000K, log g=7) models.

ACKNOWLEDGEMENT

This work is a part of the project "**Astrometrical, Astrodynamical and Astrophysical Investigations**".

References

Bates, D. R. and Damgaard, A: 1949, Trans. Roy. Soc. London, Ser. A **242**, 101.
Bolcal, C. and Didelon P.: 1987, *Elemental Abundance Analyses*, Istitut d'Astronomie de l'Université de Lausane, Chavannes-des-Bois, Switzerland, p.152
Dimitrijević, M. S.: 1989, *Bull. Obs. Astron. Belgrade* **140**, 111.
Dimitrijević, M. S. and Konjević, N.: 1980, JQSRT, **24**, 454.
Dimitrijević, M. S. and Konjević, N.: 1981, *Spectral Line Shapes*, Berlin, New York.
Kurucz, R. L.: 1979, Astrophys. J. Suppl. Series, **120**, 373.
Lakićević, I. S., Astron. Astrophys.: 1983, **127**, 37.
Pickering, J. C, Raassen, A. J. J., Uylings, P. H. M. and Johansson, S.: 1998, Astrophys. J. Suppl. Series, **117**, 261.
Popović, L. Č. and Dimitrijević, M. S.: 1996, Phys. Scr., **53**, 325.
Smith, K. I. and Dworetsky, M. M.: 1993, Astron. Astrophys., **274**, 335.
Wickramasinghe, D. T.: 1972, Mem. R. Astron. Soc., **76**, 129.

Journal of Research in Physics Vol. 28, No. 3, 303-305 (1999)

THE ELECTRON-IMPACT EFFECT IN Hg-Mn STARS: ASTROPHYSICAL IMPORTANT Zr III LINES

Luka Č. Popović and Milan S. Dimitrijević
Astronomical observatory, Volgina 7, Yu-11000 Belgrade, Serbia

1. INTRODUCTION

As it is very well known the Hg-Mn stars are non-magnetic late B type stars. In their spectra unusually strong lines of many heavy ions are present (see e.g. Preston 1971, Heacox 1979, Dworetsky 1980, Adelman 1987, Lecrone et al. 1993, Wahlgren et al. 1995). In A and B type stars the electron-impact broadening is the main pressure broadening mechanism (e.g. Dimitrijević 1989). Considering that the resonant lines of ionized heavy elements (z>30) are located in the ultraviolet spectral region, the abundance analysis of these elements has become possible due to satellite observations by high resolution spectrograph as e.g. International Ultraviolet Explorer (IUE) satellite or Goddard High Resolution Spectrograph (GHSR) installed at Hubble Space Telescope. The number of heavy ion lines observations with the higher photometric quality and spectral resolution is growing up. Consequently, experimental and theoretical spectroscopic data for modeling of these lines are required.

In order to investigate the Hg-Mn star atmospheres as well as other types of hot stars, the Stark broadening parameters for heavy ion lines are needed. Zr III lines are presented in spectra of Hg-Mn stars. E.g. in spectra of Chi Lupi, a B-type star, well-resolved lines of Zr III λ = 1937.22 Å, 1940.24 Å and 1941.06 Å have been observed. Here we present the electron-impact broadening parameters for these four astrophysical important Zr III lines as a function of temperature, calculated by using the modified semi-empirical approach (Dimitrijević and Konjević 1980, Popović and Dimitrijević 1996).

2. RESULTS AND DISCUSSION

The atomic energy levels needed for the calculations were taken from Reader and Acquista (1997). Oscillator strengths have been calculated by using the method

of Bates and Damgaard (1949) and the tables of Oertel and Shomo (1968). For calculation of Stark broadening widths the modified semi-empirical apporach has been used (Dimitrijević and Konjević 1980, Popović and Dimitrijević 1996)

Results obtained using the MSE approach for electron – impact line widths and shifts for three Zr III lines as a function of temperature are presented in Tables 1. The calculations have been performed for a perturber density of $10^{23}\mathrm{m}^{-3}$, since within the MSE formalism, the results for the electron-impact broadening parameters are linear with electron density.

Table 1. Stark widths (FWHM) of Zr III spectral lines at an electron density of $10^{23}\mathrm{m}^{-3}$ as a function of temperature.

Transition	T (K)	W (nm)
$a^3P_1 - z^3P_1^0$	5000	.452E-02
	10000	.317E-02
	20000	.220E-02
λ=194.662 nm	30000	.178E-02
	40000	.153E-02
	50000	.137E-02
$a^3P_0 - z^3P_1^0$	5000	.447E-02
	10000	.314E-02
	20000	.218E-02
λ=193.665 nm	30000	.176E-02
	40000	.152E-02
	50000	.136E-02
$a^3P_2 - z^3P_2^0$	5000	.474E-02
	10000	.332E-02
	20000	.231E-02
	30000	.187E-02
λ=194.106 nm	40000	.161E-02
	50000	.144E-02
$a^1G_4 - z^1F_3^0$	5000	.459E-02
	10000	.321E-02
	20000	.224E-02
	30000	.181E-02
λ=194.020 nm	40000	.156E-02
	50000	.140E-02

There is no experimental data for the Stark broadening parameters of Zr III spectral lines, and such data will be of importance for the refinement of the Stark broadening theory for spectral lines from complex spectra.

References

Adelman S. J.: 1987, Mon. Not. R. Astron. Soc. **228**, 573.

Bates D.R. and Damgaard A.: 1949, Trans. Roy. Soc. London, Ser. A **242**, 101.

Dimitrijević M. S.: 1989, Bull. Obs. Astron. Belgrade **140**, 111.

Dimitrijević M. S. and Konjević N.: 1980, J. Quant. Spectrosc. Radiat. Transf. **24**, 454.

Dworetsky M. M.: 1980, Astron. Astrophys. **84**, 350.

Heacox W. D.: 1979, Astrophys. J. Supl. Series **41**, 675.

Leckrone D. S., Wahlgren G. M., Johansson S. G., Adelman S. J.: 1993, ASP Conference Series **44**, 42

Oertel G.K. and Shomo L.P.: 1968, Astrophys. J. Supl. Series **16**, 175.

Preston G. W.: 1971, Publ. Astron. Soc. Pac. **83**, 571.

Popović L. Č. and Dimitrijević M. S.: 1996, Phys. Scr. **53**, 325.

Reader J. and Acquista N.: 1997, Phys. Scr. **55**, 310.

Wahlgren G. M., Leckrone D. S., Johansson S. G., Rosberg M. and Brage T.: 1995, Astrophys. J. **444**, 438.

Journal of Research in Physics Vol. 28, No. 3, 307-309 (1999)

BELDATA - THE ASTRONOMICAL DATABASE OF ASTRONOMICAL OBSERVATORY: STARK BROADENING DATA INVESTIGATIONS

L. Č. POPOVIĆ, M. S. DIMITRIJEVIĆ, N. D. MILOVANOVIĆ and N. TRAJKOVIĆ
Astronomical Observatory, Volgina 7, YU-11000 Belgrade, Serbia
lpopovic@aob.bg.ac.yu

1. INTRODUCTION

In early-type stars like B and A stars and white dwarfs, Stark broadening is the main pressure broadening mechanism, and the corresponding Stark broadening parameters are of interest for a number of investigations related to stellar plasma. One may mention as examples calculation of stellar opacities, stellar atmospheres modeling and investigations, abundance determinations, interpretation and modeling of stellar spectra and investigation and modeling of subphotospheric layers.

The interest for a very extensive list of line broadening data is additionally stimulated by the development of space astronomy where an extensive amount of spectroscopic information over large spectral regions of all kind of celestial objects has been and will be collected, stimulating the spectral-line-shape research. Consequently, the interest not only for abundant, but also for trace elements data increases. Not only in astrophysics, but also in physics and plasma technology, a number of problems depend on very extensive list of elements and line transitions with their atomic and line broadening parameters. One may mention as examples laboratory plasma diagnostic, research and modeling, radiative transfer calculations and investigation of laser produced plasmas (not only in laboratory but as well in industry during the laser welding, melting and evaporation of different targets), and plasma created in fusion research (particularly inertial confinement and pellet compression fusion), development and modeling of lasers, as well as of light sources.

In a series of papers, large scale calculations of Stark broadening parameters for a number of spectral lines of various emitters (Dimitrijević, 1996, 1997 and references therein) performed on Belgrade Observatory have been published. In order to complete as much as possible Stark broadening data needed for astrophysical and laboratory plasma research and stellar opacities calculations we are making a continuous effort to provide Stark broadening data for a large set of atoms and ions. Our calculations have been performed within the semiclassical - perturbation formalism (Sahal-Bréchot, 1969ab), for transitions when a sufficiently complete set of reliable atomic data exist and the good accuracy of obtained results is expected. From a large set of data for Stark broadening parameters we are going to make a database.

2. CONTENTS OF THE DATABASE

Extensive calculations have been performed, up to now (Dimitrijević, 1996, 1997 and references therein) for a number of radiators, and consequently, Stark broadening parameters for 79 He I, 62 Na, 51 K, 61 Li, 25 Al, 24 Rb, 3 Pd, 19 Be, 270 Mg, 31 Se, 33 Sr, 14 Ba, 189 Ca, 28 Ca II, 30 Be II, 29 Li II, 66 Mg II, 64 Ba II, 19 Si II, 3 Fe II, 2 Ni II, 12 B III, 23 Al III, 10 Sc III, 27 Be III, 32 Y III, 20 In III, 2 Tl III, 10 Ti IV, 39 Si IV, 90 C IV, 5 O IV, 114 P IV, 2 Pb IV, 19 O V, 30 N V, 25 C V, 51 P V, 34 S V, 26 V V, 30 O VI,

21 S VI, 2 F VI, 14 O VII, 10 F VII, 10 Cl VII, 20 Ne VIII, 4 K VIII, 4 Ca IX, 30 K IX, 8 Na IX, 57 Na X, 48 Ca X, 4 Sc X, 7 Al XI, 4 Si XI, 18 Mg XI, 4 Ti XI, 10 Sc XI, 9 Si XII, 27 Ti XII, 61 Si XIII and 33 V XIII multiplets become available.

Data for particular lines of F I, B II, C III, N IV, Ar II, Ga II, Ga III, Cl I, Br I, I I, Cu I, Hg II, N III, F V and S IV also exist.

In order to complete as much as possible the needed Stark broadening data, Belgrade group (Milan S. Dimitrijević, Luka Č. Popović, Vladimir Kršljanin, Dragana Tankosić, Nenad D. Milovanović) used the modified semiempirical approach developed by Dimitrijević and Konjević 1980 for radiators where there is not a sufficiently complete atomic data set for reliable semiclassical calculations. The width and in some cases the shift data for the most intensive lines for the following atom and ion species were calculated by them: Ar II, Ti II, Mn II, Fe II, Pt II, Bi II, Zn II, Cd II, As II, Br II, Sb II, I II, Xe II, La II, Y II, Zr II, Sc II, Be III, B III, Mn III, Ga III, Ge III, S III, As III, Se III, Zn III, Mg III, Ca III, La III, C III, N III, O III, F III, Ne III, Na III, Al III, Si III, P III, S III, Cl III, Ar III, B IV, Cu IV, Ge IV, C IV, N IV, O IV, Ne IV, Mg IV, Si IV, P IV, S IV, Cl IV, Ar IV, C V, O V, F V, Ne V, Al V, Si V, N VI, F VI, Ne VI, Si VI, P VI, and Cl VI lines.

3. THE STRUCTURE OF THE DATABASE

Astronomical Database System has as a goal to provide the fast and easy data exchange between Internet users and database. Astronomical Database will be placed on server of the Astronomical Observatory in Belgrade. Access will be managed through Internet with 24 hour online support on address http://www.aob.bg.ac.yu/BELDATA. Astronomical Observatory already has Internet presentation on http://www.aob.bg.ac.yu but Astronomical Database is not in function yet.

The atomic data, part of BELDATA system, will be based on the following components (Fig. 1.):

1. Database is the Stark broadening data set.
2. HTTPD (Hyper Text Transfer Protocol Daemon) or www server that has role to provide mutual HTML document communication between Internet and local server.
3. MI (Manager Interface) will transform HTML format document from HTTPD in appropriate form for DataBase Manager System.
4. DBMS (DataBase Manager System) is capable for manipulating with the database. After data processing DBMS will retrieve the data.

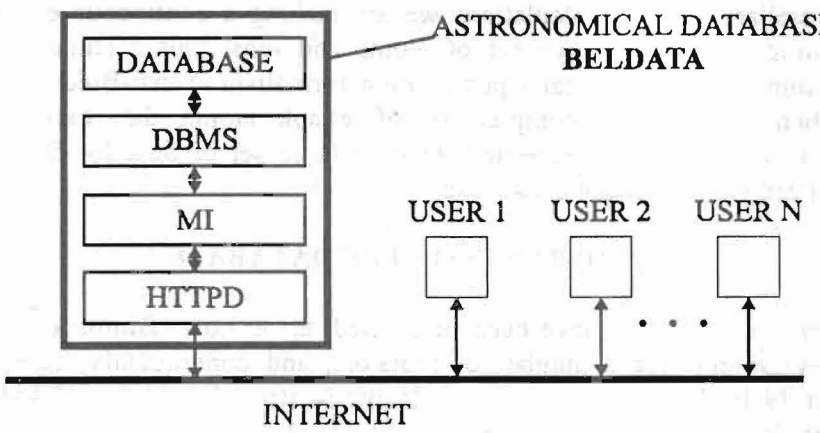

Fig. 1. Scheme of the Astronomical Database

The data will be taken by MI, transformed to HTML format document and proceeded by HTTPD over Internet to user.

Query form, which will be fulfilled by an Internet user, have two return option: data needed for laboratory plasma modeling and data needed for stellar plasma modeling. In future, BELDATA will be extended with spectra of active galactic nuclei and solar spectra. New Stark broadening parameter data will be added to the database when calculated.

Whole system needs constant maintenance effort. Moreover, we have planned to expand capabilities of DBMS. Presently, it is one executable program which may take the needed data from the database but in the future it will be a complex system with numerous functions. These functions will include various database multiple search options fully configurable within one HTML form controlled by user.

References

Dimitrijević, M. S.: 1996, *Zh. Prikl. Spektrosk.*, **63**, 810.
Dimitrijević, M. S.: 1997, *Astrophys. Space Sci.*, **252**, 415.
Dimitrijević, M.S., and Konjević, N.: 1980, *JQSRT*, **24**, 451.
Sahal-Bréchot, S.: 1969a, *Astron.Astrophys.*, **1**, 91.
Sahal-Bréchot, S.: 1969b, *Astron.Astrophys.*, **2**, 322.

Journal of Research in Physics Vol. 28, No. 3, 311-314 (1999)

The Procedure of AGN Spectra Elaboration by Using IRAF: The case of Hα of IIIZw2

E. Bon, N. Stanić and A. Kubičela, L. Č. Popović,
Astronomical Observatory Belgrade, Volgina 7, 11160 Belgrade,
e-mail: lpopovic@aob.bg.ac.yu

1. Introduction

The study of the shape and behavior of the Active Galactic Nuclei (AGNs) broad lines brings information about structure and dynamics of the emitting gas (see e.g. Osterbrock 1990). Concerning that these objects are very faint their CCD images have been obtained by using long exposition regime. That is reason that these images are very noisy and full of cosmic rays.

In order to obtain the true shape of the AGNs emission lines the CCD spectral line images should be processed by special programs. One of the procedures that could be used for extracting spectra is Image Reduction and Analysis Facility (IRAF). Here we present our experience with using the IRAF for calibrating spectra of III Zw2. The Hα and Hβ lines, have been observed at Isaac Newton Telescope (INT) at Instituto de Astrofisica de Canarias (IAC).

2. III Zw2

III Zw2 is an object classified as Syfert 1 galaxy or as a quasar, with variable central source in all wavelength, from radio to X-rays; variations of factor 2 in a few months occurs. The central part of the nucleus contain a black hole with mass of $5 \cdot 10^7 M\odot$. The central engine is powered by accretion flow of 2 solar mass per year. Total accretion disk mass is of the same order as the mass of the central black hole (Kaastra, de Korte 1987).

3. Method of elaboration

The IRAF has been developed by the National Optical Astronomical Observatory (NOAO) Kit Peak, and has been adopted by the Space Telescope Science Institute in Baltimore as a principal data analysis environment for Hubble Space Telescope (HST) data. The IRAF contains general image processing and graphic applications, plus programs for reduction and analyses of optical astronomical data. It is developed, and runs under UNIX operating system, and similar operating systems (VMS, LINUX, SOLARIS, etc.).

Also, for calibrating spectra under IRAF, we needed several small packages DATAIO, NOAO, IMRED, CCDRED, TWODSPEC, LONGSLIT, BIAS ...

Procedure of spectra elaboration start with import procedure. The spectra should be imported in a format which is compatible with the IRAF image standard. One of the standards for CCD image data is FITS. The observed spectra of III Zw2 Hα and Hβ have been given in FITS format, and have been imported by using DATAIO package. There were two spectra of III Zw2, and several types of calibrating spectra. It is very important to remove the "additive" effects: electronic pedestal level (measured from the over scan region on each of CCD image frame), pre-flash level or underlying bias structure, and dark current. The flat-field data (dome or projector flats and twilight sky exposures) will remove the multiplicative gain and illumination variation across the CCD chip. Also it is important to remove all bad pixels and cosmic ray additive effects (Massey el al. 1992). With those procedures we have calibrated CCD images, and this procedure is standard for all CCD images in general. In Fig. 1. we present a set of CCD images for calibration of CCD spectra.

After removing additive effects and normalizing CCD image, we proceed with finding the spectrum on CCD image by dividing it on several pixel rows, where the location of the spectrum position is being done. Next we define the extraction window, and we trace the center of spatial profile as a function of the dispersion axis. Last step is summing the spectrum within the extraction window. This part of extraction of the spectra gives, as a result, one-dimensional spectra. For these steps we used packet APALL. The same procedure, with the same parameters should be done on a lamp comparison spectrum, so the wavelength calibration could be done. The last step is flux calibration.

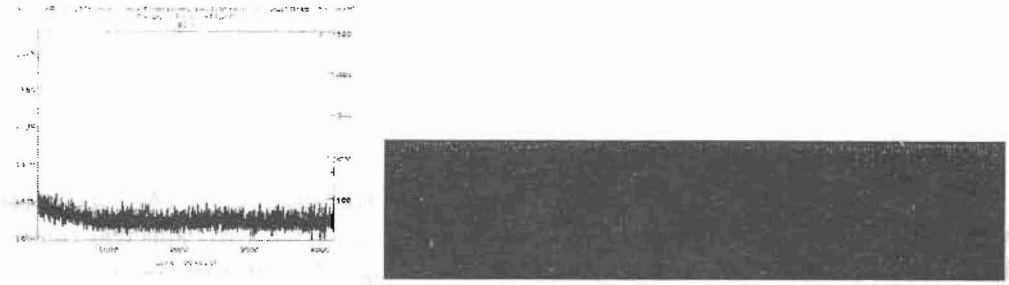

Fig.1a) The bias.

Fig. 1b) The flat field.

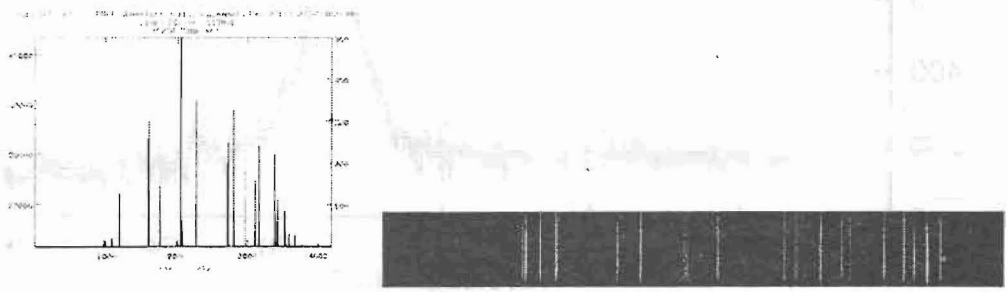

Fig. 1c) The spectrum of CuNe comparison lamp

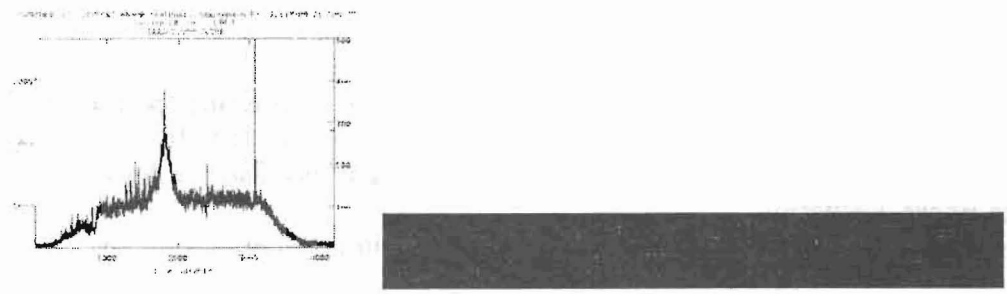

Fig. 1d) One of the spectra of the object IIIZw2

Figure 1. Representation of CCD images

Using the IRAF we have elaborated the IIIZw2 spectra observed of IAC. The observations were performed in two spectral range $\lambda = 6500$ to $\lambda = 7600$ (Hα spectral range) and $\lambda = 5000$ to $\lambda = 6100$ (Hβ spectral range). In the Fig. 2. one can see an example of calibrated spectrum.

As we can see from Fig. 2. the shape of III Zw2 is very complex. After, here described procedure of elaboration, next step is analysis of the shape of the lines. Detailed discussion of the shape of III Zw2 Hα and Hβ lines will be published elsewhere (Popović et al. 1999)

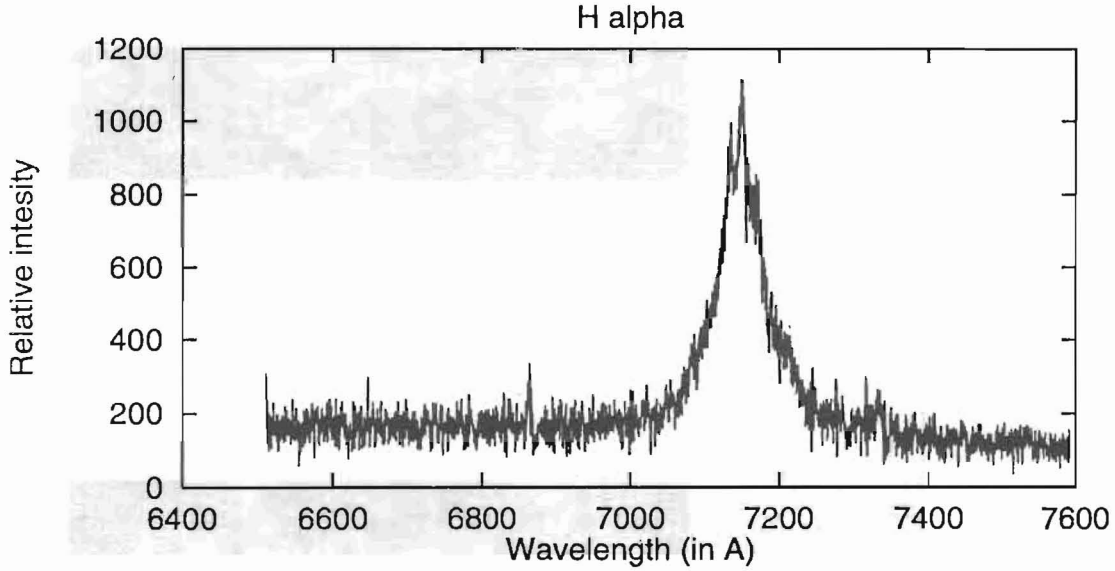

Fig. 2. The profile of Hα of IIIZw2 Hα line.

References

Massey P. , Valdes F., Barnes J. : 1992, *A User's Guide to Reducing Spectra with IRAF.*

Kaastra J. S. and de KorteP. A. J. :1987, *Astron. Astrophys.* **198**, 16.

Osterbrock D. E. :1976, *Astrophysics of Gaseous Nebulae and Galactic Nuclei*, University Science Books, California.

L. Č. Popović, A. Kubičela, N. Stanić and E. Bon, (in preparation).

Journal of Research in Physics Vol. 28, No. 3, 315-318 (1999)

BELGRADE MERIDIAN CIRCLE OBSERVATIONS OF STARS OF INTEREST FOR THE INVESTIGATIONS OF THE STARK BROADENING INFLUENCE ON STELLAR SPECTRAL LINES

MILAN S. DIMITRIJEVIĆ, ZORICA CVETKOVIĆ AND MIODRAG DAČIĆ
Astronomical Observatory, Volgina 7, 11000 Belgrade, Yugoslavia
E-mail mdimitrijevic@aob.bg.ac.yu
E-mail mdacic@aob.bg.ac.yu
E-mail zcvetkovic@aob.bg.ac.yu

Abstract. Belgrade meridian circle observations of stars of B6-A9 spectral type, which are of interest for the investigations of the Stark broadening influence on stellar spectra has been reviewed. In spectra of such stars the Stark broadening is the dominant pressure broadening mechanisme and data on their positions (right ascension and declination) are needed e.g. for the formulation of projects for space telescopes.

1. INTRODUCTION

Stark broadening data are of interest for a number of astrophysical problems as diagnostics and modeling of stellar plasma, abundance research, stellar spectra interpretation and modeling, radiative transfer etc. Among different pressure broadening mechanisms, Stark broadening is the dominant one for stars with the effective temperature larger or of the order of magnitude of 10000 K. Such stars are A, B and O type stars and white dwarfs. However, for O stars and early B type stars, electron density is so small that the pressure broadening is negligible in comparison with Doppler broadening, except for transitions involving high principal quantum numbers. The most interesting stars for the investigation of Stark broadening influence on stellar spectral lines are white dwarfs, A type and late B type stars.

With the placement of telescopes on the orbit around the Earth, and with the development of satellite observations, it becomes possible to investigate spectral lines of even trace elements and their ions. Now exist possibilities to formulate and submit various observational projects with the use of telescopes and various devices on orbit. One can see from instructions for project applications for observations with the help of Hubble Space telescope (Madau, 1994), that basic data needed, are the name of target and its precise position (right ascension and declination), total apparent magnitude, instrumental configuration and operation mode, as well as spectral elements and wavelength range. For application is needed also the number of the telescope orbits needed for observation and additional comments and requests if exist.

As one can see, the object position is one of very important basic data needed for the project application. The aim of this paper is to review observational data for the B6-A9 spectral type stars obtained with the Belgrade Meridian circle. For such stars The Stark broadening mechanism is the dominant pressure broadening mechanism, so that such data may be used for the formulation of eventual projects for stellar spectral lines investigations with the help of the Hubble telescope and similar devices on satellites.

2. B6-A9 SPECTRAL TYPE STAR OBSERVATIONS WITH THE BELGRADE MERIDIAN CIRCLE

Seven observational catalogues have been done from 1968 to 1995 on the Belgrade meridian circle, an instrument typical for astrometrical observations. During this period of almost three decads, positions of a large number of stars were determined, among them B6-A9 spectral type star positions, of interest for Stark broadening investigations. So we will review observational programs realized on the Belgrade meridian circle and will show the number of B6-A9 spectral type stars included.

The first observational program was the Belgrade Catalogue of Latitude Stars with 3957 stars included, which declinations have been determined with the relative method (Sadžakov and Šaletić, 1972). After this, follows the catalogue of right ascensions and declinations of Northern chemisphere zenith telescopes (NPZT) program stars. This catalogue (Sadžakov et al., 1981) contains the positions of 1638 stars, with more than 300 fundamental stars within the FK4 system.

From 1981 to 1987, the double star positions were deterinined (Sadžakov i Dačić, 1990), for stars whose components were not separable photographically or photoelectrically at that time. Among these stars, which number in our program is 1576, we found 483 stars with the spectral type within the B6-A9 range. We can obtain their positions for J2000.0 epoch and choose most interesting for spectral line investigations with the help of the Hubble telescope.

The Catalogue of stars in the vicinity of radio sources (Sadžakov et al., 1991) was done from 1982 up to 1987. With this catalogue, Belgrade observatory gave its contribution to the efforts to conect optical and radio interferometrical observations, i.e. to make transfer from the dynamical to the kinematical reference system. This program contains around 300 stars and we identified 48 B6-A9 spectral type stars.

Moreover, several smaller observational stellar catalogues have been made with the Belgrade meridian circle. The program of Ondrejov photograph zenith telescope contained 223 stars observed within 1985-1990 periode (Sadžakov et al., 1992). Among them 71 stars are of interest for this article.

Within the period when Hipparcos was collecting the data, high luminosity stars (HLS) and radio stars have been observed with the Belgrade meridian circle (Sadžakov et al., 1996). In the same time stars from an enlarged list of stars in the vicinity of radio sources have been observed (Sadžakov et al., 1997). In the list of FK5 fundamental stars observed for this programs, 138 B6-A9 spectral type stars have been identified..

We show here as example, a page from a catalogue of stellar positions. One can see that besides the position (right ascension and declination), some additional

Table 1. One page of the observational catalogue

No	BD	m_v	S_p	α	E_p	δ	E_p
1	41.04933	6.1	A2	0 02 02.099	1984.31	41 48 50.61	1984.31
2	36.00004	8.8	A5	0 06 16.094	1984.30	36 56 14.48	1984.30
3	45.00016	8.1	A3	0 07 26.710	1983.61	46 06 44.22	1983.61
4	53.00025	8.3	A0	0 11 56.656	1983.61	53 32 59.22	1983.61
5	42.00041	6.1	A0	0 13 43.563	1984.30	43 19 02.62	1984.30
6	53.00031	7.8	A3	0 14 01.491	1983.61	54 22 57.10	1983.62
7	35.00035	7.1	A0	0 14 06.000	1984.33	36 21 09.10	1984.30
8	25.00029	7.6	A2	0 15 54.438	1984.30	25 51 48.08	1984.30
9	53.00054	8.8	A5	0 20 09.390	1984.30	54 03 08.22	1984.30
10	-4.00040	7.8	A0	0 21 26.482	1983.87	-3 45 07.12	1983.87
11	70.00039	8.0	A0	0 39 31.085	1983.61	71 05 32.49	1984.11
12	32.00124	8.1	A3	0 41 40.970	1985.08	33 20 40.35	1984.98
13	50.00143	7.2	A0	0 45 08.322	1985.08	51 10 20.64	1985.08
14	68.00057	8.0	A2	0 49 33.628	1983.61	68 35 41.36	1983.61
15	51.00179	6.3	A0	0 50 53.942	1983.62	52 25 06.37	1983.61
16	-19.00147	7.2	A0	0 55 09.602	1984.39	-19 16 07.80	1984.39
17	43.00193	6.0	B9	0 57 13.070	1985.08	44 26 39.05	1985.08
18	46.00241	8.0	A0	0 59 53.927	1983.62	47 25 49.76	1983.61
19	-20.00191	8.7	A2	1 02 46.099	1984.39	-20 07 21.62	1984.24
20	46.00285	9.0	A0	1 09 09.629	1985.08	46 44 07.43	1985.08
21	50.00236	8.9	A0	1 09 19.693	1984.06	51 15 35.44	1984.31
22	48.00392	7.1	A0	1 14 49.088	1985.08	48 44 43.70	1985.08
23	53.00271	8.2	A2	1 14 57.706	1985.08	53 39 14.55	1985.08
24	65.00151	8.3	A0	1 15 34.065	1984.31	65 53 42.70	1984.31
25	36.00220	6.4	A3	1 15 56.394	1985.08	37 07 24.94	1985.08
26	72.00069	7.3	A0	1 20 18.976	1984.31	72 35 11.89	1984.31
27	-25.00555	6.8	A5	1 21 11.773	1985.09	-24 36 49.62	1985.09
28	-6.00270	6.8	A0	1 22 29.358	1985.08	-6 12 22.44	1985.08
29	2.00211	6.6	B8	1 24 18.352	1985.08	3 16 35.60	1985.08
30	35.00296	8.3	A2	1 31 18.652	1984.31	35 56 03.84	1984.31

characteristics enabling better identification of the star and the epoch of observation are included. The columns of the shown example represent :

The first column - the ordinal number (for the program or for the given list);

The second column - the number according to the Bon list (Bonner Durchmusterung) which contains more than 300000 northern sky stars up to 9.5 apparent magnitude;

The third column - visual apparent stellar magnitude;

The fourth column - spectral type;

The fifth column - right ascension (hour, minute and second of time);

The sixth column - epoch of the right ascension observation (determination);

The seventh column - declination (degree, minute and second of arc);

The eighth column - epoch of the declination observation (determination);

We hope that this review of Belgrade meridian circle observation and corresponding observational data will be of help to our colleagues wishing to prepare projects for satellite telescopes.

References

Madau, P. (ed.) : 1994, "Hubble Space Telescope, Cycle 5, Phase I Proposal Instructions, Space Telescope Science Institute, (Version 4.0, June 1994), 9.

Sadžakov, S., Šaletić, D. : 1972, "Catalogue of declinations of the latitude programme stars (KŠZ)", *Publ. Obs. Astron. Belgrade*, **17**.

Sadžakov, S., Šaletić, D., Dačić, M. : 1981,"Catalogue of NPZT programme stars", *Publ. Obs. Astron. Belgrade*, **30**.

Sadžakov, S., Dačić, M. : 1990, "Belgrade catalogue of double stars" *Publ. Obs. Astron. Belgrade*, **38**.

Sadžakov, S., Dačić, M., Cvetković, Z. : 1991, *Astron. Journal*, **101**, 713.

Sadžakov, S., Dačić, M., Cvetković, Z. : 1992, *Bull. Astron. Belgrade*, **146**, 1.

Sadžakov, S., Dačić, M., Cvetković, Z. : 1996, *Bull. Astron. Belgrade*, **153**, 1.

Sadžakov, S., Dačić, M., Cvetković, Z. : 1997, *Bull. Astron. Belgrade*, **155**, 3.

Journal of Research in Physics Vol. 28, No. 3, 319-322 (1999)

THE IMPORTANCE OF THE REALISTIC SPECTRAL ENERGY DISTRIBUTION IN THE LIGHT-CURVE ANALYSIS

G. ĐURAŠEVIĆ and S. ERKAPIĆ
Astronomical observatory, Volgina 7, 11050 Belgrade, Yugoslavia
E-mail: gdjurasevic@aob.aob.bg.ac.yu

1. THE IMPORTANCE OF STELLAR ATMOSPHERE MODELS

In previous versions of our programme for light-curve analysis in eclipse CB systems (Đurašević, 1992a), generalised to the case of an overcontact configuration (Đurašević et al., 1998), we had two different possibilities in using of the model with respect to the treatment of the radiation law: the simple black-body theory or the stellar atmosphere models by Carbon & Gingerich (1969, hereafter CG), the latter giving a more realistic spectral energy distribution than the black-body approximation. Further improvement of this programme can be achieved by introducing a third option: a set of tables of model atmospheres that are quite modern and reliable.Here we present our current version of the programme for the light-curve analysis which uses the new promissing Basel Stellar Library (hereafter "BaSeL") with empirically colour-calibrated flux distributions over a large domain of effective temperatures. This library (Lejeune et al. 1997, 1998) combines theoretical stellar energy distributions which are based on several original grids of blanketed model atmospheres.

To compute synthetic colours from the BaSeL models, we need effective temperature, surface gravity and metallicity.The surface gravity can be derived very accurately from the masses and radii of the CB stars by solving the inverse problem of the light-curve analysis, but the temperature determination is related to the assumed metallicity and strongly depends on photometric calibration. Consequently, the BaSeL library has been corrected in such a way as to provide synthetic "corrected" flux distributions, consistent with extant empirical calibrations at all wavelengths from near-UV through the far-IR (see Lejeune et al. 1997, 1998).

In our programme for the light-curve analysis, we have explored the "corrected" BaSeL model flux distributions, with a large range of effective temperature (2000 K $\leq T_{\rm eff} \leq$35000 K), metallicity, ($-1 \leq [Fe/H] \leq 1$) and surface gravity, ($3 \leq \log g \leq 5$).In the inverse-problem solving of the light-curve analysis, the fluxes are calculated in each iter-ation for current values of temperatures and $\log g$ by interpolation in the both of these quantites in atmosphere tables, as an input, for a given metallicity of the CB components. The metallicity of the involved system components can be different. Because of that we can use individual, different tables as an input, for each star, and, in that way, choose the best calculations for its particular atmospheric parameters. Compared to (Vaz et al., 1995) our two-dimensional flux interpolation in $T_{\rm eff}$ and $\log g$ is based on the application of the *bicubic spline* interpolation (Press et al., 1992). This proved itself as a good choice.

The programme for the light-curve analysis can be simply redirected to the Planck or CG approximation, or to the more realistic BaSeL model atmospheres. Parallel testing of these three modifications gave solutions for different passband light curves that were more consistent within the BaSeL models option than within the CG or black-body approximation. If an independant spectroscopic sources could give an estimate of metallicity of the CB components, the application of the BaSeL models option in the light-curve analysis

could really give more reliable solutions. This provides better estimates of the parameters of the CB system. Also, a change in the assumed metallicity causes a noticable change in the predicted stellar effective temperature.

2. APPLICATION TO THE LIGHT-CURVE ANALYSIS OF THE AB And

As an example we tried to estimate orbital and physical parameters of AB And from its photometric observations. This eclipsing binary is a well observed variable star, which belongs to the W subgroup of the W UMa-type systems. Here we analysed and discussed the B and V light-curves obtained by Landolt (1969) and Rigterink (1973), and the B passband curve, obtained during 1982 at the University Observatory of St. Andrews (Bell et al., 1984). The light-curve analysis was made by applying the inverse-problem method (Đurašević, 1992b).

Basic parameters of this system were estimated from quite symmetric Rigternik's (1973) light curve, which is probably cleen from spot effects. These basic parameters of the system were used then as starting points in the inverse-problem solution for other, more or less deformed and asymmetric, light curves. Rigterink (1973) and Landolt (1969) used the same comparison star BD+35°4972, while Bell et al.(1984) used BD+36°5020 as the comparison star. Through measured brightness differences between those two comparison stars all observations were expressed in the system of BD+36°4972. The light curves were then normalised to the light level at the orbital phase 0.25 of the Rigternik's (referent) light curves.

Both stars of this system have an external convective envelope which can show magnetic activity. So, we started the "spotted solution" by assuming that the components of AB And have cool spots, of the same nature as solar magnetic spots. The analysis of these asymmetric light curves begun by optimisation in the spot parameters. When the optimisation based on these parameters does not secure a further minimisation of $S = \sum (O-C)^2$, the basic system parameters have to be introduced in the iterative proces. Using this procedure we optimize all free-parameters of the model in final iterations.

With the presence of single spotted areas on both components, the Roche model gave a good fit of the observations and the basic system parameters were approximately constant for the whole set of the analysed light curves. The results are listed in Table 1, where the indexes (**h**,**c**) corespond to the less-masive (hotter) and more-massive (cooler) star respecti vely. Following from the inverse problem solutions for individual light-curves, Fig. 1 (Left) presents the observed (LCO), referent (LCR) and optimum synthetic (LCC) light curves of AB And, together with the final O-C residuals obtained by solving the inverse problem within the framework of the Roche model with spotted areas on the components. The right-hand side of this panel shows the view of the system, at a noted orbital phase, obtained with the parameters estimated by analysing the corresponding light-curves.

These results indicate that the complex nature of light curve variations during the examined period is mainly caused by the changes in the position and size of spotted areas on the system's components. The presented solutions show that AB And is in the slight over-contact configuration ($f_{over}[\%] \sim 11$ %), with the mass ratio $q = m_c / m_h \sim 1.92$.

In conclusion, the application of the "corrected" BaSeL model flux distributions in the programme for the light-curve analysis gives mutual consistency between the results obtained from different passband curves that is really better than the one obtained with simple black-body theory or CG stellar atmosphere models. We expect from these realistic spectral energy distributions to enable a certain progress in the light-curves analysis, i.e., more realistic estimates of an active CB's parameters.

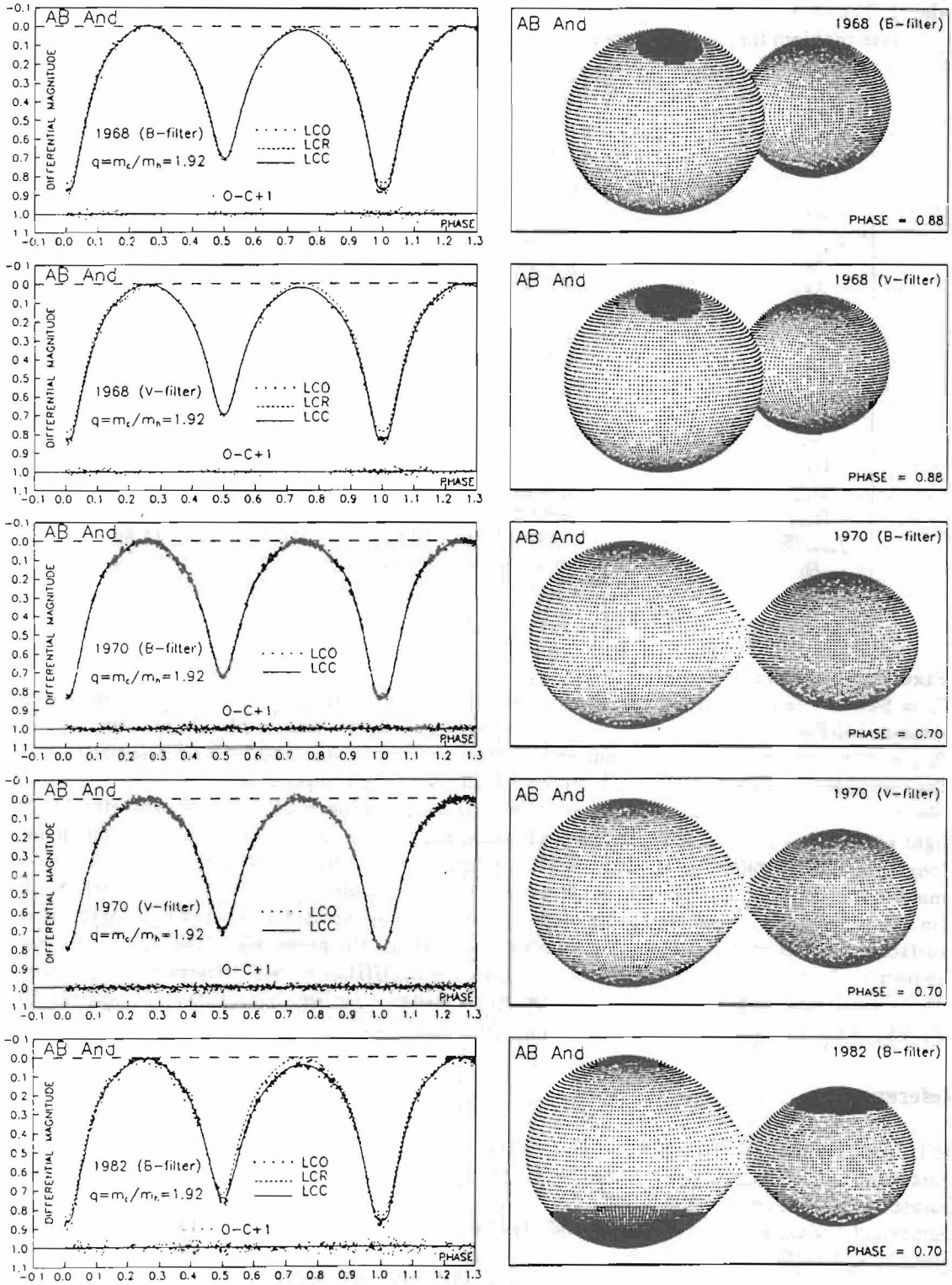

Fig.1. Left: Observed (LCO), referent (LCR) and final synthetic (LCC) light curves of AB And with O-C residuals obtained by solving the inverse problem within the framework of the Roche model with spotted areas on the components; Right: The view of the Roche model for the AB And at the noted orbital phase obtained with parameters estimated by solving the inverse problem.

Table 1. The results of the analysis for AB And (1968, 1970, 1982) light curves obtained by solving the inverse problem for the Roche model with spot areas on the system components.

Quantity	1968 (B-filter)	1968 (V-filter)	1970 (B-filter)	1970 V-filter)	1982 (B-filter)
$\Sigma(O-C)^2$	0.0270	0.0242	0.1282	0.1493	0.1308
$A_{Sh}=T_{Sh}/T_h$	0.65±0.5	0.65 ±0.19			0.909±0.007
θ_{Sh}	25.1±2.2	26.7 ±1.9			42.8±0.9
λ_{Sh}	17.4±10.6	23.2 ±10.6			234.9±14.3
φ_{Sh}	-67.9±4.1	-68.2 ±3.3			83.7±1.7
$A_{Sc}=T_{Sc}/T_c$	0.67±0.1	0.68 ±0.06			0.916±0.005
θ_{Sc}	21.1±0.6	21.2 ±0.6			52.6±0.7
λ_{Sc}	309.4±3.1	310.3 ±3.3			253.5±6.9
φ_{Sc}	61.7±1.6	62.1 ±1.5			-80.7±1.2
T_h	5692±3	5715 ±4	5679±3	5704±4	5692±2
F_h	1.019±0.001	1.017 ±0.001	1.019±0.000	1.019±0.000	1.021±0.001
i	85.0 ±0.1	85.0 ±0.1	85.2±0.1	84.9±0.1	85.0 ±0.1
u_h	0.74	0.67	0.74	0.67	0.74
u_c	0.76	0.68	0.76	0.68	0.76
$\Omega_{h,c}$	5.0736	5.0810	5.0751	5.0750	5.0674
Ω_{in}	5.1381	5.1381	5.1381	5.1381	5.1381
Ω_{out}	4.5435	4.5435	4.5435	4.5435	4.5435
f_{over}[%]	10.85	9.61	10.60	10.60	11.89
R_h	0.309	0.308	0.309	0.309	0.309
R_c	0.416	0.416	0.416	0.416	0.417
$L_h/(L_h+L_c)$	0.424	0.409	0.424	0.412	0.436

Fixed parameters :
$T_c = 5450K$ - temperature of the more-massive (cooler) star, $f_h = f_c = 1.00$ - nonsynchronous rotation coefficients of the components, $q = m_c/m_h = 1.92$ - mass ratio of the components, $\beta_{h,c} = 0.08$ - gravity-darkening coefficients of the components, $A_{h,c} = 0.5$ - albedo coefficients of the components, $[Fe/H]_{h,c} = 0.1$ - accepted metallicity of the components.
Note : $\Sigma(O-C)^2$ - final sum of squares of residuals between observed (LCO) and synthetic (LCC) light curves, $A_{Sh,c}$ - spot temperature coefficients, $\theta_{Sh,c}$, $\lambda_{Sh,c}$, $\varphi_{Sh,c}$ - spot angular dimensions. longitudes and latitudes (in arc degrees), F_h - filling coefficient for critical Roche lobe of the less-massive (hotter) star, T_c - temperature of the more-massive (cooler) component, i - orbit inclination (in arc degrees), $u_{h,c}$ - limb-darkening coefficients of the components, $\Omega_{h,c}$ - common dimensionless surface potentials of the primary and secondary, Ω_{in}, Ω_{out} - the potentials of the inner and outer contact surfaces respectively, $f_{over}[\%] = 100 \cdot (\Omega_{h,c} - \Omega_{in})/(\Omega_{out} - \Omega_{in})$ - degree of overcontact. $R_{h,c}$ - polar radii of the components in units of the distance between the component centres and $L_h/(L_h+L_c)$ - luminosity of the hotter star (including spots).

References

Bell, S. A., Hilditch, R. W. and King, D. J.: 1984, *MNRAS*, **208**, 123.
Durasevic, G.: 1992a, *Ap. & S S*, **196**, 241.
Durasevic, G.: 1992b, *Ap. & S S*, **197**, 17.
Dursevic, G., Zakirov, M., Hojaev, A. and Arzumanyants, G.: 1988, *A & A S*,**131**, 17.
Landolt, A. U.: 1969, *A J*, **74**, 1078.
Lejeune, T., Cuisinier, F., Buser, R.: 1997, *A &A*, **125**, 229.
Lejeune, T., Cuisinier, F., Buser, R.: 1998, *A & A Suppl.*, **130**, 229.
Press, W. H, Teukolsky, S. A, Vetterling, W. T., Flannery, B. P.: 1992, *Numerical Recipes in Fortran, The Art of Scientific Computing*, Second Edition, Cambridge University Press, New York, 120.
Vaz, L.P.R., Anderson, J. and Rabello Soares, M.C.A.: 1995, *A & A*, **301**, 693.

Participants of III YCSLS

Journal of Research in Physics

INFORMATION FOR CONTRIBUTORS

This Journal is devoted to the publication of original papers in **fundamental and applied physics**. The papers are in principle Articles, while Review Articles will be published by invitation only.

Contributors should send their manuscripts to Professor M. Škrinjar, Editor, Institute of Physics, Faculty of Sciences, University of Novi Sad, Trg Dositeja Obradovića 4, 21000 Novi Sad, Yugoslavia. (Fax #: +381-(21)-55-662; E-mail: fizika@uns.ns.ac.yu).

All manuscripts must be submitted in English. Manuscripts should be submitted in duplicate and should be typewritten and double spaced with wide margins. Only one side of each sheet should be used.

Manuscripts should consist of the title, followed by author(s) name(s) and adresse(s), abstract, key words, body of the text and the list of the references. Authors should *not* include references in Abstracts.

References must be numbered in the order in which they are referred to in the text: e.g. S. Wagner [1] or [1]. In the text, such abbreviations as Ref. [4] or Refs. [7-10] may be used.

The full references should be listed in the numerical order of citation in the text at the end of the article. Examples:

1. S. Autler and C. H. Townes, Phys. Rev. A **10**, 489 (1982). – for articles
2. E. U. Shirley, *The Theory of Molecules*, p. 399, (The University Press, Cambridge, 1954). – for books
3. C. E. Moore, "Selected Tables of Atomic Spectra", NSRDS-NBS3, Setion 5, National Bureau of Standards, Washington, DC 20025 (1975). – for reports.

Tables and figures should be sent with the paper on the separate pages. All photographs, graphs, and diagrams should be numbered consecutively. The legends should be typed on a separate page at the end of the article. The author's name, the figure number, and an indication of its proper orientation should be written on the back of each figure.

Line drawings must be submitted in camera-ready form and should be drawn in india ink on stiff white paper or printed on quality laser printer. The letters and symbols should be drawn so as to be clearly legible when reduced.

Authors are asked to suggest at least three referees who may revise their manuscript.

Page proofs will be sent to the author (or the first-mentioned author in a paper of multiple authorship) for checking. **Corrections to the proofs must be restricted to printer's errors**. Authors are particularly requested to return their corrected proofs as quickly as possible. Please note that **authors are urged to check their proofs carefully before return, since late corrections cannot be guaranteed for inclusion in the printed journal.**

The first-named author of each paper will receive 25 reprints free of charge.

Journal of Research in Physics
Volume 28 Number 3 December 1999

CONTENTS

CONTINUED ON INSIDE COVER